LINEAR TRANSCEIVERS FOR MIMO RELAYS

Cheng Yu Andy Shang

A thesis submitted in partial fulfilment
of the requirements for the degree of
Master of Engineering
in
Electrical and Computer Engineering
at the
University of Canterbury,
Christchurch, New Zealand.

2014

ABSTRACT

Relays can be used in wireless communication systems to provide cell coverage extension, reduce coverage holes and increase throughput. Full duplex (FD) relays, which transmit and receive in the same time slot, can have a higher transmission rate compared with half duplex (HD) relays. However, FD relays suffer from self interference (SI) problems, which are caused by the transmitted relay signal being received by the relay receiver. This can reduce the performance of FD relays. In the literature, the SI channel is commonly nulled and removed as it simplifies the problem considerably. In practice, complete nulling is impossible due to channel estimation errors. Therefore, in this thesis, we consider the leakage of the SI from the FD relay. Our goal is to reduce the SI and increase the signal to noise ratio (SNR) of the relay system. Hence, we propose different precoder and weight vector designs. These designs may increase the end to end (e2e) signal to interference and noise ratio (SINR) at the destination. Here, a precoder is multiplied to a signal before transmission and a weight vector is multiplied to the received signal after reception.

Initially, we consider an academic example where it uses a two path FD multiple input and multiple output (MIMO) system. The analysis of the SINR with the implementation of precoders and weight vectors shows that the SI component has the same underlying signal as the source signal when a relay processing delay is not being considered. Hence, to simulate the SI problem more realistically, we alter our relay design and focus on a one path FD MIMO relay system with a relay processing delay. For the implementation of precoders and weight vectors, choosing the optimal scheme is numerically challenging. Thus, we design the precoders and weight vectors using ad-hoc and near-optimal schemes. The ad-hoc schemes for the precoders are singular value decomposition (SVD), minimising the signal to leakage plus noise ratio (SLNR) using the Rayleigh Ritz (RR) method and zero forcing (ZF). The ad-hoc schemes for the weight vectors

are SVD, minimum mean squared error (MMSE) and ZF. The near-optimal scheme uses an iterative RR method to compute the source precoder and destination weight vector and the relay precoder and weight vector are computed using the ad-hoc methods which provide the best performance.

The average power and the instantaneous power normalisations are the two methods to constrain the relay precoder power. The average power normalisation method uses a novel closed form covariance matrix with an optimisation approach to constrain the relay precoder. This closed form covariance matrix is mathematically derived using matrix vectorization techniques. For the instantaneous power normalisation method, the constraint process does not require an optimisation approach. However, using this method the e2e SINR is difficult to calculate, therefore we use symbol error rate (SER) as a measure of performance.

The results from the different precoder and weight vector designs suggest that reducing the SI using the relay weight vector instead of the relay precoder results in a higher e2e SINR. Consequently, to increase the e2e SINR, performing complicated processing at the relay receiver is more effective than at the relay transmitter.

ACKNOWLEDGEMENTS

My Master's study at University of Canterbury has been a challenging and eventful journey. To be able to arrive where I am today, I need to thank many people.

First of all, I need to express my gratitude to my supervisors Prof. Peter Smith, Dr. Greame Woodward and Dr. Gayathri Kongara for their support, contribution and patience throughout my research and thesis.

Secondly, I would like to thank the members of WRC and Comms. Group. Because of them, my studies have been full with surprise and excitement. With their help and contributions, I have learnt many different aspects of communication and has widen my views of wireless communication.

Cheng Yu Andy Shang

University of Canterbury

2014

CONTENTS

LIST OF TABLES

LIST OF FIGURES

LIST OF SYMBOLS

$\mathcal{CN}(0,1)$	Circularly symmetric complex Gaussian random variable with 0 mean and variance of 1.
E{.}	Statistical expectation.
$\boldsymbol{M}$	Matrices are denoted by uppercase bold letters.
trace$\{X\}$	Trace of X.
$\boldsymbol{v}$	Vectors are denoted by lowercase bold letters.
X^*	Conjugate of X.
$X^\dagger$	Hermitian transpose of X.
X^{T}	Transpose of X.

ABBREVIATIONS

AF	amplify and forward.
AWGN	additive white Gaussian noise.
CDF	cumulative distribution function.
DF	decode and forward.
e2e	end to end.
FD	full duplex.
HD	half duplex.
INR	interference to noise ratio.
LOS	line of sight.
MIMO	multiple input multiple output.
MMSE	minimum mean squared error.
NLOS	non line of sight.
NSP	null space projection.
QPSK	quadrature phase shift keying.
RR	Rayleigh Ritz.
SC	scattered channel.
SER	symbol error rate.
SI	self interference.
SINR	signal to interference and noise ratio.
SLINR	signal to leakage plus interference ratio.
SLNR	signal to leakage and noise ratio.

SNR	signal to noise ratio.
SMSS	SVD, MMSE, SVD, SVD.
SSLS	SVD, SVD, SLNR, SVD.
SSSM	SVD, SVD, SVD, MMSE.
SSSS	SVD, SVD, SVD, SVD.
SSSS (HD)	SVD, SVD, SVD, SVD (in HD mode).
SSZS	SVD, SVD, ZF, SVD.
SZSS	SVD, ZF, SVD, SVD.
SVD	singular value decomposition.
TDC	time domain cancellation.
ZF	zero forcing.

Chapter 1

INTRODUCTION

1.1 COMMUNICATION CHANNEL AND MULTIPLE INPUT AND MULTIPLE OUTPUT SYSTEMS

Wireless communication is one of the most rapidly growing areas in the communication field today. This is due to two main factors: firstly, there has been a high demand for wireless connectivity, such as cellular telephony [1,2]. Secondly, the success of third and fourth generation digital wireless standards, such as the long term evolution (3GPP LTE) standard, provides a concrete demonstration that wireless communication theory can have a significant impact in practice and wireless technology can also be improved further [3].

There are two fundamental aspects of wireless communication that make the problem challenging and interesting. However, these aspects are not as significant in wired communication. The first aspect is the phenomenon of the dynamic and variable nature of the wireless channels. This includes the variations in channel gain due to small scale effects, multipath fading, as well as large scale effects such as path loss, distance attenuation and shadowing by obstacles [4, 5]. Secondly, unlike wired systems, where each transmitter and receiver pair can often be considered as an isolated link, wireless transmission between users is propagated over the air and there is a significant amount of interference between them. Hence, this can cause the received signal detection to be unreliable at the receiver [5, 6].

One of the most effective techniques to obtain reliable communication over a wireless channel is spatial diversity. This is achieved by using multiple antennas at the transmitter and/or at the receiver nodes to detect signals over different paths and improve the signal quality at the

receiver. The main idea of diversity is that all of the received signal being of poor quality is unlikely [7]. In this way, the communication can have a higher change of success from the transmitter to the receiver. With an appropriate system configuration, transmitted signals can be statistically independent from each other, allowing multiple signals to be detected at the receiver end [5]. Multiple-Input-Multiple-Output (MIMO) systems use additional antennas to create extra channel inputs and outputs to transmit signals from the transmitter to the receiver. Due to its potential for providing large channel capacity and high spectral efficiency [7], MIMO has become an active area of investigation.

1.2 PROBLEM STATEMENT AND FOCUS

In order to fully utilise the potential of MIMO systems, the channels need to be independent of each other [8]. This can be illustrated in the two scenarios shown in Figure 1.1. Figure 1.1(a) shows there are no objects in the transmission path and assuming the transmit and receive antennas are very close to each other, the four channels are likely to be highly dependent on each other [7]. In this case, the MIMO communication system may have a poor performance, as the receiver cannot distinguish between the two transmitted signals from the received signals [9]. Consider a more cluttered environment where objects between the transmitter and receiver introduce some reflection paths as shown in Figure 1.1(b). With these reflection paths, the different channels are less likely to be correlated as they are formed from different paths. The objects that create extra paths for signal transmission are known as scatterers. They enable MIMO systems to have multiple signal transmission by creating different channels and increasing the spatial diversity.

The scatterers can be implemented by inserting a relay between the source and destination as shown in Figure 1.2. Relays are transceivers that receive and retransmit signals with some type of processing or amplification performed on the received signal. Relays can extend network coverage, combat wireless channel impairments and reduce the transmit power required to transmit directly from the source node to the destination node [10–12]. Relays can also be useful for path extension in high frequency systems, as high frequency signals have shorter transmission paths compared to low frequency systems [13]. Relays can also be used to cooperate with a

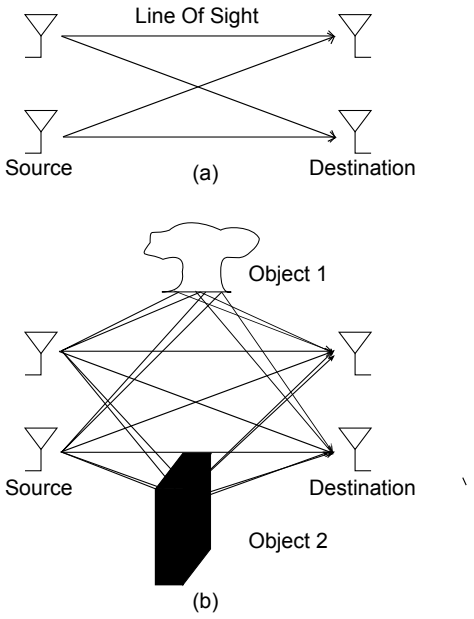

Figure 1.1 An example MIMO environment scenario with two transmit and two receive antennas a) Lack of scatterers in MIMO channel b) Scatterers in MIMO channel creating a multipath effect.

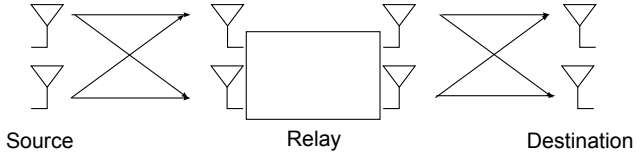

Figure 1.2 A relay that is acting like a scatterer.

source node to increase the number of streams that are received at the destination. This type of diversity is known as cooperative diversity [14–17].

Long range MIMO channels may become rank deficient due to correlated spatial fading. Such cases are referred to as a "keyhole channels" [18]. One of the methods to restore the rank of these long range MIMO channels is to deploy a relay between the source and destination. This relay can restore or increase the rank of the MIMO channels by introducing artificial scatterers [19]. This is similar to placing objects between the source and destination antenna as shown in Figure 1.1(b). This technique provides additional diversity and improves the signal quality at the destination.

There are two main types of relays that are found in the literature, these are known as amplify and forward (AF) [3, 20–26] and decode and forward (DF) [3, 27]. AF relays simply receive,

amplify and forward the received analog signal. Although these relays have a low processing delay, they amplify and transmit the received signal with the received noise [3, 28, 29]. In other words, the SNR at the output of AF relays will never be higher than their inputs. DF relays decode and re-encode the received signal before transmitting the signals to the next node [3]. This decode and re-encode process will not amplify the noise. Therefore in a low SNR environment, DF relays perform better than AF relays. However, DF relays have a longer processing delay and larger complexity compared to AF relays.

Relays have two modes of operation, these are known as half duplex (HD) and full duplex (FD) [30–32]. For HD relays, they operate in two different time slots: one is for transmitting and another is for receiving. Operating in separate time slots avoids the propagation of feedback from the relay transmitter to the relay receiver. This feedback is a particular problem because the relay receiver receives a stronger signal from the relay transmitter compared to the source transmitter [33, 34]. However, using two different time slots to operate is not spectrally efficient as the relay is only using half of its available time. In contrast to HD relays, FD relays are more spectrally efficient as they receive and transmit in the same time slot. However, FD relays are not feasible unless the loop interference between its transmitter and its receiver is mitigated or removed [25].

Currently, the relays that are most often used in communication systems are usually operating in HD mode, as the self interference (SI) power is too large to cancel out in FD mode. An example of this would be the cellular systems [35]. In traditional cellular systems, the transmit power of the relay needs to be large as the path loss at the destination receiver is high. This will cause the relay receiver to receive a stronger SI signal [36]. However, [30] shows that when the SNR at the relay input is higher than 0.75 times the SNR of the relay to destination link, then FD mode is recommended over HD mode. Furthermore, if SI can be reduced or canceled from the relays, then FD communication can be viable in practice and has the potential to outperform HD relay communication systems.

In this thesis, AF FD MIMO systems are investigated along with signal processing to reduce or remove the relay's SI and increase the end to end (e2e) signal to interference plus noise ratio (SINR).

1.3 LITERATURE REVIEW

Relays are transceivers that receive signals from one node and retransmit them to the next node with some processing or amplification performed on the received signals. Relays are used in cooperative communication systems, as they enable promising techniques to provide lower transmit power, higher throughput and larger coverage in wireless communication systems [11]. For long range MIMO systems, the link quality between the source and the destination in a wireless system is not always satisfactory. This is due to the "keyhole channel ", which results in a degenerate channel [37]. By creating additional links with a relay, the MIMO link quality can be improved [38].

1.3.1 Types of Relays Studied in Literature

Recently, there has been increased interest in FD relays, this is due to the wireless architectural progression towards short range systems [36]. For short range systems like WiFi, the path loss is less compared to traditional cellular systems, making SI reduction easier to perform. This is due to the fact that the transmit power of the relay can be lower, hence making the SI power at the relay receiver weaker. Despite the growing interest in FD relays, HD is also extensively studied in the literature. In some papers, the authors considered using HD relays in MIMO systems. Since these relays use different time slots for reception and transmission as illustrated in Figure 1.3a), the SI loop from the relay's transmitter to its receiver will not occur [38–41]. In these HD relay papers, some authors developed protocols for the case in which the source to destination link is blocked [38–40] and others exploit the source to destination link as an extra diversity branch [41]. Although much work has been done in HD relays, they are not efficient in terms of spectral efficiency and throughput compared to FD relays, which receive and transmit in the same time slot as shown in Figure 1.3b) [42, 43]. However, the challenge with FD relays is the SI that occurs from the receiver listening to its own transmitter. Another words, when a FD relay amplifies the received signal, the large amplified signal transmitted will propagate back to the relay receiver. If this feedback signal is not reduced or removed, it will distort the desired signal from the source node [44]. If this occurs, the performance of the MIMO system

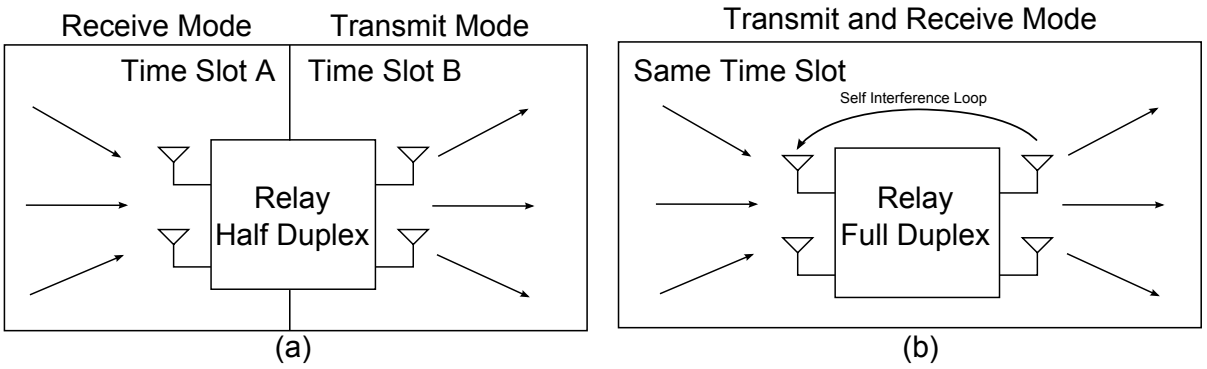

Figure 1.3 Relay schemes a) Half Duplex: receive and transmit antennas operate in different time slots b) Full Duplex: receive and transmit antennas operate in the same time slot.

degrades dramatically.

1.3.2 Self Interference in Full Duplex Relay

Many researchers have derived alternative methods to reduce the SI of FD MIMO relay systems in both theory and experimental hardware implementation [35, 45–47]. These techniques can be classified as either passive or active. The passive suppression is simply achieved by blocking the transmission path between the transmitter and receiver antenna [48]. Another technique is to have orthogonal placement of the receive and transmit antennas [35]. This will create constructive interference to eliminate the SI. The authors in [49] constructed obstacles between the transmitting and receiving antennas to effectively block the line of sight (LOS) component of the feedback channel. Furthermore, [44] used directional antennas that are pointed in opposite directions to increase SI suppression. In [50], antenna isolation is achieved by using two transmit and one receive antenna at the relay. The two transmit antennas are placed asymmetrically at l and $l + \lambda/2$ distance from the receive antenna. Offsetting the two transmitters by half a wavelength causes the signals to add destructively and cancel each other out. This creates a null position where the receiver receives a weaker signal. However, to further reduce SI, active suppression such as analog and digital cancellation are also required as proposed in [51]. In [51], they proved that FD relay systems are feasible and can achieve higher rate than that achieved by HD relay systems if SI is canceled before it reaches the relay receiver. They implemented three mechanisms for SI cancellation which are shown in Figure 1.4. These cancellation techniques

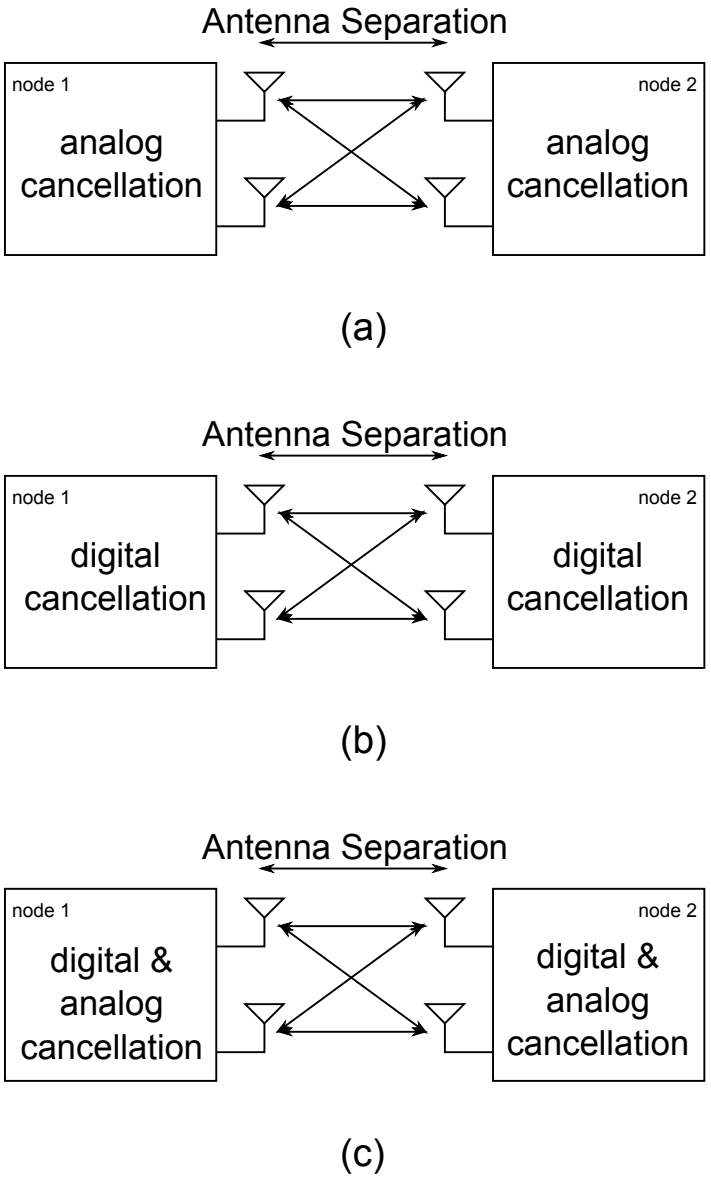

Figure 1.4 Relay cancellation techniques a) antenna separation and analog cancellation b) antenna separation and digital cancellation c)antenna separation, digital and analog cancellation.

are: antenna separation and analog cancellation (Figure 1.4(a)); antenna separation and digital cancellation (Figure 1.4(b)); and antenna separation, digital and analog cancellation (Figure 1.4(c)). Although the results in [51] demonstrated that SI reduction can be achieved in FD relays, no e2e overall performance schemes were provided.

SI cancellation work has also been done in the digital domain by other authors. The authors in [52] and [43] have analytically calculated the achievable isolation with time domain cancellation (TDC) and null space projection (NSP). It is concluded by [43, 52] that TDC is sensitive to

both channel estimation noise and transmit signal noise. On the other hand, NSP requires extra antennas for efficient mitigation. TDC techniques can suppress SI only up to the effective dynamic range of the analogue to digital converter. Hence, [36] suggests that it is more effective to reduce SI before the signal reaches the analogue to digital converter component. Other authors, such as [53], used antenna selection schemes that minimise the effect of the interference channel. They showed that antenna selection has a lower complexity compared with NSP schemes. The work in [43, 52, 53] mainly focused on reducing the SI feedback of a relay and no techniques for improving the link between the source to relay and relay to destination link were provided.

In a relay, there is always some signal processing. Since there are processing operations in the relay, there will be a delay between the transmitted signal and the received signal. However, depending on the speed and the complexity of this processing, this time delay may be negligible. Hence, some FD relay papers include the effects of processing delay [31, 54] or ignore processing delay [30] in their work. When a relay design is assumed to have no processing delay, the actual source signal component in the received signal will be identical to the transmitted signal as stated in [30]. In this case, the equation for the relay received signal becomes simpler as the SI only contains extra amplified noise. However, when a relay contains a processing delay effect, the equation of the relay received signal will be more complicated as SI is not pure amplified noise. Instead, it contains a noise term as well as a delayed signal term [52].

Most of the SI cancellation work only considers the source to relay then relay to destination link, and ignores the effect of the direct link (source to destination) in order to reduce the complexity of the analysis [25, 52, 55]. Some papers make this problem even simpler by only focusing on signal precoding and decoding at the relay node [44, 48, 49, 51].

One paper uses a two phase scheme to implement a model that considers the direct links with a FD relay [56]. In a two phase scheme, the destination node uses two time slots to receive separate information from the source and relay. The first time slot is used to receive information from the source, while the second time slot is used to receive information from the relay and the source does not transmit any information. The advantage of using this scheme is that it avoids SI. The disadvantage of this scheme is that the source is only transmitting for half of its available time.

1.3.3 Transmit and Receive Beamforming

Transmit and receive beamforming is used for improving the transmission link between the transmitter and the receiver. Signals are multiplied with a precoder before transmission and multiplied again with a weight vector after reception. Linear precoders and weight vectors have a relatively low complexity so they are used to improve the transmission quality and rate [57–60]. When a relay is operating in HD and SI is not occurring from the relay, precoders and weight vectors can be designed to maximise the SNR of the channel. One of the well known approaches to maximise the SNR of the desired channel is the singular value decomposition (SVD). The channel matrix $\boldsymbol{H}$ can be decomposed by SVD as

$$\boldsymbol{H} = \boldsymbol{U}\boldsymbol{\Sigma}\boldsymbol{V}^{\dagger}, \tag{1.1}$$

where $\boldsymbol{U}$ and $\boldsymbol{V}$ are unitary matrices and $\boldsymbol{\Sigma}$ is a diagonal matrix. The signal, $\boldsymbol{x}$, at the transmitter is multiplied by the $\boldsymbol{V}$ matrix and the received signal at the receiver is multiplied by the $\boldsymbol{U}^{\dagger}$ matrix [30, 61]. Using this process the channel can be diagonalised and this is given by the following (in the absence of noise)

$$\begin{aligned} \text{transmitter side} &= \boldsymbol{V}\boldsymbol{x} \\ \text{receiver side} &= \boldsymbol{U}^{\dagger}\boldsymbol{H}\boldsymbol{V}\boldsymbol{x} \\ &= \boldsymbol{U}^{\dagger}\boldsymbol{U}\boldsymbol{\Sigma}\boldsymbol{V}^{\dagger}\boldsymbol{V}\boldsymbol{x} \\ &= \boldsymbol{\Sigma}\boldsymbol{x}. \end{aligned} \tag{1.2}$$

Constructing the precoders and weight vector using the SVD of the channel results in parallel virtual channels, which have SNRs that correspond to the original channel eigenvalues [61]. This parallel channel decomposition helps to reduce and simplify the signal processing at the receiver, as it only needs to perform scalar decoding, rather than complex decoding [58]. This idea is feasible only when perfect channel state information is known at the transmitter and receiver [58, 61].

When there is SI at the relay, precoders and weight vectors can be designed to reduce/remove

SI and to increase the SINR. The difference between a precoder and a weight vector is that a precoder is multiplied to the signal before transmission and a weight vector is multiplied to the received signal after reception. These precoder and/or weight vector designs, which are commonly found in the literature, are: zero forcing (ZF) [62, 63], minimum mean squared error (MMSE) [64, 65] and signal to leakage plus noise ratio (SLNR) [66–70].

1.3.3.1 Precoders

An SVD precoder is often used when there is no interference in the channel as it only boost the desired channel component and ignores the noise and the interference component. However, SVD can also be used in the presence of interference to compare with other precoding techniques that deal with the interference and/or noise.

ZF is a linear precoder that is commonly used in practice [70], because it completely suppress the interference between users [71–73]. Another advantage of using ZF is its low complexity compared to other precoders [63, 74–76], as the ZF precoder is generated by simply inverting the channel matrix at the transmitter side [63]. However, ZF can suffer from high transmission power, noise inflation and extra antennas maybe required to provide enough degrees of freedom to operate [71].

Signal to leakage plus noise ratio (SLNR) is an alternative precoding technique to ZF. SLNR precoding is designed by maximising the power of the signal over the leakage plus noise [77]. This leakage is a measure of the signal power that is leaked into other users' receivers [66]. Compared to ZF, SLNR does not require any limits on the number of transmit and receive antennas [66]. This precoder also considers the influence of noise when the precoder is being designed and like ZF, there is an analytical closed form solution for the precoding matrix [67]. The SLNR precoder is obtained by the generalised eigenvalue decomposition of the channel covariance matrix and the leakage channel plus noise covariance of each user [66, 67, 69].

1.3.3.2 Weight Vectors

The SVD weight vector is similar to the SVD precoder, in that it boost the desired channel component and ignores the interference and noise of the received channel. Hence, SVD weight vector design can be used to compare with the other weight vector designs that deal with the interference and/or noise at the receiver.

Weight vectors that are used in practical systems, such as MMSE, are appealing for many applications, as they can often be implemented with low complexity [78–80]. The MMSE criterion is designed to minimise the error in MIMO channels [60]. In MIMO systems, MMSE weight vectors are adopted in some of the standards, e.g. IEEE 802.11n and 802.16e [81]. Therefore, MMSE designs are widely used in both theoretical and practical implementations. It has been shown that MMSE receivers can extract the full spatial diversity of the MIMO quasi-static channel at low data rates [79].

1.3.4 Power Constraint

A power constraint is required for designing precoders and weight vectors. This is due to the fact that transmitters have a finite power with which to transmit the signals.

One of the power constraint methods is to use an average power constraint and to set the average power of the source and relay precoder to a particular constant value as shown in [82]. In [83], they used a maximum per-relay power constraint then a total sum power constraint to find the optimum solution for the relay precoder and weight vectors. An instantaneous relay gain power constraint can also used to guarantee finite transmit power and to prevent relay oscillation as shown in [31]. Most of the literature makes the power constraint problem easier, by suppressing SI with some form of processing technique (space-time cancellation [84] precoding/decoding [85] or prenulling [86]). However, when the SI is not completely suppressed, the calculation of average power for the precoders is difficult. This is due to the fact that the relay transmitted power expression, the relay precoder and weight vector expressions are linked, leading to complex iterative equations. These equations are difficult to solve without the use of numerical methods. Hence, most of the current literature does not explicitly deal with SI in MIMO systems and it

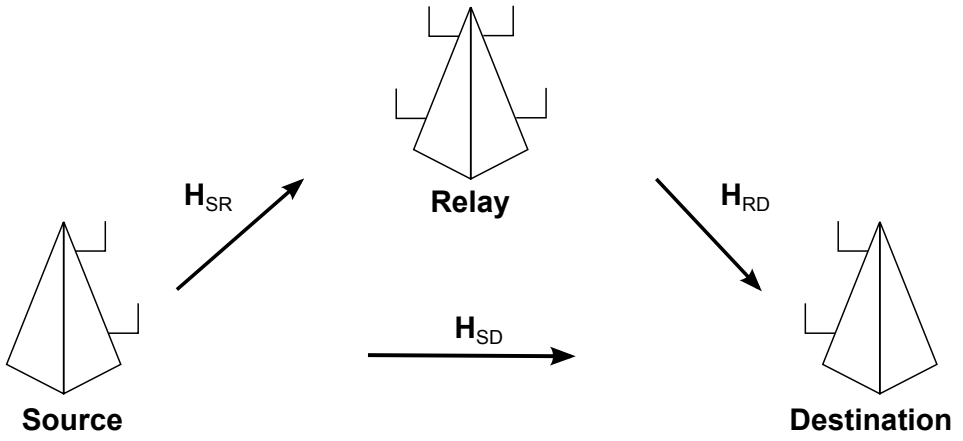

Figure 1.5 A fundamental MIMO relay design.

makes the MIMO FD relay an interesting and challenging topic to explore.

1.4 RESEARCH OBJECTIVE

Consider the fundamental FD AF relay MIMO system shown in Figure 1.5 [19]. The signal is transmitted from the source node to the destination and the relay node through channel, $\boldsymbol{H}_{SD}$, and channel, $\boldsymbol{H}_{SR}$, respectively. Before the signal is transmitted from the source node, the signal is multiplied by a precoder. At the relay node, the received signal is multiplied with a weight vector and then multiplied with a precoder to give the resultant signal. The relay transmits this new signal to the destination node through channel, $\boldsymbol{H}_{RD}$. At the destination node, the received signal is multiplied by a weight vector. All these nodes have multiple transmit and/or receive antennas. This two path cooperative design can be used to increase the receive SINR at the destination or, in the case of [19], to introduce an artificial scatterer in the channel. In [19], it was shown that SI occurs during FD relay transmission and this problem needs to be resolved for FD relays to produce a reliable link.

Using the relay design proposed in [19], we implemented a two path FD MIMO relay system including the effects of relay SI. However, we noticed that when the relays' delay effects (due to relay processing) are not considered, the source and the SI signal received by the receiver contains the same underlying source signal. As a result of this, relay processing to reduce SI is unimportant, since SI is not interfering with the source signal. Hence, without adding the

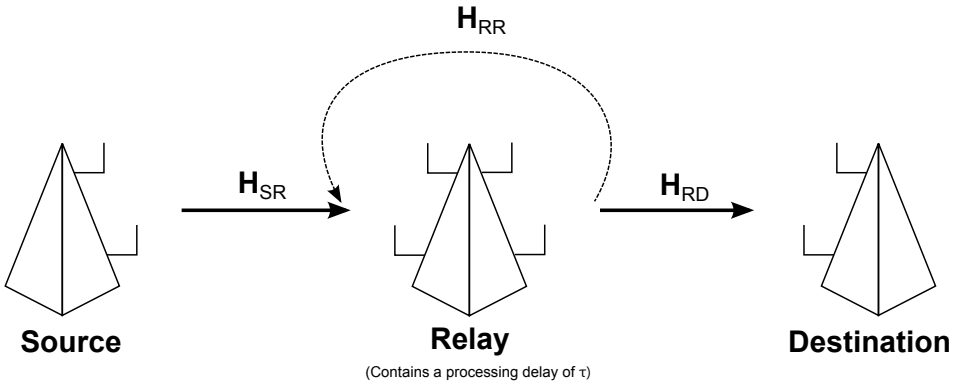

Figure 1.6 The proposed MIMO relay design.

effects of delay in the relay system, an artificial MIMO system is created, which does not model the important aspects of a real implementation.

We altered our design by constructing a one path MIMO FD AF relay system and added in the effects of a delay, τ, due to processing at the relay, as shown in Figure 1.6. In this design, we removed the source to destination link, as the MIMO relay system now includes the effects of delayed SI. Keeping the source to destination link would make the system too complex for an initial investigation.

In this relay system, the effects of the delay and SI are being considered. The signals entering the relay from the source as well as the relay transmitter will not carry the same underlying source signal, where we consider the latter as interference. In order to constrain the power of the relay using average normalisation, the power of the processed relay signal needs to be calculated. We set the power of the transmitted signal from the source to be unity. However, when the relay receives this signal, the signal power is a combination of the source signal power plus the SI power. The SI power is dependent on the relay precoder as it determines the amount of leakage that is being transmitted back to the relay receiver. However, in order to calculate and constrain the relay precoder, the relay received signal power needs to be known. This becomes an iterative scenario where one calculation is dependent upon another. A less complicated alternative method is to cancel out SI using nulling, which has been implemented in [46]. However, this is impractical, since imperfect channel state information leads to SI as represented by the $\boldsymbol{H}_{RR}$ in Figure 1.6. Hence, as SI cannot be completely removed, our research

objective is to calculate the SI signal power such that we can maximise the global e2e SINR link through different precoder and weight vector designs.

The major part of this thesis is focusing on the one path MIMO relay model. At the relay, the covariance matrix of the transmitted signal was derived with a novel closed form solution. This enables us to constrain the relay power to compare different precoder and weight vector designs. This maximises the e2e signal to interference plus noise ratio (SINR) at the destination. To the best of the authors knowledge, no such analysis and design has appeared in any literature. From these different designs, using single stream transmission, an improved e2e performance is achieved, which suggests that SI reduction at the relay receiver is preferable to pre-cancellation at the relay transmitter.

1.5 THESIS LAYOUT

This section briefly outlines the content of each chapter in this thesis.

In Chapter 2, the Rician channel model is described, as it is the base for modeling the channels in the MIMO relay with the effects of SI. This chapter also introduces ad-hoc and optimisation methods for computing the precoder and weight vector solutions. These increase the signal power and/or decrease the interference power. The ad-hoc methods include SVD, ZF, MMSE and SLNR. The optimal method that is used to calculate the source precoder and destination weight vector is based on an iterative Rayleigh-Ritz (RR) approach. The "pure ad-hoc" method is used to define all the precoders and weight vectors using only the ad-hoc approach. The "near-optimal" method is used to define the source precoder and destination weight vector using the iterative RR method, while the relay precoder and weight vector are designed using the ad-hoc approach.

Chapter 3 presents a two path MIMO relay model that is illustrated in Figure 1.5. Through analysis, we show that by ignoring the effects of the processing delay, the relay's SI effect disappears as the SI contains the desired signal. Hence, it is concluded that this is an artificial relay model which does not model the important aspects of SI.

Chapter 4 shows the performance of different precoding and weight vector designs in a one path proposed MIMO relay model that incorporates a relay processing delay. In this model, we use an average power normalisation to normalise the relay precoder. We also show that doing processing before the relay receiver to remove or reduce SI, has a higher e2e SINR than removing SI at the relay transmitter.

In Chapter 5, the MIMO relay model is extended to use instantaneous power normalisation at the relay. Using the precoder and weight vector designs from Chapter 4, which produce the best results, we present the performance of the MIMO relay model using symbol error rate (SER). To compare the results of the instantaneous power and average power normalisation models, we show an initial derivation of the SINR equation for the instantaneous power model. These derivations for the instantaneous power model are beyond the scope of this thesis and is regarded as a topic for future work.

Finally, Chapter 6 makes some conclusions and also provides some directions for future work in this topic. Part of this work has appeared at the IEEE Australian Communications Theory Workshop (AusCTW 14) [87].

Chapter 2

BACKGROUND

The main purpose of this chapter is to describe the Rician model for MIMO channels that has been used to describe all the links of a multiple input multiple output (MIMO) relay in full duplex (FD) mode and operating in amplify and forward (AF) mode. This chapter also describes the different precoder and weight vector techniques that are used to reduce or remove SI at the relay. This chapter is organised as follows: Section 2.1 describes the MIMO channel models. Section 2.2 states the problems that occur in the line of sight (LOS) MIMO channel. Section 2.3 describes the two different schemes for designing the precoder and weight vectors. These schemes are categorised as ad-hoc and near-optimal schemes which are described in Section 2.3.1 and Section 2.3.2, respectively.

2.1 CHANNEL MODELS

In this work, analytical models of wireless channels are used for comparing the performance of different precoder and weight vector designs. These models do not specifically incorporate any physical propagation mechanisms and simply reproduce the statistical properties of the MIMO matrix channel. Such analytical models are often useful when the system design is in its evaluation and verification stage. The advantage of these models is that they avoid the complex and computationally intensive reproduction of a channel's physical properties.

For our channel model, we consider a narrow band system, where the bandwidth of the signal does not exceed the coherence bandwidth. Coherence bandwidth is a statistical measure of the range of frequencies of the channel that can be considered as "flat "(i.e. all the spectral components

of the channel have approximately equal gain and linear phase) [1, 5]. The main advantage of narrowband systems is that they avoid inter symbol interference and they are very common in orthogonal frequency division multiplexing (OFDM) systems which are prevalent in current and future standards. Most narrowband analytical models are based on a multivariate complex Gaussian distribution for the MIMO channel coefficients [88]. This leads to the well known Rayleigh or Rician fading models, which are widely accepted in many wireless communication research areas [5].

2.1.1 AWGN Noise

The additive white Gaussian noise (AWGN) model is the simplest noise model for communication simulation. In this model, the received signal is degraded by thermal noise, $\boldsymbol{n}$, that may be associated with the physical channel, as well as with the electronics at the transmitter and receiver nodes [89].

The noise vector, $\boldsymbol{n}$, in AWGN is assumed to contain independent complex Gaussian random variables with a mean of zero and a variance of σ^2 [9]. A key property of AWGN is that the projection of these random vectors onto any other orthogonal vectors are independent and identically distributed [90].

2.1.2 Frequency Flat Fading Channel

In a frequency flat fading channel, the channel is assumed to have a constant gain and linear phase response over a bandwidth, which is at least as large as the bandwidth of the transmitted signal [1]. In this channel, the received signal undergoes flat fading. This is the case for narrowband systems in which the transmitted signal bandwidth is much smaller than the channel's coherence bandwidth [6].

Consider a system where the source is equipped with N_S antennas, and the destination has N_D antennas as shown in Figure 2.1. In this situation, we assume that the bandwidth of the transmitted signal is small enough, such that no inter symbol interference occurs and the channel is considered as frequency flat. Frequency flat fading corresponds to the case where the delay

spread is small with respect to the transmit signal symbol period [4]. Hence, the received signal at antenna m at one instant in time can be represented by

$$y_m = \sum_{n=1}^{N_S} h_{m,n} x_n + n_m, \tag{2.1}$$

where the signal, x_n, is being multiplied by a complex channel gain, $h_{m,n}$, between the n^{th} transmitter and m^{th} receiver. An AWGN noise term, n_m, is also being added to the received signal at the receiver. Let $\boldsymbol{x}$ and $\boldsymbol{y}$ be $N_S \times 1$ and $N_D \times 1$ vectors containing the transmitted and received data, respectively, then (2.1) can be re-written in matrix/vector format as

$$\boldsymbol{y} = \boldsymbol{H}\boldsymbol{x} + \boldsymbol{n}. \tag{2.2}$$

The $N_D \times N_S$ channel matrix, $\boldsymbol{H}$, where each element corresponds to the complex gain between a transmit and receive antenna pair, is given by

$$\boldsymbol{H} = \begin{bmatrix} h_{1,1} \cdots h_{1,N_S} \\ \vdots \ddots \vdots \\ h_{N_D,1} \cdots h_{N_D,N_S} \end{bmatrix}. \tag{2.3}$$

These channel elements vary for different types of channel environments. Hence, we consider the two well known channel types, line of sight (LOS) and scattered (SC) [91].

The LOS channel is given by [92]

$$\boldsymbol{H}_{LOS} = \boldsymbol{a}(\theta_s)^{\mathrm{T}} \boldsymbol{a}(\theta_d), \tag{2.4}$$

where $\boldsymbol{a}(\theta_s)$ and $\boldsymbol{a}(\theta_d)$ are the array responses at the transmitter and receiver, respectively. The array responses corresponding to N-element linear arrays are given by [93]

$$\begin{aligned} \boldsymbol{a}(\theta_s) &= [1, \mathrm{e}^{j2\pi d \cos(\theta_s)}, \cdots, \mathrm{e}^{j2\pi d(N-1)\cos(\theta_s)}] \\ \boldsymbol{a}(\theta_d) &= [1, \mathrm{e}^{j2\pi d \cos(\theta_d)}, \cdots, \mathrm{e}^{j2\pi d(N-1)\cos(\theta_d)}], \end{aligned} \tag{2.5}$$

where θ_d and θ_s are the angle of arrival and departure of the antenna component, respectively.

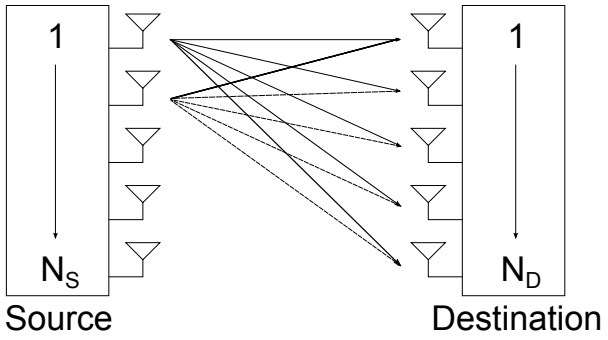

Figure 2.1 An example of a MIMO channel.

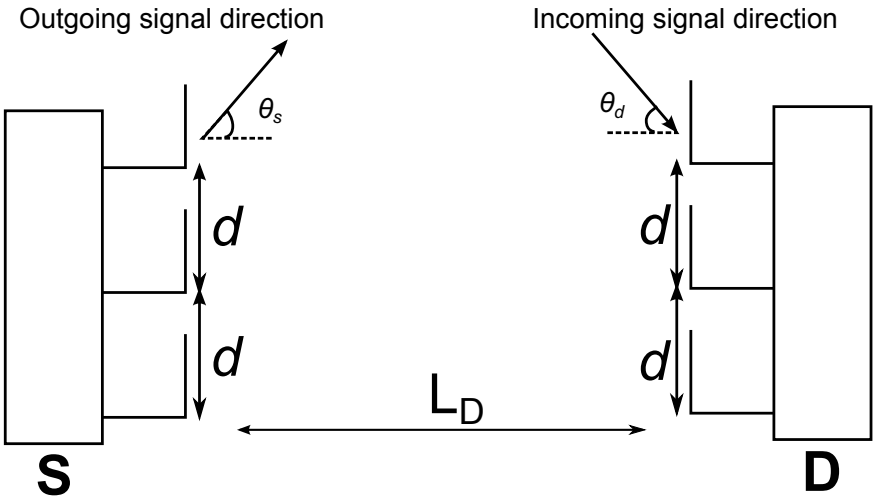

Figure 2.2 MIMO system parameters: angle of arrival (θ_d), angle of departure (θ_s), antenna spacing (d) and distance between source and destination (L).

and d is the antenna spacing measured in wavelengths. These parameters are illustrated in Figure 2.2.

In a LOS environment, when θ_s and θ_d are very small and the distance, Ł$_D$, between the source and destination antenna becomes very large, the channel matrix has a low rank. This is due to signals arriving within a narrow angle at the receiver and d is very small compared to Ł$_D$ such that $\frac{d}{\text{Ł}_D} \approx 0$ [94]. When this occurs, the elements in $\boldsymbol{a}(\theta_s)$ and $\boldsymbol{a}(\theta_d)$ become close to unity and the LOS channel matrix in (2.4) reduces to a matrix of ones given by

$$\boldsymbol{H}_{LOS} = \begin{bmatrix} 1 & \cdots & 1 \\ \vdots & \ddots & \vdots \\ 1 & \cdots & 1 \end{bmatrix}. \tag{2.6}$$

To obtain a full rank channel matrix in a LOS channel, the antenna spacing needs to be very large. However, this is limited by the size of the transmit and receive stations. An alternative method to restore the rank of the MIMO channel is to employ relays to act as scatterers [94, 95].

The channel in the scattered case is denoted by $\boldsymbol{H}_{SC}$ and the elements are statistically independent unit variance Gaussian random variables [93]. Hence, $\boldsymbol{H}_{SC}$ contains elements which are complex normal random variables with a mean of zero and a variance of one. Furthermore, the variance of the real and imaginary parts are equal [90].

The scattered channel (SC) with sufficiently rich scattering has independent matrix elements giving a high rank channel and a large channel capacity [96]. Hence, this kind of channel condition is desired for MIMO transmission. The MIMO channel is often modeled as a combination of the LOS and SC channel components. Here, the overall channel is given by

$$\boldsymbol{H} = \sqrt{P}\left(\sqrt{\frac{K}{1+K}}\boldsymbol{H}_{LOS} + \sqrt{\frac{1}{1+K}}\boldsymbol{H}_{SC}\right), \tag{2.7}$$

where $\boldsymbol{H}_{LOS}$ and $\boldsymbol{H}_{SC}$ are the LOS and SC channel matrices, respectively. We set the power of the channels ($\boldsymbol{H}_{SC}$ and $\boldsymbol{H}_{LOS}$), signal and noise to be unity. Hence, the factor P in (2.7) is the overall SNR of the received signal if and only if $\mathrm{E}\{x_i\}^2 = 1$ and $\mathrm{E}\{n_i\}^2 = 1$, where x_i and n_i are the individual i^{th} elements of the signal and noise, respectively. The term K in (2.7) is the Rician K factor that is defined as follows [89]:

$$K = \frac{\text{power in the LOS path}}{\text{power in the SC path}}. \tag{2.8}$$

When $K = 0$, the channel only contains a SC component and when $K = \infty$, the channel only contains a LOS component.

2.1.3 Quasi Static Channel

A slow fading channel, as illustrated in Figure 2.3 shows a quantised channel where the channel gain is assumed to be almost constant for non-negligible periods of time. This is called a quasi static channel [90]. This model is used for slow fading scenarios, where the delay spread is

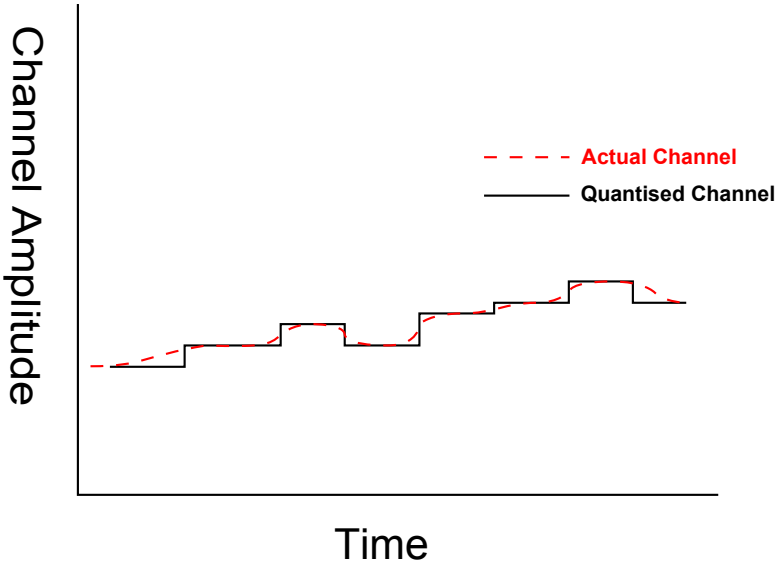

Figure 2.3 An example of a quasi static channel.

smaller than the channel coherence time[1]. The delay spread is a measure of the time it takes for all of the multiple copies of signals that are transmitted at the source to be received at the destination [97]. This constant channel period can range from the duration of a single data frame to the duration of the entire transmission process [98].

2.2 LOS MIMO CHANNEL PROBLEMS

Consider a LOS MIMO system, as shown in Figure 2.4, where the source and destination nodes experience a full LOS channel while the source and destination are separated by a long distance. In this condition, the channel is described as the well known keyhole channel as shown in Figure 2.5. In a keyhole channel, the resultant channel matrix does not contain a full rank matrix. Hence, a keyhole channel decreases the spatial diversity [7].

From this example, the LOS MIMO channel matrix is not full rank, and does not provide diversity for spatial multiplexing. Factors that will help to create a full rank matrix are:

[1]Channel coherence time is the time period in which the channel is considered as constant [90].

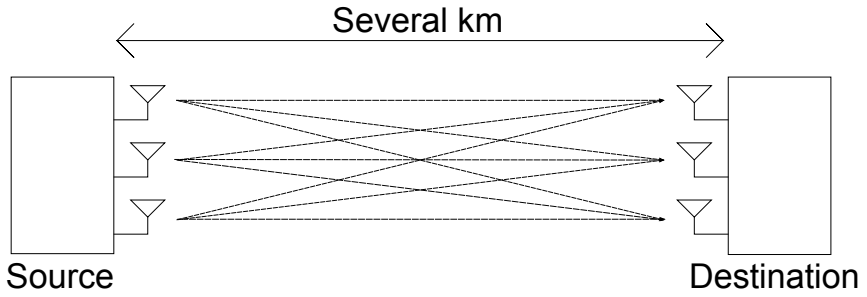

Figure 2.4 An example of an ideal LOS MIMO channel.

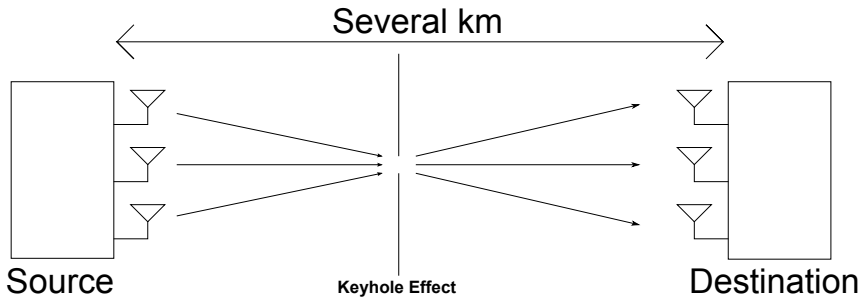

Figure 2.5 An example of a keyhole MIMO channel.

- having multipath scatterers;
- having non line of sight (NLOS) components;
- having large antenna spacings and angle spreads.

It is difficult or impossible to change the environment or to build very large antenna arrays. However, using the idea of relays to create more scatterers can help to solve this problem [19].

2.3 PRECODER AND WEIGHT VECTOR DESIGN

Precoders and weight vectors multiply signals before transmission and at the front end of receivers, respectively. If $\boldsymbol{x}$ is the data vector to be transmitted, then the transmitted signal is $\boldsymbol{M}\boldsymbol{x}$, where $\boldsymbol{M}$ is the precoder matrix, containing the precoder vectors. If $\boldsymbol{y}$ is the received signal, then $\boldsymbol{W}^{\dagger}\boldsymbol{y}$ is the output of the linear combiner, where $\boldsymbol{W}$ is the weight matrix, containing the weight vectors.

Precoders and weight matrices for the source relay and destination can be designed using different schemes. These schemes can be classified as fully optimal, near-optimal or pure ad-hoc. The fully optimal scheme uses optimal methods to design all the precoders and weight vectors that maximise the SINR of the relay MIMO system. However, the fully optimal scheme is very difficult to implement as it is usually impractical or even impossible. This is due to large computation required to compute the different precoder/weight vectors. Hence, we use a near-optimal scheme that uses optimal methods to compute the source precoder and destination weight vector. For the relay precoder and weight vector, the near-optimal scheme uses ad-hoc methods. Lastly the pure ad-hoc scheme uses ad-hoc methods to compute all of the precoders and weight vectors of the MIMO relay system.

In this thesis, we consider the "pure ad-hoc" and "near-optimal"to design the precoders and weight vectors.

2.3.1 Ad-hoc Schemes

Use ad-hoc methods. Precoder and weight vector design using ad-hoc approaches, such as singular value decomposition (SVD); minimum mean squared error (MMSE); signal to leakage and noise ratio (SLNR); and zero forcing (ZF) have lower computational complexity and are proven to give reasonable results in single transmit and receive scenario [97]. In our case, we want to design these different precoders and weight vectors in a relay environment and observe the overall e2e performance of the FD MIMO relay system.

2.3.1.1 Singular Value Decomposition

The singular value decomposition (SVD) is an important tool for MIMO radio communication. The SVD of a MIMO channel matrix is used to provide the transmitter and the receiver with the information to communicate over the available independent parallel channel modes [99].

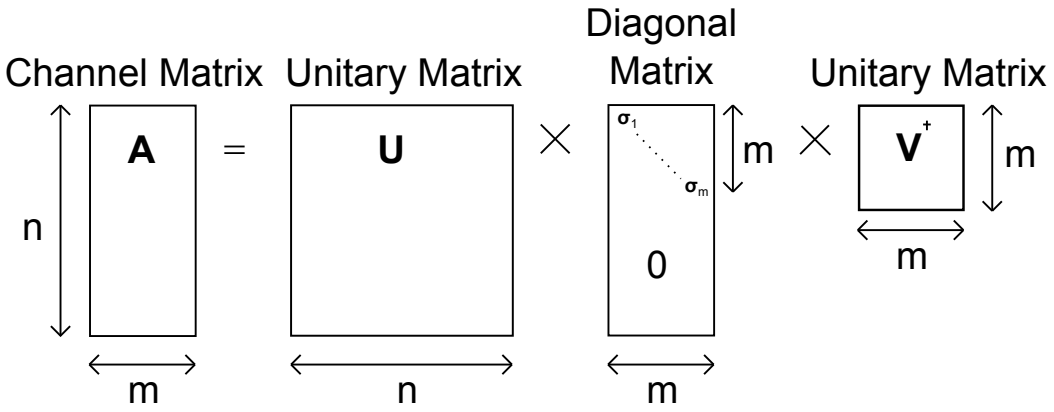

Figure 2.6 Diagrammatic interpretation of SVD.

An $n \times m$ channel matrix, $\boldsymbol{A}$, can be factored as [100]

$$\boldsymbol{A} = \boldsymbol{U}\boldsymbol{\Sigma}\boldsymbol{V}^{\dagger}, \tag{2.9}$$

where $\boldsymbol{U}$ is an $n \times n$ orthogonal matrix and $\boldsymbol{V}$ is an $m \times m$ orthogonal matrix. $\boldsymbol{\Sigma}$ is an $n \times m$ diagonal matrix given by [101, 102]

$$\boldsymbol{\Sigma} = \left(\begin{array}{ccc|c} \sigma_1 & \cdots & 0 & \\ \vdots & \ddots & \vdots & 0 \\ 0 & \cdots & \sigma_w & \\ \hline & 0 & & 0 \end{array}\right) \tag{2.10}$$

where $\sigma_1, \sigma_2, \cdots, \sigma_w$ are the singular values of σ and are ordered as $\sigma_1 \geqslant \sigma_2 \geqslant \cdots \geqslant \sigma_w > 0$. The term w is defined as $w = \min(n, m)$.

A diagrammatic interpretation of the SVD is illustrated in Figure 2.6. In this diagram, it is assumed that the number of rows (n) in the data matrix $\boldsymbol{A}$ is larger than the number of columns (m) [101].

The precoders and weight vectors are constructed by taking the leading Ł columns of the $\boldsymbol{U}$ and $\boldsymbol{V}$ matrix, respectively, where Ł represents the number of streams that are being transmitted. In this way, the signals are being transmitted through the strongest eigenchannels and this is the optimal method when there is no interference in the channel.

2.3.1.2 Zero Forcing Design

Unlike the SVD design, which focuses on transmitting the signals using the strongest links in the desired channel[2], zero forcing (ZF) aims to completely eliminate the interference between streams. However, ZF does not have any control on the power of the desired channel [7].

ZF in MIMO channels has been promoted not only for its low complexity versus nonlinear approaches but also for its good performance [62,63,103]. For example, ZF approaches in MIMO systems have a high performance in large signal to noise ratio (SNR) conditions [76]. However, ZF designs ignore the additive noise component at the receiver and these methods have antenna dimension constraints [104]. Another downside to ZF design is that high accuracy in the channel state information is essential for proper operation [75]. This is due to the numerically sensitive matrix inverses that are required to construct the ZF precoder and/or weight vectors.

Geometric View of Zero Forcing Precoder

Consider a linear precoder, $\boldsymbol{M}$, that lies in a signal space that is spanned by the vectors $\boldsymbol{u}_i$ where $\boldsymbol{u}_i$ is the incoming signal from the i^{th} of N users, i.e. $i = 1 \dots N$. This signal space represents the desired vector $\boldsymbol{u}_1$ and the interference vectors ($\boldsymbol{u}_i, i \neq 1$) that lie on the interference subspace, $\boldsymbol{S}$. If there were no interference vectors, then $\boldsymbol{M}$ is designed to be parallel with $\boldsymbol{u}_1$ to have maximum transmit channel power. However, in the case where there is interference in the channel, the ZF precoder is designed to null out these interferers. This is done by making $\boldsymbol{M}$ orthogonal to the interference subspace, $\boldsymbol{S}$. To do this, $\boldsymbol{M}$ is chosen to be the projection of $\boldsymbol{u}_1$ orthogonal to $\boldsymbol{S}$ [105]. This example is illustrated in Figure 2.7.

Zero Forcing Precoder Design

ZF precoding, which is shown in Figure 2.8, can be used to null the interference transmitted over the other channels (ie. the transmitter to the unwanted receiver, $\boldsymbol{H}_2$) [70]. In this diagram, the transmitter is equipped with N_T antennas and is transmitting signals to the desired receiver but wants to avoid transmitting signals to the unwanted receiver. The desired receiver and unwanted receiver have N_D and N_U receiving antennas, respectively. $\boldsymbol{H}_1$ and $\boldsymbol{H}_2$ are the desired channel and interference channel, respectively. The precoder, $\boldsymbol{M}$, is designed using the ZF method.

[2]The desired channel is the interference free channel that the receiver wants to receive.

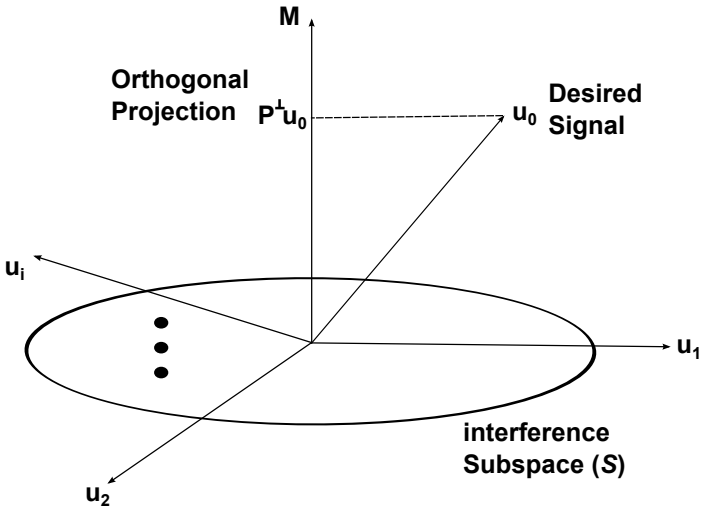

Figure 2.7 A geometric view of ZF precoder design.

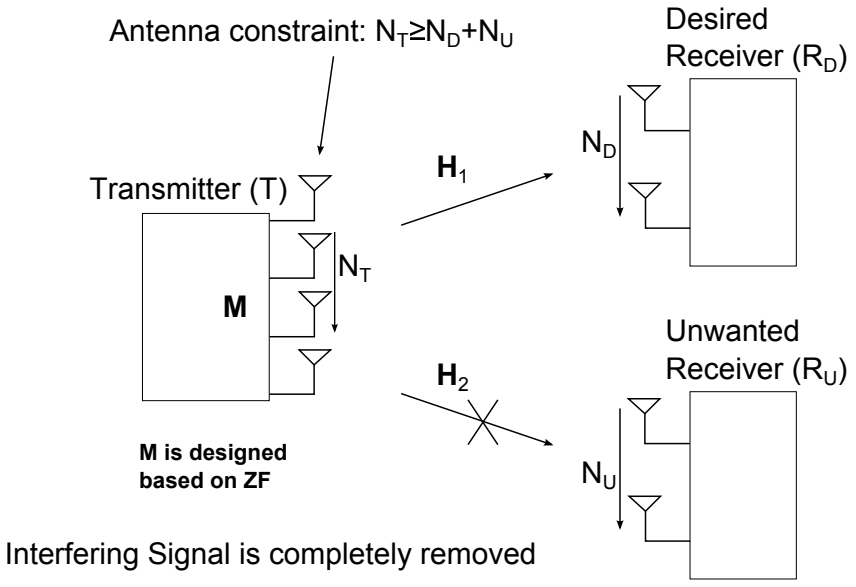

Figure 2.8 A block diagram of ZF at the relay transmitter.

Using SVD, we can decompose the interfering channel, such that we transmit the signals through the weakest eigenvectors of $\boldsymbol{H}_2$. In this way, the unwanted transmitter will not receive any signals that are transmitted from the transmitter. $\boldsymbol{H}_2$ can be decomposed as [106]

$$\begin{aligned} \boldsymbol{H}_2 &= \boldsymbol{U}\boldsymbol{\Sigma}\boldsymbol{V}^{\dagger}, \\ &= \boldsymbol{U}\boldsymbol{\Sigma}[\boldsymbol{V}^1\boldsymbol{V}^0]^{\dagger}, \end{aligned} \tag{2.11}$$

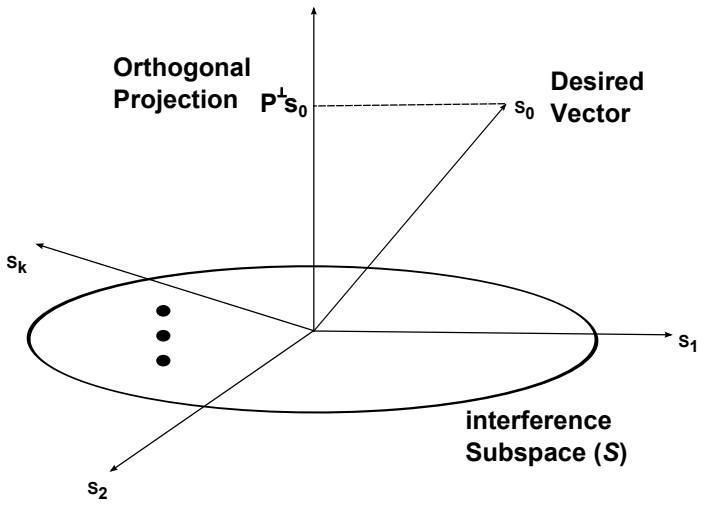

Figure 2.9 A block diagram of ZF at the relay transmitter.

where $\boldsymbol{U}$, $\boldsymbol{D}$, $\boldsymbol{V}^1$ and $\boldsymbol{V}^0$ have the dimensions $((N_D + N_U) \times (N_D + N_U))$, $((N_D + N_U) \times N_T)$, $(N_T \times N_D)$ and $(N_T \times N_U)$, respectively. From the dimensions of the singular vectors, it follows that the number of transmit antennas, N_T, needs to be greater than the sum of the receive antennas (i.e. $N_D + N_U$). The matrix, $\boldsymbol{V}^1$, contains the leading N_D columns of the right singular vectors and $\boldsymbol{V}^0$ contains the last N_U columns of the right singular vectors. The matrix, $\boldsymbol{V}^0$, forms an orthogonal basis for the null space of $\boldsymbol{H}_2$ [62]. The precoding matrix $\boldsymbol{W}$ is constructed from taking the last L columns of $\boldsymbol{V}^0$, where L represents the number of transmitted streams.

Geometric View of Zero Forcing Weight Vector Design

Consider a receiver using ZF to decode a desired transmitter in the presence of an interfering source. The ZF weight vector design is similar to the ZF precoder design, where it is designed to be the projection $\boldsymbol{P}^{\perp}\boldsymbol{s}_0$ of $\boldsymbol{s}_0$ that is orthogonal to the interference subspace $\boldsymbol{S}$, [105]. Here, $\boldsymbol{s}_i$ is the received vector from user i, where $i = 1, \ldots, N$. This is illustrated in Figure 2.9.

Zero Forcing Weight Vector Design

The ZF weight vector design can be obtained from the multiuser MIMO systems literature [71, 72, 107, 108]. The constraint for designing a ZF weight vector, as illustrated in Figure 2.10, is that the number of receive antennas (N_R) must be greater than or equal to the sum of the desired user's transmitter antennas (N_D) and the unwanted user's transmitter antennas (N_U)

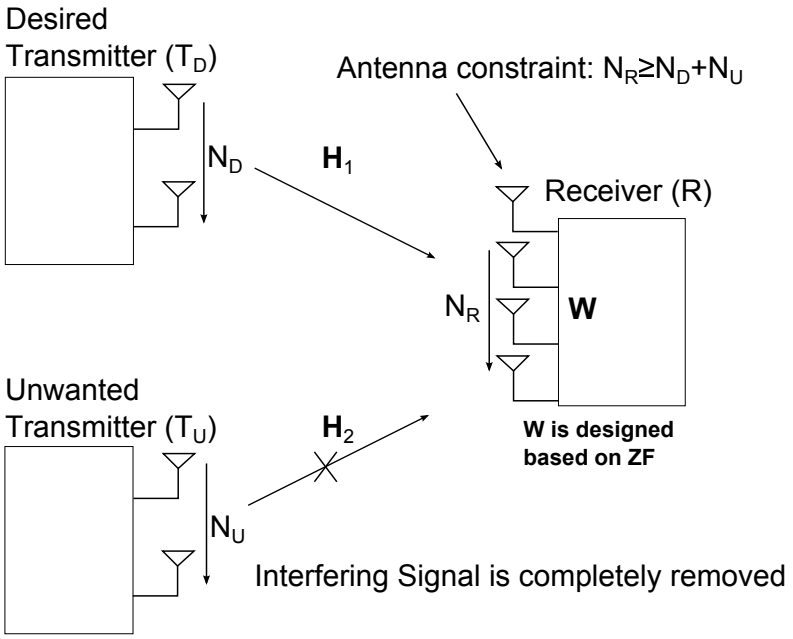

Figure 2.10 A block diagram of ZF at the receiver.

(i.e. $N_R \geq N_D + N_U$).

Consider Figure 2.10, where there are two transmitters and one receiver. The receiver, R, wants to receive the signal that is transmitted from the desired transmitter, T_D but does not want to receive any signals that are from the unwanted transmitter, T_U. Hence, the ZF weight vector can be designed such that R only receives the signals that are transmitted from T_D. The ZF weight vector is given by [76]

$$\boldsymbol{W}_{ZF} = (\boldsymbol{H}_T^{\dagger}\boldsymbol{H}_T)^{-1}\boldsymbol{H}_T^{\dagger}, \tag{2.12}$$

where the total matrix, $\boldsymbol{H}_T$, contains both the T_D to R channel, $\boldsymbol{H}_1$, and the T_U to R channel, $\boldsymbol{H}_2$, such that $\boldsymbol{H}_T = [\boldsymbol{H}_1, \boldsymbol{H}_2]$. The dimensions of $\boldsymbol{H}_1$ and $\boldsymbol{H}_2$ are $N_R \times N_D$ and $N_R \times N_U$, respectively. Hence, $\boldsymbol{H}_T$ has the dimension $N_R \times (N_D + N_U)$.

2.3.1.3 Relay Weight Vector Design using MMSE

The ZF design completely removes interference. However, it does not take into account the noise in the receive signal. An alternative design is the minimum mean squared error (MMSE) receiver, as it also takes into account the noise of the received signal by minimising the average

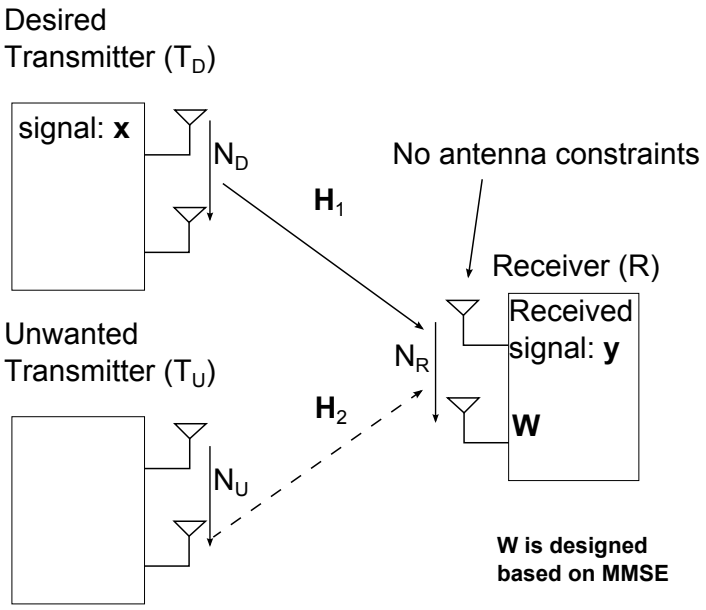

Figure 2.11 A block diagram of MMSE at the relay receiver.

squared error of the detected signals [7].

The MMSE receiver is widely used for its low complexity and its ability to suppress both interference and noise at the receiver [109]. The MMSE receiver, as shown in Figure 2.11, can be implemented at the receiver end to increase the error rate performance [24].

The MMSE expression is given by [24]

$$\boldsymbol{W}_{\text{MMSE}} = (\boldsymbol{H}_1\boldsymbol{H}_1^{\dagger} + \boldsymbol{H}_2\boldsymbol{H}_2^{\dagger} + \boldsymbol{I})^{-1}\boldsymbol{H}_1, \tag{2.13}$$

where matrices $\boldsymbol{H}_1$ and $\boldsymbol{H}_2$ represent the channel from T_D to R and the channel from T_U to R, respectively. In (2.13) it is assumed that $\mathrm{E}\{||n_i||^2 = 1\}$, where n_i is the AWGN at the i^{th} receive antenna. It is also assumed that the interfering signals have unit power.

The mathematical expression for the MMSE weight vector in (2.13) and the ZF weight vector in (2.12) are very similar, with the only difference being the extra covariance term in the MMSE equation. This extra covariance term is due to the fact that the MMSE solution considers the noise at the receiver as well as the interference, whereas ZF only considers the channel over which the signals are being transmitted.

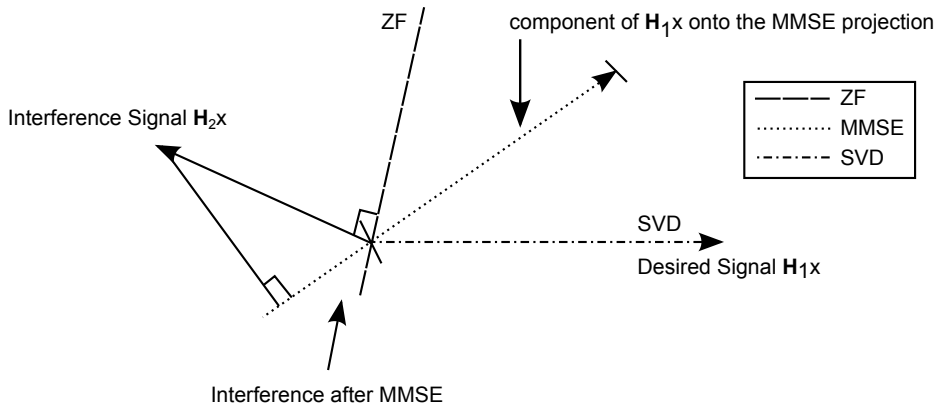

Figure 2.12 A block diagram of MMSE at the relay receiver.

The geometrical representation of the MMSE weight vector is shown in Figure 2.12, where the desired signal is being distorted by the interference signal [7]. It is clearly seen that the MMSE solution lies in between the ZF and SVD solutions. This is due to the fact that the MMSE solution reduces the interference, whereas the ZF solution completely removes the interference. At the same time, the MMSE solution will also distort the desired signal, which does not happen with the SVD approach.

2.3.1.4 Relay Precoding using Maximum SLNR

Consider a transmitter using SLNR to precode a signal such that it increases the signal to the desired user while reducing the transmitted signal to the undesired users. This is shown in the block diagram in Figure 2.13. The transmitter, T, transmits a signal, $\boldsymbol{x}$, to the desired receiver, R_D, but at the same time, this signal will also be received by the unwanted receiver, R_U. This received signal at R_U is considered as signal leakage [110] and is a measure of how much signal power leaks into the unwanted receiver [66]. The transmitter precoder, $\boldsymbol{M}$, will be selected based on maximising the signal to leakage and noise ratio (SLNR) of T.

The SLNR is defined as the ratio between the power of the desired signal and the power of the leakage and noise signal and it is defined as [66].

$$\text{SLNR} = \frac{\text{E}\{\|\boldsymbol{H}_1\boldsymbol{M}\boldsymbol{x}\|^2\}}{N_D + \text{E}\{\|\boldsymbol{H}_2\boldsymbol{M}\boldsymbol{x}\|^2\}}, \tag{2.14}$$

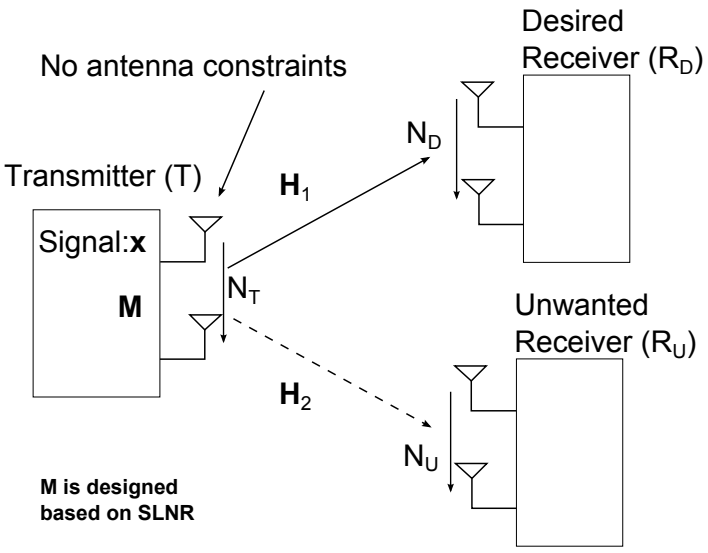

Figure 2.13 A block diagram of the SLNR approach.

where N_D is the number of the antennas at R_D and the noise (n_i at receiver i of R_D) is assumed to satisfy $\mathrm{E}\{|n_i|^2\} = 1$. $\boldsymbol{H}_1$ and $\boldsymbol{H}_2$ are the channels from the T to R_D and from T to R_U, respectively. $\boldsymbol{M}$ is the precoder that is designed to maximise the SLNR and $\boldsymbol{x}$ is the signal at the transmitter. The solution for $\boldsymbol{M}$ is computed using the Rayleigh Ritz (RR) method[3]. From (2.14), the SLNR can be written as

$$\mathrm{SLNR} = \frac{\mathrm{trace}\{\boldsymbol{H}_1\boldsymbol{M}\boldsymbol{I}\boldsymbol{M}^\dagger\boldsymbol{H}_1^\dagger\}}{N_D + \mathrm{trace}\{\boldsymbol{H}_2\boldsymbol{M}\boldsymbol{I}\boldsymbol{M}^\dagger\boldsymbol{H}_2^\dagger\}}, \tag{2.15}$$

where $\boldsymbol{I} = \mathrm{E}\{\boldsymbol{x}\boldsymbol{x}^\dagger\}$. Using the properties of trace ($\mathrm{trace}\{\boldsymbol{A}\boldsymbol{B}\boldsymbol{B}^\dagger\boldsymbol{A}^\dagger\} = \mathrm{trace}\{\boldsymbol{B}^\dagger\boldsymbol{A}^\dagger\boldsymbol{A}\boldsymbol{B}\}$), (2.15) can be written as

$$\mathrm{SLNR} = \frac{\mathrm{trace}\{\boldsymbol{M}^\dagger\boldsymbol{H}_1^\dagger\boldsymbol{H}_1\boldsymbol{M}\}}{N_D + \mathrm{trace}\{\boldsymbol{M}^\dagger\boldsymbol{H}_2^\dagger\boldsymbol{H}_2\boldsymbol{M}\}}. \tag{2.16}$$

To compute the solution for $\boldsymbol{M}$, the SLNR equation is converted to have a RR structure. Hence, (2.16) is rewritten as

$$\begin{aligned}\mathrm{SLNR} &= \frac{\mathrm{trace}\{\boldsymbol{M}^\dagger\boldsymbol{H}_1^\dagger\boldsymbol{H}_1\boldsymbol{M}\}}{N_D\frac{\mathrm{trace}\{\boldsymbol{M}^\dagger\boldsymbol{M}\}}{\mathrm{trace}\{\boldsymbol{M}^\dagger\boldsymbol{M}\}} + \mathrm{trace}\{\boldsymbol{M}^\dagger\boldsymbol{H}_2^\dagger\boldsymbol{H}_2\boldsymbol{M}\}}, \\ &= \frac{\mathrm{trace}\{\boldsymbol{M}^\dagger\boldsymbol{H}_1^\dagger\boldsymbol{H}_1\boldsymbol{M}\}}{\mathrm{trace}\{\boldsymbol{M}^\dagger(\frac{N_D}{\mathrm{trace}\{\boldsymbol{M}^\dagger\boldsymbol{M}\}}\boldsymbol{I} + \boldsymbol{H}_2^\dagger\boldsymbol{H}_2)\boldsymbol{M}\}}.\end{aligned} \tag{2.17}$$

[3]The full explanation of RR is in Section 2.3.2.1

If $\boldsymbol{M}$ is orthogonal then $\text{trace}\{\boldsymbol{M}^\dagger\boldsymbol{M}\} = Ł$, where Ł is the number of streams, i.e., the number of columns of $\boldsymbol{M}$. Hence

$$\begin{aligned}\text{SLNR} &= \frac{\text{trace}\{\boldsymbol{M}^\dagger\boldsymbol{H}_1^\dagger\boldsymbol{H}_1\boldsymbol{M}\}}{\text{trace}\{\boldsymbol{M}^\dagger(\frac{N_D}{Ł}\boldsymbol{I} + \boldsymbol{H}_2^\dagger\boldsymbol{H}_2)\boldsymbol{M}\}}, \\ &= \frac{\text{trace}\{\boldsymbol{M}^\dagger\boldsymbol{A}\boldsymbol{M}\}}{\text{trace}\{\boldsymbol{M}^\dagger\boldsymbol{B}\boldsymbol{M}\}}. \end{aligned} \tag{2.18}$$

The established solution for maximising the SLNR [66] is to use the Ł largest eigenvectors of

$$\boldsymbol{B}^{-1}\boldsymbol{A} = (\frac{N_D}{Ł}\boldsymbol{I} + \boldsymbol{H}_2^\dagger\boldsymbol{H}_2)^{-1}\boldsymbol{H}_1^\dagger\boldsymbol{H}_1. \tag{2.19}$$

Hence, $\boldsymbol{M}$ is computed by taking the Ł largest eigenvectors of $(\frac{N_D}{Ł}\boldsymbol{I} + \boldsymbol{H}_2^\dagger\boldsymbol{H}_2)^{-1}\boldsymbol{H}_1^\dagger\boldsymbol{H}_1$.

2.3.2 Near-optimal Scheme

Optimisation is when the best solution for a particular problem is used for the parameters given. This involves using the constraints imposed on the parameters and finding the minimums and maximums of the objective function [111].

However, the function is so complex with numerous variables, finding the optimum value for every variable at one time proved to be nearly impossible. One way to solve this problem is to fix and estimate some variables. This allows the remaining variables to be optimised. Then these values are fixed and the original variables are optimised. This is an iterative process until the best overall optimisation is achieved. Initially we used a MATLAB function called "*fmincon*" to compute all the precoder and weight vector that maximises the SINR equation. However, when the results were calculated, we found out that the power of the precoder and weight vectors needed to be constrained in order to compare with the results from the ad-hoc designs. When we set the power constrain into the *fmincon*, the optimisd result is very similar or exactly the same as the ad-hoc design solutions.

In this work we use the RR method to partly optimise the signal to interference and noise ratio (SINR) of the MIMO relay system. This is done by using an iterative RR method to optimise the source precoder and destination weight vector and the relay precoder and weight vector are

designed using ad-hoc approaches.

2.3.2.1 Rayleigh-Ritz Method in Optimisation

The Rayleigh-Ritz (RR) method, which is also known as the Rayleigh Quotient, is an optimisation scheme that is based on eigenvector decomposition [100]. RR uses the eigenvalues and eigenvectors of Hermitian matrices. As the eigenvalues of a Hermitian matrix are real, they can be labeled according to increasing size [112]

$$\lambda_{\mathbf{min}} = \lambda_1 \leqslant \lambda_2 \leqslant \cdots \leqslant \lambda_{n-1} \leqslant \lambda_n = \lambda_{\mathbf{max}}. \tag{2.20}$$

The smallest and largest eigenvalues are characterised as the solution to a constrained minimum and maximum problem [112]. The method of RR considers optimising quadratic functions such as

$$\boldsymbol{Q} = \frac{\boldsymbol{x}^\dagger \boldsymbol{A} \boldsymbol{x}}{\boldsymbol{x}^\dagger \boldsymbol{x}}, \tag{2.21}$$

where $\boldsymbol{x}$ is the vector that we can select and $\boldsymbol{Q}$ is to be maximised or minimised. $\boldsymbol{Q}$ is then maximised or minimised by choosing $\boldsymbol{x}$ as the maximum or minimum eigenvector of $\boldsymbol{A}$ [112]. This method is also used to find the solution for SLNR, where it wants to maximise the signal power over the leakage power.

The RR method can also be extended to matrix quadratic forms of the form

$$\boldsymbol{Q} = \frac{\text{trace}\{\boldsymbol{X}^\dagger \boldsymbol{A} \boldsymbol{X}\}}{\text{trace}\{\boldsymbol{X}^\dagger \boldsymbol{X}\}}, \tag{2.22}$$

where the matrix $\boldsymbol{X}$ has $m \leqslant n$ columns and $\boldsymbol{A}$ is an $n \times n$ matrix. Here, the solution for $\boldsymbol{Q}$ is near-optimal. However, it very close to optimal, and is given by the leading m eigenvectors of A (to increase $\boldsymbol{Q}$) and the lowest m eigenvectors of A (to decrease $\boldsymbol{Q}$).

2.4 POWER CONSTRAINT FOR PRECODERS AND WEIGHT VECTORS USING FROBENIUS NORMALISATION

In this work, the Frobenius norm, which is also known as the Hilbert Schmidt norm, is widely used to compute the total power of a vector signal and also to constrain the power of precoder and weight vectors. In this situation, we have for a vector, $\boldsymbol{v}$, the norm given by,

$$||\boldsymbol{v}||_F = \sqrt{\boldsymbol{v}^\dagger \boldsymbol{v}} = \sqrt{\text{trace}\{\boldsymbol{v}\boldsymbol{v}^\dagger\}}. \tag{2.23}$$

2.5 SUMMARY

In this chapter, we have explained the structure of the MIMO channel and the two different schemes (ad-hoc and near-optimal) for designing the precoder and weight vectors. The channel model is constructed by using the Rician channel model that includes the LOS component and the NLOS component.

The precoder and weight vectors are designed using near-optimal and ad-hoc schemes. The near-optimal scheme is built on RR and the ad-hoc schemes consist of SLNR, SVD, MMSE and ZF. Our aim is to use these different ad-hoc methods and select the solution that gives the best end to end (e2e) SINR for our relay MIMO model. Then to compare the performance between the best ad-hoc and near-optimal methods.

Chapter 3

MIMO TRANSMIT AND RECEIVE RELAY MODEL WITH NO DELAY

In this chapter, we provide an analysis of the SINR of a two path MIMO relay model that assumes zero processing delay. This is an extension work of [19]. Our analysis shows that the self interference (SI) from the relay carries a signal that is identical to within a scale factor to the desired signal that is being transmitted from the source. Hence, any processing to remove or reduce SI does not seem to be worthwhile, as the SI is not distorting the desired signal. This motivates the work of Chapter 4 where a more representative MIMO relay model is developed to incorporate the effect of a delay.

3.1 MIMO RELAY MODEL

Consider the MIMO relay channel system model shown in Figure 3.1. The source, S, is transmitting to the relay, R, through the source to relay channel, $\boldsymbol{H}_{SR}$, and to the destination, D, through the source to destination channel $\boldsymbol{H}_{SD}$. The source is equipped with N_S transmit antennas and the relay is equipped with N_{RR} receiving and N_{RT} transmitting antennas. The destination receives the transmitted signal from the source and relay with N_D antennas through the channels $\boldsymbol{H}_{SD}$ and $\boldsymbol{H}_{RD}$, respectively. $\boldsymbol{H}_{RD}$ is the channel from the relay to the destination.

In this model, the relay is receiving and transmitting instantaneously in full duplex (FD) mode and SI occurs at the relay receiver through the channel $\boldsymbol{H}_{RR}$. In order to reduce SI and boost the end to end (e2e) signal to interference plus noise ratio (SINR), source precoders, $\boldsymbol{M}_S$, relay precoder, $\boldsymbol{M}_R$, relay weight vectors, $\boldsymbol{W}_R$ and destination weight vector, $\boldsymbol{W}_D$, are considered in

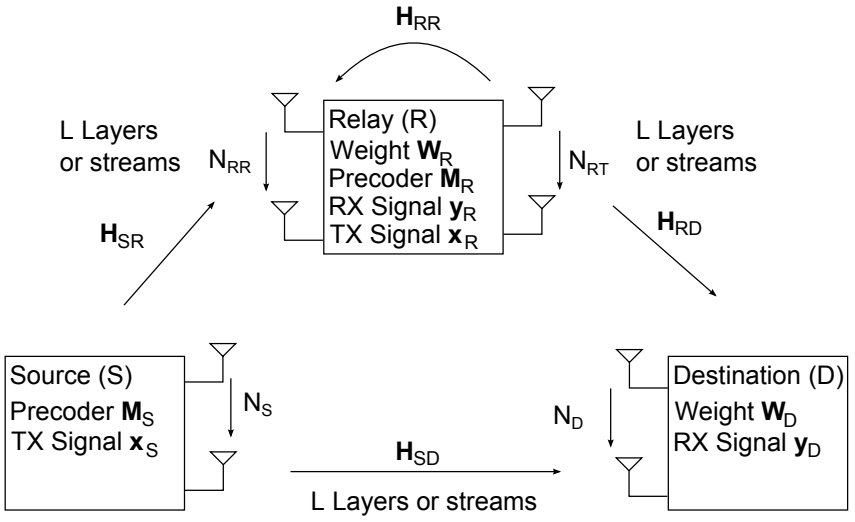

Figure 3.1 A block diagram for a relay MIMO wireless communications system.

this MIMO relay system.

3.2 MIMO RELAY MODEL SYSTEM EQUATIONS

Consider the MIMO relay scenario discussed in [19]. In this study, a basic MIMO system was constructed to simulate the effects of the relay MIMO channel. However, they ignored the effects of relay SI which is an essential aspect of a FD relay. In our MIMO FD relay system, we used the same design as in [19] and added the effects of SI at the relay through the channel, $\boldsymbol{H}_{RR}$, as shown at the top of Figure 3.1.

The overall received signal at the destination is the sum of the direct path and the relay forwarded signal. At the destination of the relay MIMO system, the output of the linear combiner is

$$\boldsymbol{y}_D = \boldsymbol{W}_D^{\dagger}(\boldsymbol{H}_{SD}\boldsymbol{x}_S + \boldsymbol{H}_{RD}\boldsymbol{x}_R + \boldsymbol{n}_D), \tag{3.1}$$

where $\boldsymbol{W}_D \in \mathbb{C}^{\mathrm{N}_D \times \mathrm{Ł}}$ is the destination weight vector. $\boldsymbol{x}_S \in \mathbb{C}^{\mathrm{N}_S \times 1}$ and $\boldsymbol{x}_R \in \mathbb{C}^{\mathrm{N}_{RT} \times 1}$ are the signals transmitted from the source and relay, respectively. $\boldsymbol{H}_{SD} \in \mathbb{C}^{\mathrm{N}_D \times \mathrm{N}_S}$ and $\boldsymbol{H}_{RD} \in \mathbb{C}^{\mathrm{N}_D \times \mathrm{N}_{RT}}$ are the source to destination and relay to destination channels, respectively. $\boldsymbol{n}_D \in \mathbb{C}^{\mathrm{N}_D \times 1}$ is the destination noise vector. Ł represents the number of streams. The transmitted

source signal is given by

$$\boldsymbol{x}_S = \boldsymbol{M}_S \boldsymbol{d}_S, \tag{3.2}$$

where $\boldsymbol{M}_S \in \mathbb{C}^{\mathrm{N}_S \times \mathrm{L}}$ is the source precoder. $\boldsymbol{d}_S \in \mathbb{C}^{\mathrm{L} \times 1}$ is the source signal and it is assumed to have unit power, i.e. $\mathrm{E}\{||\boldsymbol{d}_S||^2\} = 1$.

At the output of the linear combiner of the relay, the signal is given by

$$\boldsymbol{y}_R = \boldsymbol{W}_R^{\dagger}(\boldsymbol{H}_{SR}\boldsymbol{x}_S + \boldsymbol{H}_{RR}\boldsymbol{x}_R + \boldsymbol{n}_R), \tag{3.3}$$

where $\boldsymbol{H}_{RR} \in \mathbb{C}^{\mathrm{N}_{RR} \times \mathrm{N}_{RT}}$ is the relay to relay channel and $\boldsymbol{n}_R \in \mathbb{C}^{\mathrm{N}_R \times 1}$ is the relay noise vector. The transmitted signal at the relay is given by

$$\boldsymbol{x}_R = \boldsymbol{M}_R \boldsymbol{y}_R. \tag{3.4}$$

Substituting $\boldsymbol{y}_R$ from (3.3) in (3.4) gives

$$\boldsymbol{x}_R = \boldsymbol{M}_R \boldsymbol{W}_R^{\dagger}(\boldsymbol{H}_{SR}\boldsymbol{x}_S + \boldsymbol{H}_{RR}\boldsymbol{x}_R + \boldsymbol{n}_R). \tag{3.5}$$

On separating terms containing $\boldsymbol{x}_R$, the equation is rearranged to

$$\begin{aligned}(\boldsymbol{I}_{N_{RT}} - \boldsymbol{M}_R \boldsymbol{W}_R^{\dagger}\boldsymbol{H}_{RR})\boldsymbol{x}_R &= \boldsymbol{M}_R \boldsymbol{W}_R^{\dagger}(\boldsymbol{H}_{SR}\boldsymbol{x}_S + \boldsymbol{n}_R), \\ \boldsymbol{x}_R &= (\boldsymbol{I}_{N_{RT}} - \boldsymbol{M}_R \boldsymbol{W}_R^{\dagger}\boldsymbol{H}_{RR})^{-1}\boldsymbol{M}_R \boldsymbol{W}_R^{\dagger}(\boldsymbol{H}_{SR}\boldsymbol{x}_S + \boldsymbol{n}_R),\end{aligned} \tag{3.6}$$

where $\boldsymbol{I}_{N_{RT}}$ is an $N_{RT} \times N_{RT}$ identity matrix. Defining $\boldsymbol{F}_R = \boldsymbol{M}_R \boldsymbol{W}_R^{\dagger}$, $\boldsymbol{x}_R$ can be simplified to give

$$\boldsymbol{x}_R = (\boldsymbol{I}_{N_{RT}} - \boldsymbol{F}_R \boldsymbol{H}_{RR})^{-1}\boldsymbol{F}_R(\boldsymbol{H}_{SR}\boldsymbol{x}_S + \boldsymbol{n}_R). \tag{3.7}$$

Substituting (3.7) into (3.1) gives the total signal after precoding at the destination.

$$\boldsymbol{y}_D = \boldsymbol{W}_D^{\dagger}\{\boldsymbol{H}_{SD}\boldsymbol{x}_S + \boldsymbol{H}_{RD}(\boldsymbol{I}_{N_{RT}} - \boldsymbol{F}_R \boldsymbol{H}_{RR})^{-1}\boldsymbol{F}_R(\boldsymbol{H}_{SR}\boldsymbol{x}_S + \boldsymbol{n}_R) + \boldsymbol{n}_D\}. \tag{3.8}$$

The overall signal can be rearranged to be represented as the sum of the desired signal, and the

interference plus noise term at the destination. This equation is shown as

$$\begin{aligned}\boldsymbol{y}_D = \boldsymbol{W}_D^{\dagger} \big\{ &[\boldsymbol{H}_{SD} + \boldsymbol{H}_{RD}(\boldsymbol{I}_{N_{RT}} - \boldsymbol{F}_R\boldsymbol{H}_{RR})^{-1}\boldsymbol{F}_R\boldsymbol{H}_{SR}]\boldsymbol{x}_S \\ &+\boldsymbol{H}_{RD}(\boldsymbol{I}_{N_{RT}} - \boldsymbol{F}_R\boldsymbol{H}_{RR})^{-1}\boldsymbol{F}_R\boldsymbol{n}_R + \boldsymbol{n}_D \big\}. \end{aligned} \tag{3.9}$$

By setting $\boldsymbol{H}_{RD}(\boldsymbol{I}_{RT} - \boldsymbol{F}_R\boldsymbol{H}_{RR})^{-1}\boldsymbol{F}_R = \boldsymbol{G}$, (3.9) is simplified to

$$\boldsymbol{y}_D = \boldsymbol{W}_D^{\dagger}\{(\boldsymbol{H}_{SD} + \boldsymbol{G}\boldsymbol{H}_{SR})\boldsymbol{x}_S + (\boldsymbol{G}\boldsymbol{n}_R + \boldsymbol{n}_D)\}. \tag{3.10}$$

In the final equation of the MIMO relay system shown in (3.10), the effect of SI has essentially been removed by combining the transmit and receive relay signals as shown in (3.6). As can be seen in (3.10), the source signal, $\boldsymbol{x}_S$, is received at the destination through the effective channel, $\boldsymbol{H}_{SD} + \boldsymbol{G}\boldsymbol{H}_{SR}$, with no interference. The relay does cause noise inflation via the $\boldsymbol{G}\boldsymbol{n}_R$ term but no interference terms are present. This means that relay processing designed at removing or reducing SI is unnecessary. This MIMO relay scenario is unrealistic for modeling the effects of SI as it has ingored the effect of the delay introduced at the relay. As a result of this, we need to include the effect of a relay processing delay into the system model. When there is a processing delay of τ, as shown in Figure 3.2, the relay receiver will receive two sets of signals that are defined as

$$\boldsymbol{y}_R(t) = \boldsymbol{W}_R^{\dagger}(\boldsymbol{H}_{SR}\boldsymbol{x}_S(t) + \boldsymbol{n}_R(t)), \tag{3.11}$$

and

$$\begin{aligned}\bar{\boldsymbol{y}}_R(t) &= \boldsymbol{W}_R^{\dagger}\boldsymbol{H}_{RR}\boldsymbol{x}_R(t), \\ \boldsymbol{x}_R(t) &= \boldsymbol{M}_R\boldsymbol{W}_R^{\dagger}(\boldsymbol{H}_{SR}\boldsymbol{x}_S(t-\tau) + \boldsymbol{H}_{RR}\boldsymbol{x}_R(t-\tau) + \boldsymbol{n}_R(t-\tau)). \end{aligned} \tag{3.12}$$

As seen from (3.11) and (3.12), there will be a time difference between the signal, $\boldsymbol{x}_S(t)$, carried in $\boldsymbol{y}_R(t)$ and $\boldsymbol{x}_S(t-\tau)$ carried in the SI link. Since there is a time difference between these two signals, they will interfere with each other, decreasing the performance of the MIMO system. This is a more appropriate design for simulating the SI effect as now it will degrade the MIMO relay system in a more realistic fashion. More complex processing techniques would use temporal

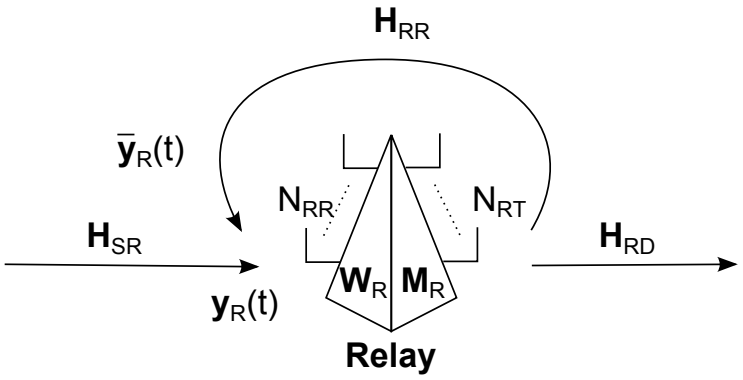

Figure 3.2 The effect of introducing a processing relay delay.

processing and use both $\boldsymbol{x}_S(t)$ and $\boldsymbol{x}_S(t-\tau)$ in the decoding process. However, we consider simple schemes where the delayed signals are treated as interference.

As a result of this, the destination node will receive two sets of information that are not synchronised. This will increase the complexity of the MIMO relay system as further processing is required to recover the signal at the destination. Also there is already a complicated SI scenario at the relay that needs to be solved and extra complexity will make the relay system even harder to analyse. Hence, the complexity of the MIMO relay system can be reduced by changing from a two path system to a one path system, where the source to destination link is discarded. This one path MIMO relay system which includes the effects of a relay processing delay will be described in more detail in Chapter 4.

3.3 SUMMARY

In this chapter, we showed, through the use of analysis, that SI is non-detrimental when the relay is receiving and transmitting instantaneously. The reason for this is that the transmitted signal is the same (within a scaling factor) as the received signal at the relay. This implies that doing relay processing to remove SI is unlikely to increase the e2e performance. In other words, this MIMO relay system is an artificial system to model as in practice there will always be a delay between the receive stage and the transmit stage at the relay node. As a result of this delay, the signal transmitted from the relay will not be the same as the signal received at any given instant in time. Hence, these two signals will interfere with each other and reduce the

quality of the signal at the relay transmitter. In order to model this SI effect, we construct a one path MIMO relay system with the effects of a relay processing delay which will be proposed in Chapter 4.

Chapter 4

MIMO TRANSMIT AND RECEIVE MODEL WITH A DELAY AT THE RELAY

In Chapter 3, we derived the two path MIMO relay model equations and discussed the influence of SI when the relay processing delay has been ignored. We also proposed a one path MIMO relay model to simulate the SI at the relay to reduce the complexity of the MIMO relay model.

In this chapter, using the one path MIMO model, the precoder and weight vector designs are described in Section 4.1, the derivation of the SINR equations is shown in Section 4.2 and the relay power constraint is shown in Section 4.3. We implement different ad-hoc methods in Section 4.4.1 as well as a near-optimal method using Rayleigh-Ritz (RR) in Section 4.4.2. At the end of this chapter, the simulated results from this MIMO relay model are presented in Section 4.5

4.1 MIMO RELAY MODEL

Consider a one path communication MIMO relay system, shown in Figure 4.1, where there is a delay due to the processing of the relay.

As there is a processing delay between the receive and transmit sides of the relay, the transmitted signal from the relay will not be identical to the signal that is received from the source. Since the relay receives two different signals from the source and the feedback channel, we consider the latter one as interference.

The precoders and weight vectors are designed using near-optimal and ad-hoc schemes as shown in Table 4.1. The near-optimal scheme is implemented using beamforming methods to calculate

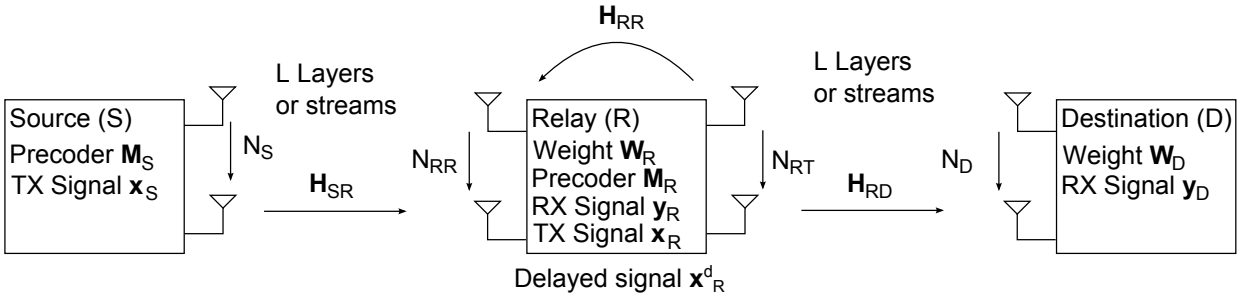

Figure 4.1 MIMO relay model.

Table 4.1 The different processing schemes for the precoders & weight vectors for the MIMO system

Schemes	Relay (R)	Source (S) & Destination (D)	Methods
Near-optimal	Ad-hoc Solution	Optimal Solution	Beamforming, (RR)
Ad-hoc	Ad-hoc Solution	Ad-hoc Solution	Beamforming

the relay precoder and weight vector, then the source precoder and destination weight vector are calculated using RR methods. The ad-hoc scheme uses different beamforming methods to compute the precoders and weight vectors of the source, relay and destination nodes. The source precoder is computed using singular value decomposition (SVD). The destination weight vector is computed using minimum-mean-squared-error (MMSE) and SVD. The relay precoder is designed using signal to leakage and noise ratio (SLNR), zero forcing (ZF) and SVD. The relay weight vector is designed using MMSE, ZF and SVD. The SVD method is used as it provides the optimal solution when there is no interference. In the situation, where there is SI, SVD can be used to provide a lower bound to compare with other precoder and weight vector techniques. Such precoder and weight vector designs at the relay are the MMSE weight vector and SLNR precoder as they can be used to increase the signal and also decrease SI. However, these two techniques will not completely remove SI. Although, ZF precoder and weight vector designs can completely remove SI, they do not increase the signal component. Hence, by implementing the different techniques as summarised in Table 4.2, we can determine which of these methods will provide the largest e2e SINR.

Table 4.2 The different beamforming methods that are used in the ad-hoc schemes

Source Precoder ($\boldsymbol{M}_S$)	Relay Weight Vector ($\boldsymbol{W}_R$)	Relay Precoder ($\boldsymbol{M}_R$)	Destination Weight Vector ($\boldsymbol{W}_D$)
SVD	SVD	SVD	SVD
	MMSE	SLNR	MMSE
	ZF	ZF	

4.2 MIMO RELAY MODEL SYSTEM EQUATIONS

Consider the MIMO relay scenario shown in Figure 4.1. At the destination, the received signal after processing is

$$\boldsymbol{y}_D = \boldsymbol{W}_D^{\dagger}(\boldsymbol{H}_{RD}\boldsymbol{x}_R + \boldsymbol{n}_D), \tag{4.1}$$

where $\boldsymbol{W}_D \in \mathbb{C}^{\mathrm{N}_D \times \mathrm{Ł}}$ is the destination weight vector with $||\boldsymbol{W}_D||_F = 1$, $\boldsymbol{x}_R$ is the relay signal with $\mathrm{E}\{||\boldsymbol{x}_R||_F^2\} = 1$, $\boldsymbol{H}_{RD} \in \mathbb{C}^{\mathrm{N}_D \times \mathrm{N}_{RT}}$ is the relay to destination channel, $\boldsymbol{n}_D \in \mathbb{C}^{\mathrm{Ł} \times 1}$ is the destination noise vector and the elements of $\boldsymbol{n}_D$ are assumed to be $\mathcal{CN}(0,1)$ without loss of generality. Ł is the number of data streams. The relay input after processing is

$$\boldsymbol{y}_R = \boldsymbol{W}_R^{\dagger}(\boldsymbol{H}_{SR}\boldsymbol{x}_S + \boldsymbol{H}_{RR}\boldsymbol{x}_R^d + \boldsymbol{n}_R), \tag{4.2}$$

where $\boldsymbol{H}_{SR} \in \mathbb{C}^{\mathrm{N}_{RR} \times \mathrm{N}_S}$ and $\boldsymbol{H}_{RR} \in \mathbb{C}^{\mathrm{N}_{RR} \times \mathrm{N}_{RT}}$ are the source to relay and relay to relay channels, respectively. The relay noise vector is given by $\boldsymbol{n}_R \in \mathbb{C}^{\mathrm{N}_{RR} \times 1}$ and the elements of $\boldsymbol{n}_R$ are assumed to be $\mathcal{CN}(0,1)$ without loss of generality. $\boldsymbol{x}_R^d$ is the delayed relay signal. $\boldsymbol{W}_R \in \mathbb{C}^{\mathrm{N}_{RR} \times L}$ is the relay weight vector with $||\boldsymbol{W}_R||_F = 1$ and $\boldsymbol{M}_S \in \mathbb{C}^{\mathrm{N}_S \times \mathrm{Ł}}$ is the source precoder with $\mathrm{E}\{||\boldsymbol{x}_S||_F^2\} = 1$, where $\boldsymbol{x}_S \in \mathbb{C}^{\mathrm{N}_S \times \mathrm{Ł}}$ is the transmitted source signal and is given by

$$\boldsymbol{x}_S = \boldsymbol{M}_S\boldsymbol{d}_S, \tag{4.3}$$

where $\boldsymbol{d}_S \in \mathbb{C}^{\mathrm{Ł} \times 1}$ is the source signal.

The transmitted signal at the relay is given by

$$\begin{aligned} \boldsymbol{x}_R &= \boldsymbol{M}_R\boldsymbol{y}_R, \\ &= \boldsymbol{M}_R\boldsymbol{W}_R^{\dagger}(\boldsymbol{H}_{SR}\boldsymbol{x}_S + \boldsymbol{H}_{RR}\boldsymbol{x}_R^d + \boldsymbol{n}_R), \end{aligned} \tag{4.4}$$

where $\boldsymbol{M}_R \in \mathbb{C}^{N_{RT} \times Ł}$ is the relay precoder matrix with $\mathrm{E}\{||\boldsymbol{M}_R \boldsymbol{y}_R||_F^2\} = 1$, where the expectation is taken over the ensemble of the channel realisations.

In (4.2), $\boldsymbol{x}_R^d$ the delayed version of the signal, $\boldsymbol{x}_R$, transmitted from the relay transmitter to the relay receiver through channel $\boldsymbol{H}_{RR}$. The occurrence of the delayed signal, $\boldsymbol{x}_R^d$, is due to a relay processing delay of τ. Hence, the relationship between the two signals is $\boldsymbol{x}_R^d(t) = \boldsymbol{x}_R(t-\tau)$ and the delayed signal is considered as relay SI.

To simplify the analysis, we consider this delayed signal as pure interference. Combining (4.2) with (4.1), the received signal at the destination is given by

$$\begin{aligned}\boldsymbol{y}_D = &\boldsymbol{W}_D^\dagger \boldsymbol{H}_{RD} \boldsymbol{F}_R \boldsymbol{H}_{SR} \boldsymbol{M}_S \boldsymbol{d}_S + \boldsymbol{W}_D^\dagger \boldsymbol{H}_{RD} \boldsymbol{F}_R \boldsymbol{H}_{RR} \boldsymbol{x}_R^d \\ &+ \boldsymbol{W}_D^\dagger \boldsymbol{H}_{RD} \boldsymbol{F}_R \boldsymbol{n}_R + \boldsymbol{W}_D^\dagger \boldsymbol{n}_D, \end{aligned} \tag{4.5}$$

where $\boldsymbol{F}_R = \boldsymbol{M}_R \boldsymbol{W}_R^\dagger$. The signal power is given by

$$\frac{\mathrm{trace}\{\boldsymbol{W}_D^\dagger \boldsymbol{H}_{RD} \boldsymbol{F}_R \boldsymbol{H}_{SR} \boldsymbol{M}_S \boldsymbol{M}_S^\dagger \boldsymbol{H}_{SR}^\dagger \boldsymbol{F}_R^\dagger \boldsymbol{H}_{RD}^\dagger \boldsymbol{W}_D\}}{Ł}, \tag{4.6}$$

using

$$\mathrm{E}\{\boldsymbol{d}_S \boldsymbol{d}_S^\dagger\} = \frac{1}{Ł} \boldsymbol{I}_L, \tag{4.7}$$

and the interference plus noise is given by

$$\mathrm{trace}\{\boldsymbol{W}_D^\dagger \boldsymbol{H}_{RD} \boldsymbol{F}_R \boldsymbol{H}_{RR} \boldsymbol{C} \boldsymbol{H}_{RR}^\dagger \boldsymbol{F}_R^\dagger \boldsymbol{H}_{RD}^\dagger \boldsymbol{W}_D + \boldsymbol{W}_D^\dagger \boldsymbol{H}_{RD} \boldsymbol{F}_R \boldsymbol{F}_R^\dagger \boldsymbol{H}_{RD}^\dagger \boldsymbol{W}_D + \boldsymbol{W}_D^\dagger \boldsymbol{W}_D\}, \tag{4.8}$$

using

$$\mathrm{E}\{\boldsymbol{x}_R^d \boldsymbol{x}_R^{d\dagger}\} = \mathrm{E}\{\boldsymbol{x}_R \boldsymbol{x}_R^\dagger\} = \boldsymbol{C}. \tag{4.9}$$

Table 4.3 Precoder, weight and signal vectors power constraint

Precoder & Weight Vector	Constraint
Relay Weight Vector ($\boldsymbol{W}_R$)	$\|\|\boldsymbol{W}_R\|\|_F = 1$
Destination Weight Vector ($\boldsymbol{W}_D$)	$\|\|\boldsymbol{W}_D\|\|_F = 1$
Source Signal Vector ($\boldsymbol{x}_S$)	$\mathrm{E}\{\|\|\boldsymbol{x}_S\|\|_F^2\} = 1$
Relay Signal Vector ($\boldsymbol{x}_R$)	$\mathrm{E}\{\|\|\boldsymbol{x}_R\|\|_F^2\} = 1$
Delayed Relay Signal Vector ($\boldsymbol{x}_R^d$)	$\mathrm{E}\{\|\|\boldsymbol{x}_R^d\|\|_F^2\} = 1$
Transmitted Source Signal (Arbitrary $\boldsymbol{M}_S$)	$\mathrm{E}\{\|\|\boldsymbol{M}_S\boldsymbol{d}_S\|\|_F^2\} = 1$
Transmitted Source Signal ($\boldsymbol{M}_S$ is Orthogonal)	$\boldsymbol{M}_S^\dagger\boldsymbol{M}_S = \boldsymbol{I}_L \Rightarrow \mathrm{E}\{\|\|\boldsymbol{d}_S\|\|_F^2\} = 1$

Combining (4.6) and (4.8), the SINR is given by

$$\mathrm{SINR} = \frac{\frac{1}{\mathrm{L}}\mathrm{trace}\{\boldsymbol{W}_D^\dagger\boldsymbol{H}_{RD}\boldsymbol{F}_R\boldsymbol{H}_{SR}\boldsymbol{M}_S\boldsymbol{M}_S^\dagger\boldsymbol{H}_{SR}^\dagger\boldsymbol{F}_R^\dagger\boldsymbol{H}_{RD}^\dagger\boldsymbol{W}_D\}}{\mathrm{trace}\{\boldsymbol{W}_D^\dagger\boldsymbol{H}_{RD}\boldsymbol{F}_R\boldsymbol{H}_{RR}\boldsymbol{C}\boldsymbol{H}_{RR}^\dagger\boldsymbol{F}_R^\dagger\boldsymbol{H}_{RD}^\dagger\boldsymbol{W}_D + \boldsymbol{W}_D^\dagger\boldsymbol{H}_{RD}\boldsymbol{F}_R\boldsymbol{F}_R^\dagger\boldsymbol{H}_{RD}^\dagger\boldsymbol{W}_D + \boldsymbol{W}_D^\dagger\boldsymbol{W}_D\}}. \tag{4.10}$$

To compare the different precoder and weight vector designs, $\boldsymbol{M}_S$, $\boldsymbol{W}_R$ and $\boldsymbol{W}_D$ are all normalised to have a unit norm while $\boldsymbol{M}_R$ is normalised to $\mathrm{E}\{||\boldsymbol{M}_R\boldsymbol{x}_R||^2\} = 1$. The normalisation constraints are all summarised in Table 4.3.

4.3 RELAY SIGNAL POWER CONSTRAINT

The relay signal needs to be constrained to a fixed power in order to simulate the system, as the relay cannot transmit using an unbounded amount of power. By fixing the relay signal power, it also allows different precoder and weight vector designs to be compared. Consider the relay signal in (4.4)

$$\boldsymbol{x}_R = \boldsymbol{M}_R\boldsymbol{W}_R^\dagger(\boldsymbol{H}_{SR}\boldsymbol{M}_S\boldsymbol{x}_S + \boldsymbol{H}_{RR}\boldsymbol{x}_R^d + \boldsymbol{n}_R), \tag{4.11}$$

where we set $\boldsymbol{F}_R = \boldsymbol{M}_R\boldsymbol{W}_R^\dagger$, $\boldsymbol{x}_R$ can be written as

$$\boldsymbol{x}_R = \boldsymbol{F}_R\boldsymbol{H}_{SR}\boldsymbol{M}_S\boldsymbol{x}_S + \boldsymbol{F}_R\boldsymbol{H}_{RR}\boldsymbol{x}_R^d + \boldsymbol{F}_R\boldsymbol{n}_R. \tag{4.12}$$

The power of the transmitted signal needs to be constrained such that

$$\mathrm{E}\{||\boldsymbol{x}_R||_F^2\} = \mathrm{E}\{\boldsymbol{x}_R^\dagger \boldsymbol{x}_R\} = \mathrm{trace}\{\mathrm{E}\{\boldsymbol{x}_R \boldsymbol{x}_R^\dagger\}\} = 1. \tag{4.13}$$

Hence, we need to compute the covariance matrix ($\mathrm{E}\{\boldsymbol{x}_R \boldsymbol{x}_R^\dagger\}$). From (**??**), we have

$$\begin{aligned}\mathrm{E}\{\boldsymbol{x}_R \boldsymbol{x}_R^\dagger\} = \mathrm{E}\{&(\boldsymbol{F}_R \boldsymbol{H}_{SR} \boldsymbol{M}_S \boldsymbol{d}_S + \boldsymbol{F}_R \boldsymbol{H}_{RR} \boldsymbol{x}_R^d + \boldsymbol{F}_R \boldsymbol{n}_R) \\ &(\boldsymbol{F}_R \boldsymbol{H}_{SR} \boldsymbol{M}_S \boldsymbol{d}_S + \boldsymbol{F}_R \boldsymbol{H}_{RR} \boldsymbol{x}_R^d + \boldsymbol{F}_R \boldsymbol{n}_R)^\dagger\}.\end{aligned} \tag{4.14}$$

When (4.14) is expanded, it becomes

$$\begin{aligned}\mathrm{E}\{\boldsymbol{x}_R \boldsymbol{x}_R^\dagger\} = \mathrm{E}\{&\boldsymbol{F}_R \boldsymbol{H}_{SR} \boldsymbol{M}_S \boldsymbol{d}_S \boldsymbol{d}_S^\dagger \boldsymbol{M}_S^\dagger \boldsymbol{H}_{SR}^\dagger \boldsymbol{F}_R^\dagger \\ &+ \boldsymbol{F}_R \boldsymbol{H}_{RR} \boldsymbol{x}_R^d \boldsymbol{x}_R^{d\dagger} \boldsymbol{H}_{RR}^\dagger \boldsymbol{F}_R^\dagger + \boldsymbol{F}_R \boldsymbol{n}_R \boldsymbol{n}_R^\dagger \boldsymbol{F}_R^\dagger\},\end{aligned} \tag{4.15}$$

where the covariance matrices of $\boldsymbol{d}_S$ and $\boldsymbol{n}_R$ are given by

$$\begin{aligned}\mathrm{E}\{\boldsymbol{d}_S \boldsymbol{d}_S^\dagger\} &= \frac{1}{\text{Ł}} \boldsymbol{I}_L, \\ \mathrm{E}\{\boldsymbol{n}_R \boldsymbol{n}_R^\dagger\} &= \boldsymbol{I}_{N_{RR}}.\end{aligned} \tag{4.16}$$

It is clearly seen that the covariance matrix ($\boldsymbol{C} = \mathrm{E}\{\boldsymbol{x}_R \boldsymbol{x}_R^\dagger\}$) appears on both sides of (4.15) under the assumption that the covariance matrix of $\boldsymbol{x}_R$ and $\boldsymbol{x}_R^d$ are the same. In order to solve for $\boldsymbol{C}$, we simplify (4.15) to

$$\boldsymbol{C} = \boldsymbol{A}\boldsymbol{C}\boldsymbol{A}^\dagger + \boldsymbol{B}, \tag{4.17}$$

where

$$\begin{aligned}\boldsymbol{A} &= \boldsymbol{F}_R \boldsymbol{H}_{RR}, \\ \boldsymbol{B} &= \frac{1}{\text{Ł}} \boldsymbol{F}_R \boldsymbol{H}_{SR} \boldsymbol{M}_S \boldsymbol{M}_S^\dagger \boldsymbol{H}_{SR}^\dagger \boldsymbol{F}_R^\dagger + \boldsymbol{F}_R \boldsymbol{F}_R^\dagger.\end{aligned} \tag{4.18}$$

Using matrix vectorization [1], (4.17) can be expressed as

$$\begin{bmatrix} \boldsymbol{c}_1 \\ \boldsymbol{c}_2 \\ \vdots \\ \boldsymbol{c}_{N_{RT}} \end{bmatrix} = \begin{bmatrix} \boldsymbol{A}\boldsymbol{C}\boldsymbol{a}_1^{\dagger} \\ \boldsymbol{A}\boldsymbol{C}\boldsymbol{a}_2^{\dagger} \\ \vdots \\ \boldsymbol{A}\boldsymbol{C}\boldsymbol{a}_{N_{RT}}^{\dagger} \end{bmatrix} + \begin{bmatrix} \boldsymbol{b}_1 \\ \boldsymbol{b}_2 \\ \vdots \\ \boldsymbol{b}_{N_{RT}} \end{bmatrix}, \tag{4.19}$$

where

$$\begin{aligned} \boldsymbol{A} &= \begin{bmatrix} \boldsymbol{a}_1 \\ \boldsymbol{a}_2 \\ \vdots \\ \boldsymbol{a}_{N_{RT}} \end{bmatrix}, \\ \boldsymbol{B} &= \begin{bmatrix} \boldsymbol{b}_1, & \boldsymbol{b}_2, & \cdots & \boldsymbol{b}_{N_{RT}} \end{bmatrix}, \\ \boldsymbol{C} &= \begin{bmatrix} \boldsymbol{c}_1, & \boldsymbol{c}_2, & \cdots & \boldsymbol{c}_{N_{RT}} \end{bmatrix}. \end{aligned} \tag{4.20}$$

The stacked vectors of $\boldsymbol{C}$ and $\boldsymbol{B}$ in (4.19) are denoted by

$$\begin{aligned} \boldsymbol{v}_C &= \begin{bmatrix} \boldsymbol{c}_1 \\ \boldsymbol{c}_2 \\ \vdots \\ \boldsymbol{c}_{N_{RT}} \end{bmatrix}, \\ \boldsymbol{v}_B &= \begin{bmatrix} \boldsymbol{b}_1 \\ \boldsymbol{b}_2 \\ \vdots \\ \boldsymbol{b}_{N_{RT}} \end{bmatrix}. \end{aligned} \tag{4.21}$$

[1] Vectorization of a matrix is a linear transform that converts the matrix into a column vector. This implies that it is stacking the columns of the matrix on top of one another.

With this notation, (4.19) can be written as

$$\boldsymbol{v}_C = \begin{bmatrix} \boldsymbol{A} & 0 & \cdots & 0 \\ 0 & \ddots & \ddots & \vdots \\ \vdots & \ddots & \ddots & 0 \\ 0 & \cdots & 0 & \boldsymbol{A} \end{bmatrix} \begin{bmatrix} \boldsymbol{C}\boldsymbol{a}_1^\dagger \\ \vdots \\ \boldsymbol{C}\boldsymbol{a}_{N_{RT}}^\dagger \end{bmatrix} + \boldsymbol{v}_B. \tag{4.22}$$

The second matrix on the right hand side of (4.22) can be arranged to give

$$\begin{bmatrix} \boldsymbol{C}\boldsymbol{a}_1^\dagger \\ \vdots \\ \boldsymbol{C}\boldsymbol{a}_{N_{RT}}^\dagger \end{bmatrix} = \bar{\boldsymbol{A}}\boldsymbol{v}_C. \tag{4.23}$$

In order to compute $\bar{\boldsymbol{A}}$, consider one of the vector terms in (4.23). The i^{th} term, $\boldsymbol{C}\boldsymbol{a}_i^\dagger$, can be expanded as

$$\boldsymbol{C}\boldsymbol{a}_i^\dagger = \begin{bmatrix} \boldsymbol{c}_1^\dagger \boldsymbol{a}_i^\dagger \\ \vdots \\ \vdots \\ \boldsymbol{c}_{N_{RT}}^\dagger \boldsymbol{a}_i^\dagger \end{bmatrix}. \tag{4.24}$$

The j^{th} element of this vector, $\boldsymbol{C}\boldsymbol{a}_i^\dagger$, is given by

$$\begin{aligned}
\boldsymbol{c}_j^\dagger \boldsymbol{a}_i^\dagger = \boldsymbol{a}_i^* \boldsymbol{c}_j^* &= \begin{pmatrix} A_{i,1}^*, & \cdots & A_{i,N_{RT}}^* \end{pmatrix} \begin{pmatrix} C_{1,j}^* \\ \vdots \\ C_{N_{RT},j}^* \end{pmatrix}, \\
&= \begin{pmatrix} A_{i,1}^*, & \cdots & A_{i,N_{RT}}^* \end{pmatrix} \begin{pmatrix} C_{j,1} \\ \vdots \\ C_{j,N_{RT}} \end{pmatrix}, \\
&= \begin{pmatrix} \mathbf{0} & A_{i,1}^*, & \mathbf{0}, & A_{i,2}^*, & \cdots \end{pmatrix} \begin{pmatrix} C_{1,1} \\ C_{2,1} \\ \vdots \\ C_{j,1} \\ \vdots \\ C_{N_{RT},1} \\ \vdots \\ C_{1,N_{RT}} \\ \vdots \\ C_{N_{RT},N_{RT}} \end{pmatrix},
\end{aligned} \tag{4.25}$$

where the $\mathbf{0}$ term on the left hand side of $A_{i,1}^*$ is a zero vector of length $j-1$ and similarly, the $\mathbf{0}$ at the right hand side of $A_{i,1}^*$ is a zero vector of length $N-1$. The vector in (4.24) can be rewritten in matrix form using (4.25) to give

$$\boldsymbol{C}\boldsymbol{a}_i^\dagger = \begin{pmatrix} A_{i,1}^* \boldsymbol{I}_{N_{RT}}, & \cdots & A_{i,N_{RT}}^* \boldsymbol{I}_{N_{RT}} \end{pmatrix} \boldsymbol{v}_C. \tag{4.26}$$

Stacking these terms for $i = 1, \ldots, N_{RT}$ gives

$$\begin{bmatrix} \boldsymbol{C}\boldsymbol{a}_1^{\dagger} \\ \vdots \\ \vdots \\ \boldsymbol{C}\boldsymbol{a}_{N_{RT}}^{\dagger} \end{bmatrix} = \begin{bmatrix} A_{1,1}^{*}\boldsymbol{I}_{N_{RT}} & \cdots & A_{1,N_{RT}}^{*}\boldsymbol{I}_{N_{RT}} \\ \vdots & \ddots & \vdots \\ A_{N_{RT},1}^{*}\boldsymbol{I}_{N_{RT}} & \cdots & A_{N_{RT},N_{RT}}^{*}\boldsymbol{I}_{N_{RT}} \end{bmatrix} \boldsymbol{v}_C, \tag{4.27}$$

$$= (\boldsymbol{A}^{*} \otimes \boldsymbol{I}_{N_{RT}})\boldsymbol{v}_C.$$

Hence, $\bar{\boldsymbol{A}} = (\boldsymbol{A}^{*} \otimes \boldsymbol{I}_{N_{RT}})\boldsymbol{v}_C$ and using (4.24) we have

$$\boldsymbol{v}_C = \begin{bmatrix} \boldsymbol{A} & 0 & \cdots & 0 \\ 0 & \ddots & \ddots & \vdots \\ \vdots & \ddots & \ddots & 0 \\ 0 & \cdots & 0 & \boldsymbol{A} \end{bmatrix} (A^{*} \otimes \boldsymbol{I}_{N_{RT}})\boldsymbol{v}_C + \boldsymbol{v}_B, \tag{4.28}$$

where $\otimes$ is the Kronecker product [2]. The large matrix containing $\boldsymbol{A}$ in its block diagonal entries in (4.28) can also be expressed as

$$\begin{bmatrix} \boldsymbol{A} & 0 & \cdots & 0 \\ 0 & \ddots & \ddots & \vdots \\ \vdots & \ddots & \ddots & 0 \\ 0 & \cdots & 0 & \boldsymbol{A} \end{bmatrix} = (\boldsymbol{I}_{N_{RT}} \otimes \boldsymbol{A}). \tag{4.29}$$

Substituting (4.29) in (4.28), $\boldsymbol{v}_C$ is written as

$$\boldsymbol{v}_C = (\boldsymbol{I}_{N_{RT}} \otimes \boldsymbol{A})(\boldsymbol{A}^{*} \otimes \boldsymbol{I}_{N_{RT}})\boldsymbol{v}_C + \boldsymbol{v}_B. \tag{4.30}$$

On separating terms containing $\boldsymbol{v}_C$ and rearranging this equation, we have

$$\boldsymbol{v}_C = [\boldsymbol{I}_{N_{RT}^2} - (\boldsymbol{I}_{N_{RT}} \otimes \boldsymbol{A})(\boldsymbol{A}^{*} \otimes \boldsymbol{I}_{N_{RT}})]^{-1}\boldsymbol{v}_B. \tag{4.31}$$

[2] Given an $m \times n$ matrix A and a $p \times q$ matrix B, the Kronecker product of matrix A and B is an $(mp) \times (nq)$ matrix.

Using (4.31), the power of the covariance matrix can be calculated. Since $\boldsymbol{M}_S$ and $\boldsymbol{W}_R$ have unit norm, the only variable in (4.17) to control the size of $\boldsymbol{C}$ is $\boldsymbol{M}_R$. Hence, a scaling factor, α, is used to scale the power of $\boldsymbol{M}_R$ such that the power constraint in (4.13) can be satisfied. The value of α is determined by finding the roots of

$$\text{trace}\{\boldsymbol{C}\} - 1 = \text{trace}\{\text{E}\{\boldsymbol{x}_R \boldsymbol{x}_R^{\dagger}\}\} - 1 = 0, \tag{4.32}$$

where $\boldsymbol{x}_R$ is given by

$$\boldsymbol{x}_R = \boldsymbol{M}_R \boldsymbol{W}_R^{\dagger} \boldsymbol{H}_{SR} \boldsymbol{M}_S \boldsymbol{x}_S + \boldsymbol{M}_R \boldsymbol{W}_R^{\dagger} \boldsymbol{H}_{RR} \boldsymbol{x}_R^d + \boldsymbol{M}_R \boldsymbol{W}_R^{\dagger} \boldsymbol{n}_R, \tag{4.33}$$

and $\boldsymbol{M}_R$ is given by

$$\boldsymbol{M}_R = \alpha \boldsymbol{M}_R^U, \tag{4.34}$$

where $\boldsymbol{M}_R^U$ is the unnormalised version of $\boldsymbol{M}_R$.

This numerical method of finding α is implemented using the "*fzero*" function in MATLAB, which uses a combination of bisection, secant and inverse quadratic interpolation methods. The *fzero* function computes α based on (4.31) such that the $\boldsymbol{C}$ in (4.32) is being satisfied.

4.4 NORMALISING THE PRECODER AND WEIGHT VECTOR SOLUTIONS

When the precoders and weight vectors are calculated using the different techniques, they are initially computed in an unnormalised form which are denoted by $\boldsymbol{M}_S^U$, $\boldsymbol{W}_R^U$ and $\boldsymbol{W}_D^U$ with the full solution given by $\boldsymbol{M}_S = \boldsymbol{M}_S^U / ||\boldsymbol{M}_S^U||_F$, $\boldsymbol{W}_R = \boldsymbol{W}_R^U / ||\boldsymbol{W}_R^U||_F$ and $\boldsymbol{W}_D = \boldsymbol{W}_D^U / ||\boldsymbol{W}_D^U||_F$. Similarly, the value of $\boldsymbol{M}_R$ is normalised by computing the scaling factor, α, using the procedure in Section 4.3.

From (4.17), it is clear that the calculation of $\boldsymbol{C}$ requires $\boldsymbol{F}_R$ ($\boldsymbol{F}_R = \boldsymbol{M}_R \boldsymbol{W}_R$). However, some of the $\boldsymbol{M}_R$ and $\boldsymbol{W}_R$ solutions require the value of $\boldsymbol{C}$ in order to compute the answer, such as the SLNR and MMSE methods. Hence, these calculations tend to become iterative. To make the precoding and weight vector designs clearer, we summarise the requirements for the different precoder and weight vector designs in Table 4.4.

To compute and normalise $\boldsymbol{M}_R$, $\boldsymbol{C}$ is required in all of the designs, as it is essential to find the scaling factor to normalise $\boldsymbol{M}_R$. Hence, an iteration procedure for calculating $\boldsymbol{C}$ and normalising $\boldsymbol{M}_R$ cannot be avoided.

For the MMSE solution at the relay, we consider two approximations for $\boldsymbol{C}$ to avoid the iterative process. The first approximation of $\boldsymbol{C}$ is

$$\boldsymbol{C} \approx \frac{1}{\mathrm{L}} \boldsymbol{I}_{N_{RT}}, \tag{4.35}$$

which is based on assuming that $\boldsymbol{C}$ is white[3]. The second approximation of $\boldsymbol{C}$ is

$$\boldsymbol{C} = \mathrm{E}\{\boldsymbol{x}_R \boldsymbol{x}_R^{\dagger}\} = \mathrm{E}\{\boldsymbol{M}_R \boldsymbol{y}_R \boldsymbol{y}_R^{\dagger} \boldsymbol{M}_R^{\dagger}\} \approx \frac{\boldsymbol{M}_R^U \boldsymbol{M}_R^{U\dagger}}{\mathrm{trace}\{\boldsymbol{M}_R^U \boldsymbol{M}_R^{U\dagger}\}}. \tag{4.36}$$

In this case, the $\boldsymbol{y}_R \boldsymbol{y}_R^{\dagger}$ term is assumed to be white rather than the $\boldsymbol{C}$ term, which is used in the first approximation of $\boldsymbol{C}$. We use these two approximations to calculate the MMSE relay weight vector and find which of these approximations provides a better MMSE solution.

For the MMSE solution at the destination, $\boldsymbol{C}$ has been calculated, therefore an iteration is not required for computing the MMSE destination weight vector.

The SVD method, as shown in Table 4.4, is used for all of the precoder and weight vector designs. Since this approach only increases the desired signal and ignores the interference, it provides a useful baseline for comparing other techniques that increase the signal and/or account for the SI at the relay. As there is no interference at the source, the best method is to increase the channel power using SVD. At the relay receiver, the antenna receives the desired signal and SI. Hence, the ZF and MMSE weight vectors are used to null or minimise SI as well as increasing the desired signal, respectively. At the relay transmitter, ZF and SLNR precoder designs are being implemented, as ZF can null SI and SLNR can increase the desired signal and can also decrease the SI that is transmitted to the relay receiver. At the destination receiver, the MMSE design is used to minimise SI and noise.

[3]A discrete signal where the samples are regarded as uncorrelated random variables with zero mean and finite variance.

Table 4.4 Precoder, weight vector and covariance matrix design requirements.

Precoder / Weight Vector / Covariance Matrix	Methods	The values that are used for computing the precoders or weight vectors
$\boldsymbol{M}_S$	SVD	$\boldsymbol{H}_{SR}$
$\boldsymbol{W}_R$	SVD	$\boldsymbol{H}_{SR}$
	ZF	$\boldsymbol{H}_{SR}$ $\boldsymbol{H}_{RR}$
	MMSE	$\boldsymbol{H}_{RR}$ $\boldsymbol{H}_{SR}$ $\boldsymbol{M}_S$ $\boldsymbol{M}_R$ $\boldsymbol{C}$
$\boldsymbol{M}_R$	SVD	$\boldsymbol{H}_{RD}$ $\boldsymbol{C}$
	SLNR	$\boldsymbol{H}_{RD}$ $\boldsymbol{H}_{RR}$ $\boldsymbol{C}$
	ZF	$\boldsymbol{H}_{RR}$ $\boldsymbol{C}$
$\boldsymbol{W}_D$	SVD	$\boldsymbol{H}_{RD}$
	MMSE	$\boldsymbol{H}_{SR}$ $\boldsymbol{H}_{RR}$ $\boldsymbol{M}_S$ $\boldsymbol{M}_S$ $\boldsymbol{M}_R$ $\boldsymbol{C}$
$\boldsymbol{C}$		$\boldsymbol{M}_R$ $\boldsymbol{W}_R$ $\boldsymbol{M}_S$ $\boldsymbol{H}_{SR}$ $\boldsymbol{H}_{RR}$

Table 4.5 Implementation methods to determine the precoders and weights at the relay

Weights ($\boldsymbol{W}$)	Precoders ($\boldsymbol{M}$)
Minimum Mean Square Error (MMSE)	Signal to Leakage and Noise Ratio (SLNR)
Zero Forcing (ZF)	Zero Forcing (ZF)
Singular Value Decomposition (SVD)	Singular Value Decomposition (SVD)

4.4.1 Pure Ad-hoc Schemes

We implemented different precoders and weight vectors and compared their effects on the e2e SINR performance, these designs are categorised in Table 4.5. They are also shown in Table 4.2 for the different source, relay and destination precoder and/or weight vector designs.

4.4.1.1 Precoder and Weight Design using SVD

The SVD designs for the source precoder and relay weight vector are computed by taking the leading Ł (the number of data streams) columns of the left singular vectors of $\boldsymbol{H}_{SR}$ then the leading Ł columns of the right singular vectors of $\boldsymbol{H}_{SR}$, respectively. Similarly, the relay precoder and destination weight vector are computed by taking the leading Ł columns of the left singular vectors of $\boldsymbol{H}_{RD}$ then the leading Ł columns of the right singular vectors of $\boldsymbol{H}_{RD}$, respectively. These matrices are shown in Table 4.6, where $\boldsymbol{M}(:, 1:Ł)$ denotes the leading Ł columns of a matrix, $\boldsymbol{M}$.

Table 4.6 SVD approach for $\boldsymbol{M}_S$, $\boldsymbol{M}_R$, $\boldsymbol{W}_R$ and $\boldsymbol{W}_D$

Precoder / Weight Matrix	Methods
$\boldsymbol{M}_S$	$\boldsymbol{V}_{SR}(:, 1:Ł)$
$\boldsymbol{W}_R$	$\boldsymbol{U}_{SR}(:, 1:Ł)$
$\boldsymbol{M}_R^U$	$\boldsymbol{V}_{RD}(:, 1:Ł)$
$\boldsymbol{W}_D$	$\boldsymbol{U}_{RD}(:, 1:Ł)$

In Table 4.6, the notation, $\boldsymbol{H}_{ab} = \boldsymbol{U}_{ab}\boldsymbol{D}_{ab}\boldsymbol{V}_{ab}^{\dagger}$, is used for the SVD design.

4.4.1.2 ZF Weight Vector at Relay

From (2.12), the ZF weight vector is given by

$$\hat{\boldsymbol{W}}_{ZF} = (\bar{\boldsymbol{H}}_T^{\dagger}\bar{\boldsymbol{H}}_T)^{-1}\bar{\boldsymbol{H}}_T^{\dagger}, \tag{4.37}$$

where $\bar{\boldsymbol{H}}_T$ is a composite matrix containing $\boldsymbol{H}_{RR}$ and $\boldsymbol{H}_{SR}$, defined as

$$\bar{\boldsymbol{H}}_T = [\boldsymbol{H}_{SR}\boldsymbol{H}_{RR}]\,. \tag{4.38}$$

The ZF weight vector is constructed by taking the first N_S rows of $\hat{\boldsymbol{W}}_{ZF}$, such that $\boldsymbol{W}_{ZF}^U = \hat{\boldsymbol{W}}_{ZF}(:, 1:N_S)$. The constraint for the ZF weight vector is, the number of antennas for the relay receiver, N_{RR}, needs to be greater than $N_S + N_T$.

4.4.1.3 ZF Precoder at the Relay

The relay ZF precoder is designed to null the interference channel, $\boldsymbol{H}_{RR}$. Hence, from (2.11), the ZF precoder is constructed by taking Ł-smallest right singular vectors of $\boldsymbol{H}_{RR}$. This is given by

$$\boldsymbol{W}_{ZF}^U = \boldsymbol{V}_{RR}(:, (N_{RR} - Ł) + 1 : N_{RT}), \tag{4.39}$$

where $\boldsymbol{V}_{RR}$ contains the right singular vectors of $\boldsymbol{H}_{RR}$, given by $\boldsymbol{H}_{RR} = \boldsymbol{U}_{RR}\boldsymbol{D}_{RR}\boldsymbol{V}_{RR}^{\dagger}$. The ZF precoder has an antenna requirement that the number of relay transmit antennas, N_{RT}, must be greater than or equal to $N_{RR} + Ł$, where Ł is the number of data streams that the relay

transmits.

4.4.1.4 MMSE Equation for Relay Weight Vector

The MMSE solution for the relay weight vector is given by

$$\boldsymbol{W}_R^U = (\bar{\boldsymbol{H}}\bar{\boldsymbol{H}}^\dagger + \bar{\boldsymbol{C}})^{-1}\bar{\boldsymbol{H}}, \tag{4.40}$$

where $\bar{\boldsymbol{H}}$ is the equivalent channel matrix and $\bar{\boldsymbol{C}}$ is the noise plus interference covariance matrix, defined as

$$\begin{aligned}\bar{\boldsymbol{C}} &= (\boldsymbol{I}_{N_{RR}} + \boldsymbol{H}_{RR}\boldsymbol{C}\boldsymbol{H}_{RR}^\dagger),\\ \bar{\boldsymbol{H}} &= \boldsymbol{H}_{SR}\boldsymbol{M}_S.\end{aligned} \tag{4.41}$$

The covariance matrix of the relay transmitted signal, $\boldsymbol{C} = \mathrm{E}\{\boldsymbol{x}_R\boldsymbol{x}_R^\dagger\}$, needs to be approximated, since the calculation of the MMSE solution for $\boldsymbol{W}_R$ requires the values of $\boldsymbol{M}_R$ and $\boldsymbol{C}$, shown in Table 4.4. However, the calculation of $\boldsymbol{C}$ also requires the value of $\boldsymbol{W}_R$. As a result, using an approximated $\boldsymbol{C}$ value, the calculation for the MMSE weight vector does not require an iterative process.

We consider two approximations for $\boldsymbol{C}$, the first approximation is to assume that $\boldsymbol{C}$ is approximately an identity matrix with a scaling factor of $\frac{1}{\mathrm{L}}$, which is given by

$$\boldsymbol{C} \approx \frac{1}{\mathrm{L}}\boldsymbol{I}_{N_{RT}}. \tag{4.42}$$

The second approximation is computed by observing (4.4) and $\boldsymbol{x}_R$ is given by

$$\boldsymbol{x}_R = \boldsymbol{M}_R\boldsymbol{y}_R. \tag{4.43}$$

Hence, $\boldsymbol{C}$ is given by

$$\boldsymbol{C} = \mathrm{E}\{\boldsymbol{x}_R \boldsymbol{x}_R^{\dagger}\} = \mathrm{E}\{\boldsymbol{M}_R \boldsymbol{y}_R \boldsymbol{y}_R^{\dagger} \boldsymbol{M}_R^{\dagger}\} \approx \frac{\boldsymbol{M}_R^U \boldsymbol{M}_R^{U\dagger}}{\mathrm{trace}\{\boldsymbol{M}_R^U \boldsymbol{M}_R^{U\dagger}\}}, \tag{4.44}$$

where $\boldsymbol{y}_R$ is assumed to be white in (4.44) and $\boldsymbol{M}_R^U$ is the unnormalised form of $\boldsymbol{M}_R$ which can be computed from the relay precoder using SVD. Using these approximations, the computation complexity of the iterative processing for calculating the covariance matrix is avoided.

4.4.1.5 MMSE Equation for Destination Weight Vector

The MMSE solution for the destination weight vector is given by

$$\boldsymbol{W}_{MMSE\text{-}D}^U = (\boldsymbol{H}_1 \boldsymbol{H}_1^{\dagger} + \boldsymbol{H}_2 \boldsymbol{H}_2^{\dagger} + \boldsymbol{B})^{-1} \boldsymbol{H}_1, \tag{4.45}$$

where $\boldsymbol{H}_1$, $\boldsymbol{H}_2$ and $\boldsymbol{B}$ are given by

$$\begin{aligned} \boldsymbol{H}_1 &= \boldsymbol{H}_{RD} \boldsymbol{M}_R \boldsymbol{W}_R^{\dagger} \boldsymbol{H}_{SR} \boldsymbol{M}_S, \\ \boldsymbol{H}_2 &= \boldsymbol{H}_{RD} \boldsymbol{M}_R \boldsymbol{W}_R^{\dagger} \boldsymbol{H}_{RR} \boldsymbol{C}^{1/2}, \\ \boldsymbol{B} &= \boldsymbol{H}_{RD} \boldsymbol{M}_R \boldsymbol{W}_R^{\dagger} \boldsymbol{W}_R \boldsymbol{M}_R^{\dagger} \boldsymbol{H}_{RD}^{\dagger} + \boldsymbol{I}_{N_D}. \end{aligned} \tag{4.46}$$

In (4.46), $\boldsymbol{C}$ is the covariance matrix that is described and calculated in Section 4.3. The MMSE solution for the relay weight vector, calculation of the covariance matrix, $\boldsymbol{C}$, requires an iteration or an approximation. Here, the MMSE solution at the destination can obtain $\boldsymbol{C}$ from the relay node, as $\boldsymbol{C}$ has already been calculated at the relay.

From (4.46), it follows that the desired channel, $\boldsymbol{H}_1$, the interference channel, $\boldsymbol{H}_2$, and the noise covariance, $\boldsymbol{B}$, all contain the same leading term of $\boldsymbol{H}_{RD} \boldsymbol{M}_R \boldsymbol{W}_R^{\dagger}$. Hence, this implies that when the MMSE solution is reducing the interference and noise component, it is also reducing the desired signal component. Hence, the best approach is likely to be based on a simple boosting of the desired signal which is the basis of the SVD approach. Therefore the MMSE approach may have a similar performance as the SVD solution.

4.4.1.6 SLNR Equation

The SLNR equation for the relay precoder is complicated compared to the standard SLNR equation, as the leakage is in two directions, i) a delayed version of the desired signal that is leaked into the relay receiver and ii) the SI signal that is amplified then forwarded onto the destination. Nevertheless, the signals at the destination can be identified as the total leakage of the delayed signal to the destination plus SI and noise at the destination. Therefore the SLNR equation can be formed.

At the relay, the transmitted signal is given by

$$\begin{aligned}\boldsymbol{x}_R &= \boldsymbol{M}_R\boldsymbol{W}_R^{\dagger}(\boldsymbol{H}_{SR}\boldsymbol{M}_S\boldsymbol{d}_S + \boldsymbol{H}_{RR}\boldsymbol{x}_R^d + \boldsymbol{n}_R),\\ &= \boldsymbol{M}_R\boldsymbol{W}_R^{\dagger}\boldsymbol{H}_{SR}\boldsymbol{M}_S\boldsymbol{d}_S + \boldsymbol{M}_R\boldsymbol{W}_R^{\dagger}\boldsymbol{H}_{RR}\boldsymbol{x}_R^d + \boldsymbol{M}_R\boldsymbol{W}_R^{\dagger}\boldsymbol{n}_R.\end{aligned} \tag{4.47}$$

This signal can be decomposed into

$$\begin{aligned}\text{Desired signal} &= \boldsymbol{M}_R\boldsymbol{W}_R^{\dagger}\boldsymbol{H}_{SR}\boldsymbol{M}_S\boldsymbol{d}_S,\\ \text{SI} &= \boldsymbol{M}_R\boldsymbol{W}_R^{\dagger}\boldsymbol{H}_{RR}\boldsymbol{x}_R^d,\\ \text{Amplified noise} &= \boldsymbol{M}_R\boldsymbol{W}_R^{\dagger}\boldsymbol{n}_R.\end{aligned} \tag{4.48}$$

The signal in (4.47) is transmitted through both $\boldsymbol{H}_{RD}$ and $\boldsymbol{H}_{RR}$. The signal through $\boldsymbol{H}_{RD}$ is given by

$$\boldsymbol{H}_{RD}\boldsymbol{M}_R\boldsymbol{W}_R^{\dagger}(\boldsymbol{H}_{SR}\boldsymbol{M}_S\boldsymbol{d}_S + \boldsymbol{H}_{RR}\boldsymbol{x}_R^d + \boldsymbol{n}_R), \tag{4.49}$$

which can also be decomposed into

$$\begin{aligned}\text{Desired signal} &= \boldsymbol{H}_{RD}\boldsymbol{M}_R\boldsymbol{W}_R^{\dagger}\boldsymbol{H}_{SR}\boldsymbol{M}_S\boldsymbol{d}_S,\\ \text{Interference at destination} &= \boldsymbol{H}_{RD}\boldsymbol{M}_R\boldsymbol{W}_R^{\dagger}\boldsymbol{H}_{RR}\boldsymbol{x}_R^d,\\ \text{Extra noise at destination} &= \boldsymbol{H}_{RD}\boldsymbol{M}_R\boldsymbol{W}_R^{\dagger}\boldsymbol{n}_R,\\ \text{Destination noise} &= \boldsymbol{n}_D.\end{aligned} \tag{4.50}$$

The signal[4] through $\boldsymbol{H}_{RR}$ is given by

$$\begin{aligned}&\boldsymbol{H}_{RR}(\boldsymbol{M}_R\boldsymbol{W}_R^{\dagger}\boldsymbol{H}_{SR}\boldsymbol{M}_S\boldsymbol{d}_S+\boldsymbol{M}_R\boldsymbol{W}_R^{\dagger}\boldsymbol{H}_{RR}\boldsymbol{x}_R^d+\boldsymbol{M}_R\boldsymbol{W}_R^{\dagger}\boldsymbol{n}_R),\\&=\boldsymbol{H}_{RR}\boldsymbol{M}_R\boldsymbol{W}_R^{\dagger}(\boldsymbol{H}_{SR}\boldsymbol{M}_S\boldsymbol{d}_S+\boldsymbol{H}_{RR}\boldsymbol{x}_R^d+\boldsymbol{n}_R).\end{aligned}\tag{4.51}$$

Using the information in (4.50) and (4.51), the SLNR structure can be written in the form of

$$\begin{aligned}\text{Signal}&=\boldsymbol{H}_{RD}\boldsymbol{M}_R\boldsymbol{W}_R^{\dagger}\boldsymbol{H}_{SR}\boldsymbol{M}_S\boldsymbol{d}_S,\\\text{Leakage}&=\boldsymbol{H}_{RD}\boldsymbol{M}_R\boldsymbol{W}_R^{\dagger}\boldsymbol{H}_{RR}\boldsymbol{x}_R^d+\boldsymbol{H}_{RR}\boldsymbol{M}_R\boldsymbol{W}_R^{\dagger}(\boldsymbol{H}_{SR}\boldsymbol{M}_S\boldsymbol{x}_S+\boldsymbol{H}_{RR}\boldsymbol{x}_R^d+\boldsymbol{n}_R),\\\text{Noise}&=\boldsymbol{H}_{RD}\boldsymbol{M}_R\boldsymbol{W}_R^{\dagger}\boldsymbol{n}_R+\boldsymbol{n}_D.\end{aligned}\tag{4.52}$$

From (4.52), the signal power is given by

$$\mathrm{E}\{\mathrm{trace}\{\boldsymbol{H}_{RD}\boldsymbol{M}_R\boldsymbol{W}_R^{\dagger}\boldsymbol{H}_{SR}\boldsymbol{M}_S\boldsymbol{d}_S\boldsymbol{d}_s^{\dagger}\boldsymbol{M}_S^{\dagger}\boldsymbol{H}_{SR}^{\dagger}\boldsymbol{W}_R\boldsymbol{M}_R^{\dagger}\boldsymbol{H}_{RD}^{\dagger}\}\},\tag{4.53}$$

and can be simplified to

$$\mathrm{E}\{\mathrm{trace}\{\boldsymbol{H}_{RD}\boldsymbol{M}_R\hat{\boldsymbol{A}}\boldsymbol{M}_R^{\dagger}\boldsymbol{H}_{RD})\}\},\tag{4.54}$$

using

$$\hat{\boldsymbol{A}}=\boldsymbol{W}_R^{\dagger}\boldsymbol{H}_{SR}\boldsymbol{M}_S\boldsymbol{d}_S\boldsymbol{d}_S^{\dagger}\boldsymbol{M}_S^{\dagger}\boldsymbol{H}_{SR}^{\dagger}\boldsymbol{W}_R.\tag{4.55}$$

By setting $\mathrm{E}\{\hat{\boldsymbol{A}}\}=\boldsymbol{A}$, the signal power can be written as

$$\mathrm{trace}\{(\boldsymbol{M}_R^{\dagger}\boldsymbol{H}_{RD}^{\dagger}\boldsymbol{H}_{RD}\boldsymbol{M}_R)\boldsymbol{A}\},\tag{4.56}$$

where $\boldsymbol{A}$ is given by

$$\boldsymbol{A}=\frac{1}{\mathrm{L}}\boldsymbol{W}_R^{\dagger}\boldsymbol{H}_{SR}\boldsymbol{M}_S\boldsymbol{M}_S^{\dagger}\boldsymbol{H}_{SR}^{\dagger}\boldsymbol{W}_R,\tag{4.57}$$

assuming $\mathrm{E}\{\boldsymbol{d}_S\boldsymbol{d}_S^{\dagger}\}=\frac{1}{\mathrm{L}}\boldsymbol{I}_{N_S}$.

In the case of one data stream, $\mathrm{L}=1$, $\boldsymbol{A}$ is a scalar and the signal power is given by

$$(\boldsymbol{M}_R^{\dagger}\boldsymbol{H}_{RD}^{\dagger}\boldsymbol{H}_{RD}\boldsymbol{M}_R)\boldsymbol{A}.\tag{4.58}$$

[4]This entire signal is considered as SI at the relay receiver.

For Ł > 1, the $\boldsymbol{A}$ matrix in (4.56) complicates the analysis and an SLNR solution appears to be unattainable.

The noise power from (4.52) is given by

$$\mathrm{E}\{\mathrm{trace}\{(\boldsymbol{H}_{RD}\boldsymbol{M}_R\boldsymbol{W}_R^{\dagger}\boldsymbol{n}_R+\boldsymbol{n}_D)(\boldsymbol{n}_R^{\dagger}\boldsymbol{W}_R\boldsymbol{M}_R^{\dagger}\boldsymbol{H}_{RD}^{\dagger}+\boldsymbol{n}_D^{\dagger})\}\}. \tag{4.59}$$

By setting $\mathrm{E}\{\boldsymbol{n}_D\boldsymbol{n}_D^{\dagger}\}=\boldsymbol{I}_{N_D}$ and $\mathrm{E}\{\boldsymbol{n}_R\boldsymbol{n}_R^{\dagger}\}=\boldsymbol{I}_{N_{RR}}$, (4.59) can be simplified to

$$\begin{aligned}&\mathrm{E}\{\mathrm{trace}\{\boldsymbol{H}_{RD}\boldsymbol{M}_R\boldsymbol{W}_R^{\dagger}\boldsymbol{W}_R\boldsymbol{M}_R^{\dagger}\boldsymbol{H}_{RD}^{\dagger}+\boldsymbol{I}_{N_D}\}\},\\&=\mathrm{trace}\{(\boldsymbol{M}_R^{\dagger}\boldsymbol{H}_{RD}^{\dagger}\boldsymbol{H}_{RD}\boldsymbol{M}_R)\boldsymbol{B}\}+\mathrm{trace}\{\boldsymbol{I}_{N_D}\},\end{aligned} \tag{4.60}$$

where $\boldsymbol{B}$ is given by

$$\boldsymbol{B}=\boldsymbol{W}_R^{\dagger}\boldsymbol{W}_R. \tag{4.61}$$

In the case of one data stream, Ł = 1, $\boldsymbol{B}$ is a scalar and (4.60) simplifies to

$$(\boldsymbol{M}_R^{\dagger}\boldsymbol{H}_{RD}^{\dagger}\boldsymbol{H}_{RD}\boldsymbol{M}_R)\boldsymbol{B}+\boldsymbol{N}_D. \tag{4.62}$$

The leakage power from (4.52) is given by

$$\begin{aligned}&\mathrm{E}\{\mathrm{trace}\{(\boldsymbol{H}_{RD}\boldsymbol{M}_R\boldsymbol{W}_R^{\dagger}\boldsymbol{H}_{RR}\boldsymbol{x}_R^{d}+\boldsymbol{H}_{RR}\boldsymbol{x}_R)(\boldsymbol{x}_R^{\dagger}\boldsymbol{H}_{RR}^{\dagger}+\boldsymbol{x}_R^{d\dagger}\boldsymbol{H}_{RR}^{\dagger}\boldsymbol{W}_R\boldsymbol{M}_R^{\dagger}\boldsymbol{H}_{RD}^{\dagger})\}\},\\&=\mathrm{E}\{\mathrm{trace}\{\boldsymbol{H}_{RD}\boldsymbol{M}_R\boldsymbol{W}_R^{\dagger}\boldsymbol{H}_{RR}\boldsymbol{C}\boldsymbol{H}_{RR}^{\dagger}\boldsymbol{W}_R\boldsymbol{M}_R^{\dagger}\boldsymbol{H}_{RD}^{\dagger}+\boldsymbol{H}_{RR}\boldsymbol{C}\boldsymbol{H}_{RR}^{\dagger}\}\},\\&=\mathrm{trace}\{(\boldsymbol{M}_R^{\dagger}\boldsymbol{H}_{RD}^{\dagger}\boldsymbol{H}_{RD}\boldsymbol{M}_R)\boldsymbol{D}+\boldsymbol{E}\},\end{aligned} \tag{4.63}$$

where

$$\begin{aligned}\boldsymbol{C}&=\mathrm{E}\{\boldsymbol{x}_R\boldsymbol{x}_R^{\dagger}\}=\mathrm{E}\{\boldsymbol{x}_R^{d}\boldsymbol{x}_R^{d\dagger}\},\\\boldsymbol{D}&=\boldsymbol{W}_R^{\dagger}\boldsymbol{H}_{RR}\boldsymbol{C}\boldsymbol{H}_{RR}^{\dagger}\boldsymbol{W}_R,\\\boldsymbol{E}&=\boldsymbol{H}_{RR}\boldsymbol{C}\boldsymbol{H}_{RR}^{\dagger}.\end{aligned} \tag{4.64}$$

In the case of one data stream, Ł = 1, $\boldsymbol{D}$ is a scalar and (4.63) simplifies to

$$(\boldsymbol{M}_R^{\dagger}\boldsymbol{H}_{RD}^{\dagger}\boldsymbol{H}_{RD}\boldsymbol{M}_R)\boldsymbol{D} + \text{trace}\{\boldsymbol{E}\}. \tag{4.65}$$

Using the signal power in (4.58) with the noise power in (4.62) and the leakage power in (4.65), the SLNR equation for Ł = 1 can be expressed as

$$\frac{\boldsymbol{A}(\boldsymbol{M}_R^{\dagger}\boldsymbol{H}_{RD}^{\dagger}\boldsymbol{H}_{RD}\boldsymbol{M}_R)}{\boldsymbol{B}(\boldsymbol{M}_R^{\dagger}\boldsymbol{H}_{RD}^{\dagger}\boldsymbol{H}_{RD}\boldsymbol{M}_R) + N_D + \boldsymbol{D}(\boldsymbol{M}_R^{\dagger}\boldsymbol{H}_{RD}^{\dagger}\boldsymbol{H}_{RD}\boldsymbol{M}_R) + \text{trace}\{\boldsymbol{E}\}}. \tag{4.66}$$

In order to compute the solution for the relay precoder, $\boldsymbol{M}_R$, (4.66) needs to be converted into the RR form. We rewrite (4.66) as

$$\frac{\boldsymbol{M}_R^{\dagger}\boldsymbol{Q}_1\boldsymbol{M}_R}{\boldsymbol{M}_R^{\dagger}\boldsymbol{Q}_2\boldsymbol{M}_R}, \tag{4.67}$$

where $\boldsymbol{Q}_1$ and $\boldsymbol{Q}_2$ are given by

$$\begin{aligned} \boldsymbol{Q}_1 &= \boldsymbol{A}\boldsymbol{H}_{RD}^{\dagger}\boldsymbol{H}_{RD}, \\ \boldsymbol{Q}_2 &= \frac{(\text{trace}\{\boldsymbol{E}\} + N_D)\boldsymbol{I}_{N_{RT}}}{(\boldsymbol{M}_R^{\dagger}\boldsymbol{M}_R)} + \boldsymbol{H}_{RD}^{\dagger}\boldsymbol{H}_{RD}(\boldsymbol{B} + \boldsymbol{D}). \end{aligned} \tag{4.68}$$

The SLNR precoder, $\boldsymbol{M}_R^U$, is constructed by taking the first leading eigenvector of $\boldsymbol{Q}_2^{-1}\boldsymbol{Q}_1$. This can only be done when using Ł = 1, as we have simplified the SLNR equation with the assumption that Ł = 1.

Obtaining this SLNR solution for the relay precoder is complicated and this is due to two issues:

Firstly, the solution for the SLNR cannot be computed without the assumption that Ł = 1. The reason is that using Ł = 1, some of the matrix constants can be converted to scalars and we can simplify the SLNR equation as shown in (4.66).

Secondly, the denominator in $\boldsymbol{Q}_2$ as shown in (4.68) contains the $\boldsymbol{M}_R^{\dagger}\boldsymbol{M}_R$ term. This means that initially, when we compute for the $\boldsymbol{M}_R$ using SLNR, we need to set an initial estimate of $\boldsymbol{M}_R$, i.e. $\boldsymbol{M}_R = [1, 0, \cdots, 0]^{\text{T}}$. Then update $\boldsymbol{M}_R$ using SLNR method, afterwards we update the $\boldsymbol{M}_R^{\dagger}\boldsymbol{M}_R$ term in $\boldsymbol{Q}_2$ and compute for the new $\boldsymbol{M}_R$ using the SLNR equation. We iterate this process until $\boldsymbol{M}_R$ converges.

Observing the signal term, $\boldsymbol{Q}_1$, with the noise and interference term, $\boldsymbol{Q}_2$, in (4.68), shows that they both contain the relay to destination channel, $\boldsymbol{H}_{RD}$. This means that when the SLNR wants to increase the signal term, at the same time it wants to increase the noise and interference term. Therefore the best approach is to increase the signal term only, which is similar to the SVD approach. Thus, the performance of SLNR is likely to be similar to SVD.

4.4.2 Near-optimal Scheme

In this section, we use a near-optimal scheme that uses RR to compute the source precoder and destination weight vector. The relay precoder and weight vector are computed using ad-hoc methods.

4.4.2.1 Iterative Near-optimal Scheme for the Source

The near-optimal scheme to compute the precoder, $\boldsymbol{M}_S$, and weight vector, $\boldsymbol{W}_D$, at the source and destination, respectively, uses an iterative algorithm based on the SINR in (4.10). The SINR is given by

$$\frac{\frac{1}{\text{Ł}}\text{trace}\{\boldsymbol{W}_D^\dagger \boldsymbol{H}_{RD}\boldsymbol{F}_R\boldsymbol{H}_{SR}\boldsymbol{M}_S\boldsymbol{M}_S^\dagger\boldsymbol{H}_{SR}^\dagger\boldsymbol{F}_R^\dagger\boldsymbol{H}_{RD}^\dagger\boldsymbol{W}_D\}}{\text{trace}\{\boldsymbol{W}_D^\dagger \boldsymbol{H}_{RD}\boldsymbol{F}_R\boldsymbol{H}_{RR}\boldsymbol{C}\boldsymbol{H}_{RR}^\dagger\boldsymbol{F}_R^\dagger\boldsymbol{H}_{RD}^\dagger\boldsymbol{W}_D + \boldsymbol{W}_D^\dagger \boldsymbol{H}_{RD}\boldsymbol{F}_R\boldsymbol{F}_R^\dagger\boldsymbol{H}_{RD}^\dagger\boldsymbol{W}_D + \boldsymbol{W}_D^\dagger\boldsymbol{W}_D\}}, \tag{4.69}$$

where Ł is the number of signal streams from the relay, $\boldsymbol{M}_S$ is the source precoder matrix, and $\boldsymbol{W}_D$ is the destination weight vector. $\boldsymbol{F}_R = \boldsymbol{M}_R\boldsymbol{W}_R^\dagger$ is the product of the relay precoder and weight vector. Setting

$$\begin{aligned}\boldsymbol{A}_{RR} &= \boldsymbol{H}_{RD}\boldsymbol{F}_R\boldsymbol{H}_{SR},\\ \boldsymbol{B}_{RR} &= \boldsymbol{H}_{RD}\boldsymbol{F}_R\boldsymbol{H}_{RR}\boldsymbol{C}\boldsymbol{H}_{RR}^\dagger\boldsymbol{F}_R^\dagger\boldsymbol{H}_{RD}^\dagger + \boldsymbol{H}_{RD}\boldsymbol{F}_R\boldsymbol{F}_R^\dagger\boldsymbol{H}_{RD}^\dagger + \boldsymbol{I}_{N_{RT}},\end{aligned} \tag{4.70}$$

(4.69) can be simplified to

$$\frac{\text{trace}\{\boldsymbol{W}_D^\dagger\boldsymbol{A}_{RR}\boldsymbol{M}_S\boldsymbol{M}_S^\dagger\boldsymbol{A}_{RR}^\dagger\boldsymbol{W}_D\}}{\text{Ł}\text{trace}\{\boldsymbol{W}_D^\dagger\boldsymbol{B}_{RR}\boldsymbol{W}_D\}}. \tag{4.71}$$

Table 4.7 Algorithm to compute source precoder ($\boldsymbol{M}_S$) and destination weight ($\boldsymbol{W}_D$)

Step	Procedure
1.	Create a $(N_D \times L)$ identity rectangular matrix $\boldsymbol{W}_D$
2.	Use (4.73) to update $\boldsymbol{M}_S$
3.	Use (4.74) to update $\boldsymbol{W}_D$
4.	Compute step 2 and 3 until convergence is reached

Consider the numerator in (4.71). Using the properties of the trace operator, (trace$\{\boldsymbol{A}\boldsymbol{B}\boldsymbol{B}^\dagger\boldsymbol{A}^\dagger\}$ = trace$\{\boldsymbol{B}^\dagger\boldsymbol{A}^\dagger\boldsymbol{A}\boldsymbol{B}\}$), the numerator can be rearranged to

$$\text{trace}\{\boldsymbol{M}_S^\dagger\boldsymbol{A}_{RR}^\dagger\boldsymbol{W}_D\boldsymbol{W}_D^\dagger\boldsymbol{A}_{RR}\boldsymbol{M}_S\}. \tag{4.72}$$

Using the known values of $\boldsymbol{W}_D, \boldsymbol{M}_R$ and $\boldsymbol{W}_R$ with the RR technique in (2.22), $\boldsymbol{M}_S$ is calculated by taking the leading Ł (data streams) eigenvectors of

$$\boldsymbol{A}_{RR}^\dagger\boldsymbol{W}_D\boldsymbol{W}_D^\dagger\boldsymbol{A}_{RR}. \tag{4.73}$$

The destination weight vector, $\boldsymbol{W}_D$, in (4.71) is calculated (with the known values of $\boldsymbol{M}_S, \boldsymbol{M}_R, \boldsymbol{W}_R$) using the SLNR equation in (2.14). Then $\boldsymbol{W}_D$ is computed by taking the leading Ł eigenvectors of

$$\boldsymbol{B}_{RR}^{-1}\boldsymbol{A}_{RR}\boldsymbol{M}_S\boldsymbol{M}_S^\dagger\boldsymbol{A}_{RR}^\dagger. \tag{4.74}$$

As this is an iterative process, we initialise $\boldsymbol{M}_S$ and $\boldsymbol{W}_D$ to a starting value (e.g. an identity matrix). Then we iterate between (4.73) and (4.74) to compute the values of $\boldsymbol{M}_S$ and $\boldsymbol{W}_D$ until both of them converge.

Using (4.73) and (4.74), the source precoder and destination decoder can be calculated using the algorithm shown in Table 4.7.

4.5 SIMULATION RESULTS

The performances of different precoder and weight vector designs, such as SSSS, SSZS, SMSS, SSSM and SSLS (See Table 4.8), are simulated over 5,000 different channel realisations. We set all of the precoders and weight vectors to SVD as a base design then alter each of the

precoders and weight vectors individually to compare the different design techniques. Therefore, a character change in each of the design names and the placement of the changed character shows which precoder or weight vector has been altered. The simulation results are calculated by computing the source precoder, $\boldsymbol{M}_S$, relay weight vector, $\boldsymbol{W}_R$, relay precoder, $\boldsymbol{M}_R$, and destination weight vector, $\boldsymbol{W}_D$, then substituting them into the SINR equation (4.10). The results plotted are the cumulative distribution function (CDF) of rate and the CDF SINR. The rate (capacity) is calculated using $R = \log_2(1 + \text{SINR})$ and the SINR is calculated using (4.10).

For comparison purposes, we use the SVD design in both HD and FD modes, labeled as SSSS (HD) and SSSS, respectively. In HD mode, there is no LI and the optimal approach is to transmit signals through the strongest eigenchannel using SVD. In FD mode, the SSSS design does not consider SI, but it is deployed in the presence of SI. Hence, SSSS (HD) and SSSS are useful benchmarks. Where SSSS (HD) corresponds to a system with no SI effects and SSSS is a system, which is optimised for the zero SI secnario, but is deployed in the presence of SI. The rate calculation for the SSSS (HD) design is given by

$$R = \frac{1}{2}\log_2(1 + \text{SINR}) \tag{4.75}$$

4.5.1 Pure Ad-hoc Solution

4.5.1.1 Individual Design Performance

In this section, we compare the different ad-hoc methods as shown in Table 4.8. These designs are simulated using single stream transmission ($L = 1$) in a LOS ($K = 10$dB for all of the channels) environment. The SNR at the relay, $\text{SNR}_{\text{H}_{\text{SR}}}$, and destination, $\text{SNR}_{\text{H}_{\text{RD}}}$, receiver are both 10dB and the interference to noise ratio, INR, at the relay receiver, $\text{INR}_{\text{H}_{\text{RR}}}$, is 5dB. The antenna number configurations are $N_S = 2$, $N_{RR} = 2$, $N_{RT} = 3$, $N_D = 2$ for Figure 4.2 to Figure 4.5 and $N_S = 2$, $N_{RR} = 4$, $N_{RT} = 2$, $N_D = 2$ for Figure 4.6. The reason for a different antenna configuration for Figure 4.6, is to satisfy the antenna constraint for the ZF weight vector. The SINR results from Figure 4.2 to Figure 4.6 show that the SSSS (HD) design always has a greater SINR compared to other FD designs due to no interference at the relay. However, in the plots

Table 4.8 Precoder and weight vector specifications

Design	$\boldsymbol{M}_S$	$\boldsymbol{W}_R$	$\boldsymbol{M}_R$	$\boldsymbol{W}_D$
SSSS	SVD	SVD	SVD	SVD
SMSS	SVD	MMSE	SVD	SVD
SSZS	SVD	SVD	ZF	SVD
SSLS	SVD	SVD	SLNR	SVD
SSSM	SVD	SVD	SVD	MMSE
SZSS	SVD	ZF	SVD	SVD
SSSS (HD)	SVD	SVD	SVD	SVD

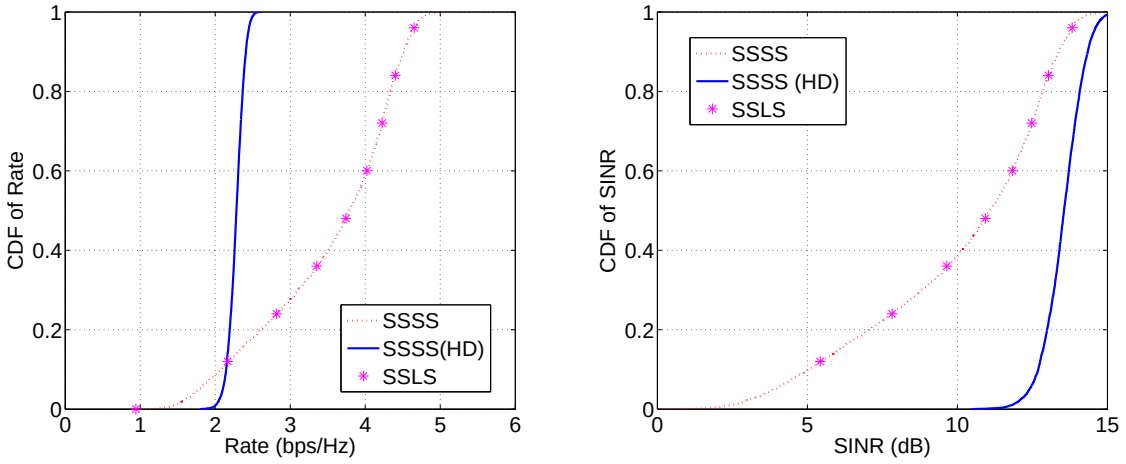

Figure 4.2 Rate and SINR CDFs for SSSS, SSLS and SSSS (HD) designs. ($\text{SNR}_{\text{H}_{\text{SR}}} = 10$ dB, $\text{INR}_{\text{H}_{\text{RR}}} = 5$ dB, $\text{SNR}_{\text{H}_{\text{RD}}} = 10$ dB, $N_S = 2$, $N_{RR} = 2$, $N_{RT} = 3$, $N_D = 2$, $K_{\text{SR}} = 10$ dB, $K_{\text{RR}} = 10$ dB, $K_{\text{RD}} = 10$ dB) .

using rates, the SSSS (HD) design, has a decreased performance compared to the other FD designs. This is caused by halving the rate for SSSS (HD), since SSSS (HD) requires two time slots for transmission and reception.

Figure 4.2 shows the CDF plots for the rate using the SSLS design. It is noted that SSLS and SSSS designs have similar performance. The reason is that in the SLNR precoder design, the desired term and the noise term both contain the relay to destination channel, $\boldsymbol{H}_{RD}$[5]. Hence, when the SLNR increases the signal term, it will also increase the noise term. Thus, a better option is to increase the signal term, which has the same effect as the SVD solution.

Figure 4.3 shows the results of two different MMSE relay weight vector designs, SMSS-I and SMSS-MR, which are compared to the benchmark SSSS and SSSS (HD) designs. The MMSE

[5]The full SLNR analysis is described in 4.4.1.6.

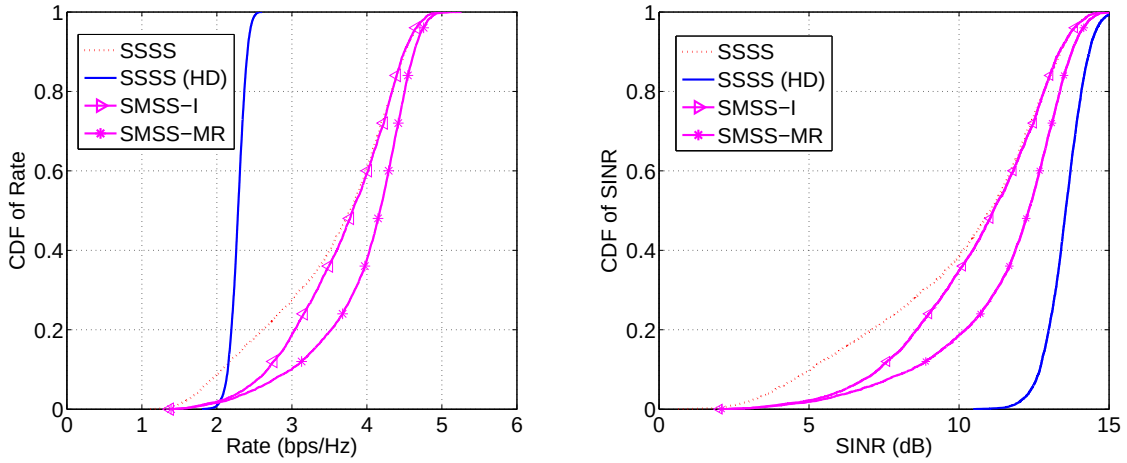

Figure 4.3 Rate and SINR CDFs for SSSS, SMSS-I, SMSS-MR and SSSS (HD) designs. ($\mathrm{SNR}_{\mathrm{H_{SR}}} = 10$ dB, $\mathrm{INR}_{\mathrm{H_{RR}}} = 5$ dB, $\mathrm{SNR}_{\mathrm{H_{RD}}} = 10$ dB, $N_S = 2$, $N_{RR} = 2$, $N_{RT} = 3$, $N_D = 2$, $K_{\mathrm{SR}} = 10$ dB, $K_{\mathrm{RR}} = 10$ dB, $K_{\mathrm{RD}} = 10$ dB) .

designs are classified by the different approximations used for the covariance matrix, $\boldsymbol{C}$. The approximations are given by

$$\begin{aligned} \boldsymbol{C} &= \frac{1}{\mathrm{L}}\boldsymbol{I}_{N_{RT}}, \\ \boldsymbol{C} &= K\boldsymbol{M}_R\boldsymbol{M}_R^{\dagger}, \end{aligned} \tag{4.76}$$

respectively. The constant, $K = \frac{1}{\mathrm{trace}\{\boldsymbol{M}_R\boldsymbol{M}_R^{\dagger}\}}$ is a scaling factor for $\boldsymbol{C}$ which is defined to have a unit trace.

Figure 4.3, shows that using $K\boldsymbol{M}_R\boldsymbol{M}_R^{\dagger}$ as the approximation for $\boldsymbol{C}$ gives a better performance compared to using an identity matrix. Using $\frac{1}{\mathrm{L}}\boldsymbol{I}_{N_{RT}}$ oversimplifies the approximation and the results show that the identity matrix is not the best substitute for $\boldsymbol{C}$.

As the SMSS-MR design has a better performance than SMSS-I, we use SMSS-MR as the SMSS design throughout this thesis.

Figure 4.4 shows that the SSSM design has a similar performance to the SSSS design. This is due to the desired channel, interference channel and the covariance noise all containing the same leading term, $\boldsymbol{H}_{RD}\boldsymbol{M}_R\boldsymbol{W}_R^{\dagger}$, as shown in (4.46). This shows that when the MMSE destination weight vector is reducing the interference and noise, it also reduces the desired signal. Hence,

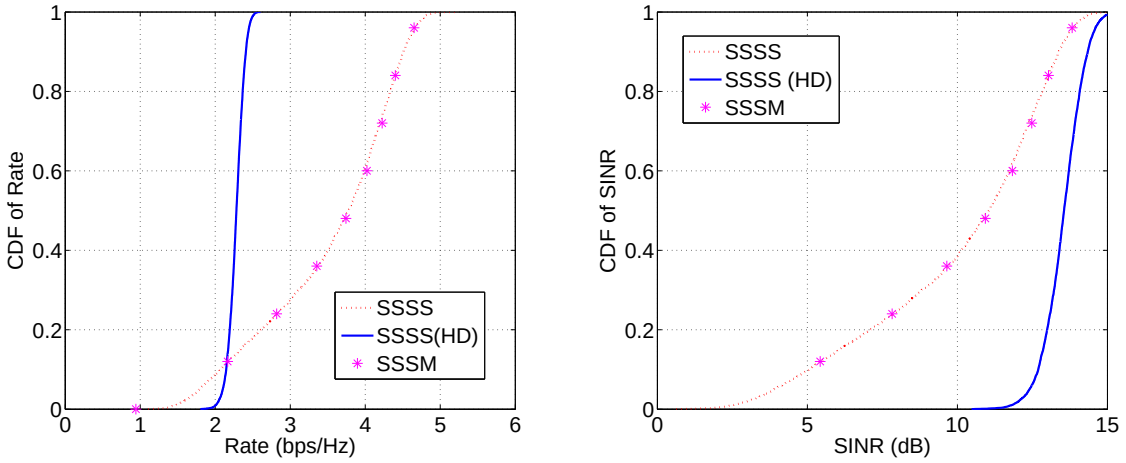

Figure 4.4 Rate and SINR CDFs for SSSS, SSSM and SSSS (HD) designs. ($\mathrm{SNR}_{\mathrm{H_{SR}}} = 10$ dB, $\mathrm{INR}_{\mathrm{H_{RR}}} = 5$ dB, $\mathrm{SNR}_{\mathrm{H_{RD}}} = 10$ dB, $N_S = 2$, $N_{RR} = 2$, $N_{RT} = 3$, $N_D = 2$, $K_{\mathrm{SR}} = 10$ dB, $K_{\mathrm{RR}} = 10$ dB, $K_{\mathrm{RD}} = 10$ dB) .

similar to the SLNR solution, the best approach is to increase the desired signal.

Figure 4.5 and Figure 4.6 show the performance of the ZF relay precoder and weight vector designs, respectively. These figures show that the ZF precoder, SSZS, has a better performance than the ZF weight vector, SZSS. The reason for this is, at the relay receiver, the SSZS design uses SVD to increase the desired channel, which also increases the e2e SINR. However, SZSS only removes the interference channel. For AF relays, the SNR at the relay's input will not be higher than the output. Hence, increasing the desired channel at the relay receiver has a better overall performance compared to increasing the desired channel at the relay transmitter. Since SSZS has a better performance than SZSS, we use SSZS for the ZF design to compare with the other designs.

4.5.1.2 Comparison Between Different Designs in a Rician Fading Channel

In this section, we compare the performance between different designs for a range of INR values, i.e. INR is set to 0dB (low), 5 dB(medium) and 10dB (high). The results are given in terms of rate CDFs. The plots shown on the left hand side of Figure 4.7 to Figure 4.9 represent a one stream scenario ($\mathrm{L} = 1$) system. The two stream ($\mathrm{L} = 2$) scenario is shown on the right hand side of Figure 4.7 to Figure 4.9. The rate for $\mathrm{L} = 2$ is given by $R = \log_2(1+\mathrm{SINR}_1)+\log_2(1+\mathrm{SINR}_2)$, where SINR_1 is the SINR for the first stream and SINR_2 is the SINR for the second stream. For

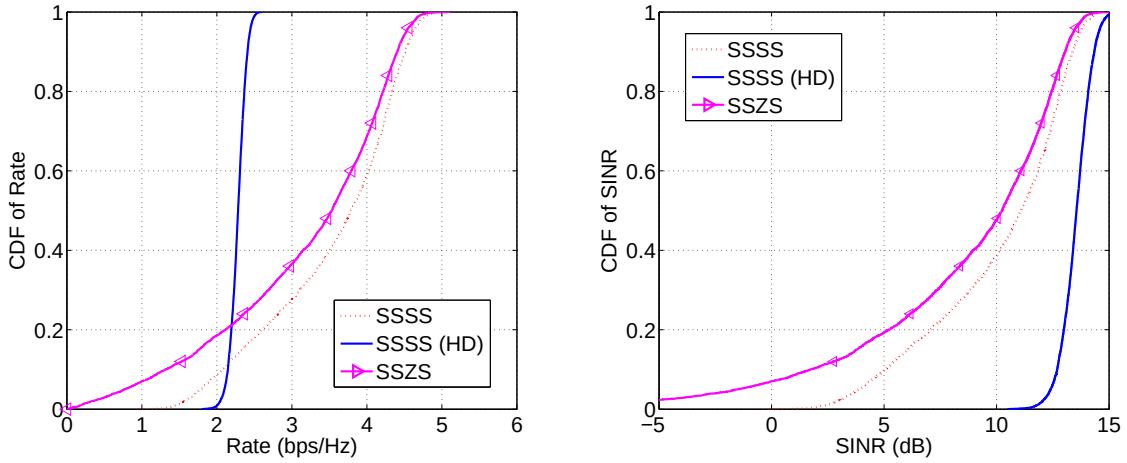

Figure 4.5 Rate and SINR CDFs for SSSS, SZSS and SSSS (HD) designs. ($\mathrm{SNR}_{\mathrm{H_{SR}}} = 10$ dB, $\mathrm{INR}_{\mathrm{H_{RR}}} = 5$ dB, $\mathrm{SNR}_{\mathrm{H_{RD}}} = 10$ dB, $N_S = 2$, $N_{RR} = 2$, $N_{RT} = 3$, $N_D = 2$, $K_{\mathrm{SR}} = 10$ dB, $K_{\mathrm{RR}} = 10$ dB, $K_{\mathrm{RD}} = 10$ dB) .

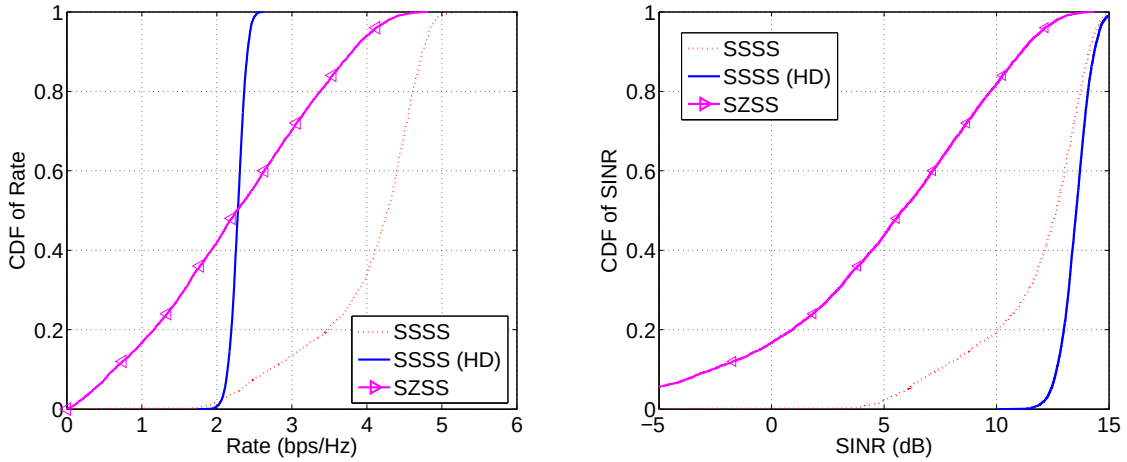

Figure 4.6 Rate and SINR CDFs for SSSS, SSZS and SSSS (HD) designs. ($\mathrm{SNR}_{\mathrm{H_{SR}}} = 10$ dB, $\mathrm{INR}_{\mathrm{H_{RR}}} = 5$ dB, $\mathrm{SNR}_{\mathrm{H_{RD}}} = 10$ dB, $N_S = 2$, $N_{RR} = 3$, $N_{RT} = 2$, $N_D = 2$, $K_{\mathrm{SR}} = 10$ dB, $K_{\mathrm{RR}} = 10$ dB, $K_{\mathrm{RD}} = 10$ dB) .

the SSSS (HD) design, when Ł = 2, the rate is given by $R = \frac{1}{2}\log_2(1+\mathrm{SINR}_1)+\frac{1}{2}\log_2(1+\mathrm{SINR}_2)$.

Figure 4.7 to Figure 4.9 show the performance of the SSSS, SMSS, SSZS, SSSS (HD) and SSSM designs when the INR at the relay is decreased. The SSLS design is only used in the Ł = 1 case which is only designed for a one stream system. For a two stream system, the solution of the SLNR is difficult or impossible to obtain as the constant terms do not reduce to scalars. From these figures, both SSLS and SSSM have virtually the same performance as SSSS for every scenario. The reason for this is, in both designs, the interference term contains the same channel,

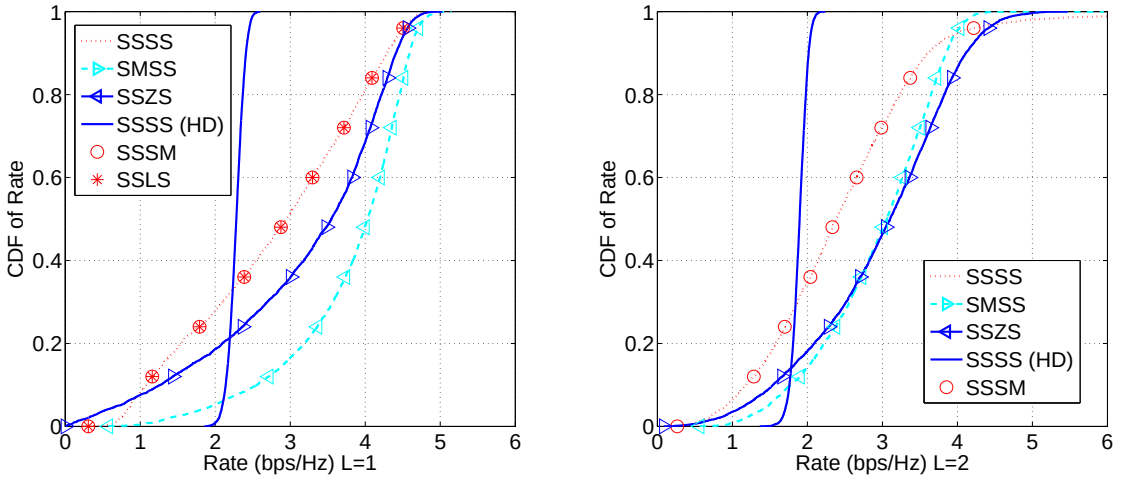

Figure 4.7 High SI. Rate CDFs for SSSS, SZSS, SSSM, SMSS, SSLS and SSSS (HD) designs. ($\mathrm{SNR}_{\mathrm{H_{SR}}}$ = 10 dB, $\mathrm{INR}_{\mathrm{H_{RR}}}$ = 10 dB, $\mathrm{SNR}_{\mathrm{H_{RD}}}$ = 10 dB, K_{SR} = 10 dB, K_{RR} = 10 dB, K_{RD} = 10 dB)(N_S = 2, N_{RR} = 2, N_{RT} = 3, N_D = 2 for L=1), (N_S = 2, N_{RR} = 2, N_{RT} = 4, N_D = 2 for L=2) .

the relay to destination channel, as the desired signal. Hence, the best approach is to increase the desired channel component, which is similar to the process of SVD.

The SMSS design has the best performance. The SSSS design has a better performance than SZSS when the INR is small (0 dB) but the SZSS has a better performance compared with SSSS when INR is large (10 dB). Here, when the interference is large, it needs to be removed using the ZF technique in the SSZS design. In contrast, when the interference is small, the system can have a higher transmission rate by increasing the signal channel using the SVD technique in the SSSS design.

Note that the overall performance of Ł = 2 is a lower than Ł = 1 as the energy of each source is halved. With Ł = 2, the energy is divided between the two streams, where generally one stream has a greater SNR than the the other. This results in a decrease in the overall received SNR. In the case of the one stream, Ł = 1, all the energy is transmitted only through the channel that has the highest SNR.

Figure 4.10 shows a comparison between SSSS, SMSS and SSZS designs by adjusting the INR value at the relay receiver (High: $\mathrm{INR}_{\mathrm{H_{RR}}}$=10dB, Mid: $\mathrm{INR}_{\mathrm{H_{RR}}}$=5dB and Low: $\mathrm{INR}_{\mathrm{H_{RR}}}$=0dB). The designs that only contain a line in the graph show the simulation when the INR is set 0 dB. The design that contain both a line and a marker in the graph show that the design is simulated

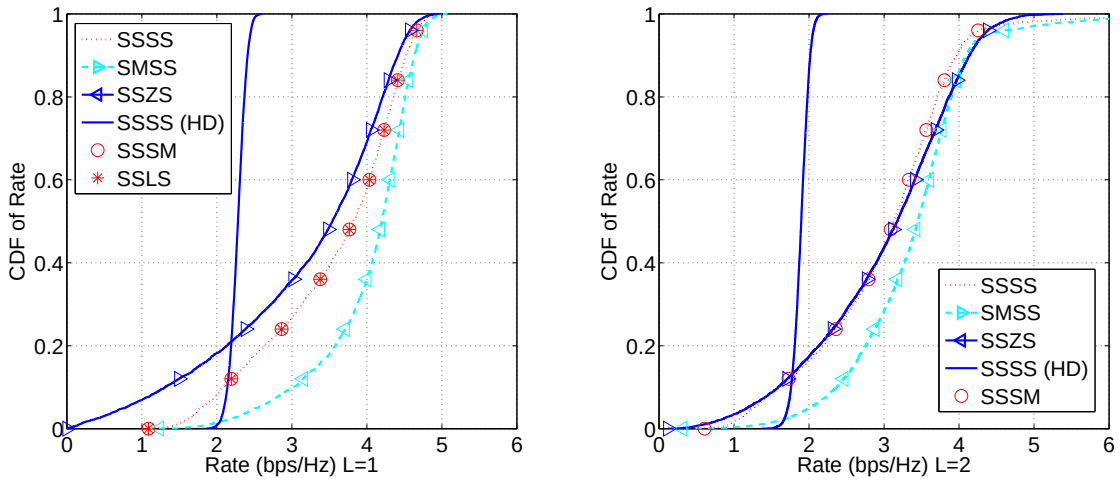

Figure 4.8 Medium SI. Rate CDFs for SSSS, SZSS, SSSM, SMSS, SSLS and SSSS (HD) designs ($\mathrm{SNR}_{\mathrm{H_{SR}}} = 10$ dB, $\mathrm{INR}_{\mathrm{H_{RR}}} = 5$ dB, $\mathrm{SNR}_{\mathrm{H_{RD}}} = 10$ dB, $K_{\mathrm{SR}} = 10$ dB, $K_{\mathrm{RR}} = 10$ dB, $K_{\mathrm{RD}} = 10$ dB)($N_S = 2$, $N_{RR} = 2$, $N_{RT} = 3$, $N_D = 2$ for L=1), ($N_S = 2$, $N_{RR} = 2$, $N_{RT} = 4$, $N_D = 2$ for L=2) .

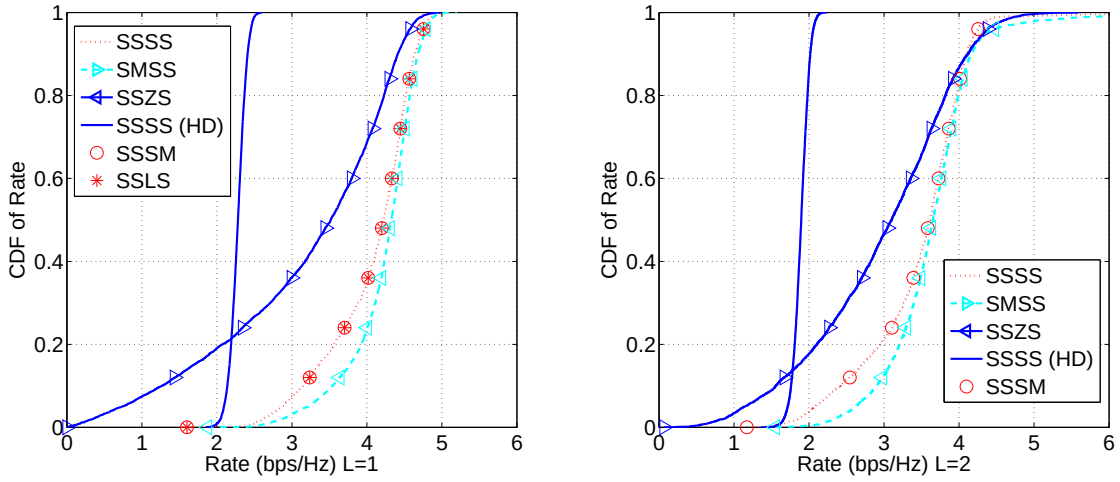

Figure 4.9 Low SI. Rate CDFs for SSSS, SZSS, SSSM, SMSS, SSLS and SSSS (HD) designs ($\mathrm{SNR}_{\mathrm{H_{SR}}} = 10$ dB, $\mathrm{INR}_{\mathrm{H_{RR}}} = 0$ dB, $\mathrm{SNR}_{\mathrm{H_{RD}}} = 10$ dB, $K_{\mathrm{SR}} = 10$ dB, $K_{\mathrm{RR}} = 10$ dB, $K_{\mathrm{RD}} = 10$ dB)($N_S = 2$, $N_{RR} = 2$, $N_{RT} = 3$, $N_D = 2$ for L=1), ($N_S = 2$, $N_{RR} = 2$, $N_{RT} = 4$, $N_D = 2$ for L=2) .

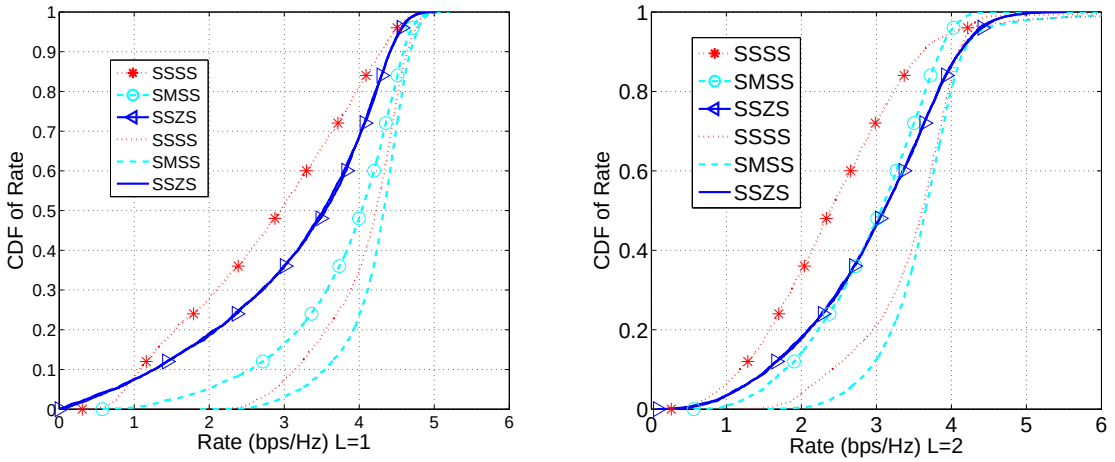

Figure 4.10 Rate CDFs for SSSS, SZSS and SMSS designs (Line: $\mathrm{SNR}_{\mathrm{H_{SR}}} = 10$ dB, $\mathrm{INR}_{\mathrm{H_{RR}}} = 0$ dB, $\mathrm{SNR}_{\mathrm{H_{RD}}} = 10$ dB),(Marker: $\mathrm{SNR}_{\mathrm{H_{SR}}} = 10$ dB, $\mathrm{INR}_{\mathrm{H_{RR}}} = 10$ dB, $\mathrm{SNR}_{\mathrm{H_{RD}}} = 10$ dB) ($K_{\mathrm{SR}} = 10$ dB, $K_{\mathrm{RR}} = 10$ dB, $K_{\mathrm{RD}} = 10$ dB)($N_S = 2$, $N_{RR} = 2$, $N_{RT} = 3$, $N_D = 2$ for L=1), ($N_S = 2$, $N_{RR} = 2$, $N_{RT} = 4$, $N_D = 2$ for L=2) .

when the INR is set to 10 dB. This shows that SSSS and SMSS increase their performance when the INR is reduced. However, the SSZS design remains constant when the INR is being altered. This is because ZF only removes the interference signal component and does not improve the desired channel link.

Figure 4.10 shows that it is easier to reduce the interference signal and increase the desired signal using processing such as MMSE at the front end of the relay receiver. The desired signal and the interference signal are independent of each other, because they are transmitted from two different channels. However, processing at the front end of the relay transmitter is difficult as the signal has already a combination of the desired and interference signal. This is also a property of AF relays where the SNR of the signal at the relay receiver will be the same or lower than at the relay transmitter.

4.5.1.3 Comparison Between Different Designs in a Rayleigh Fading Channel

In this section, we use the same precoder and weight vector designs as before but simulate the relay MIMO system in a Rayleigh fading channel.

Figure 4.11 to Figure 4.13 show the performance of different precoder and weight vector designs

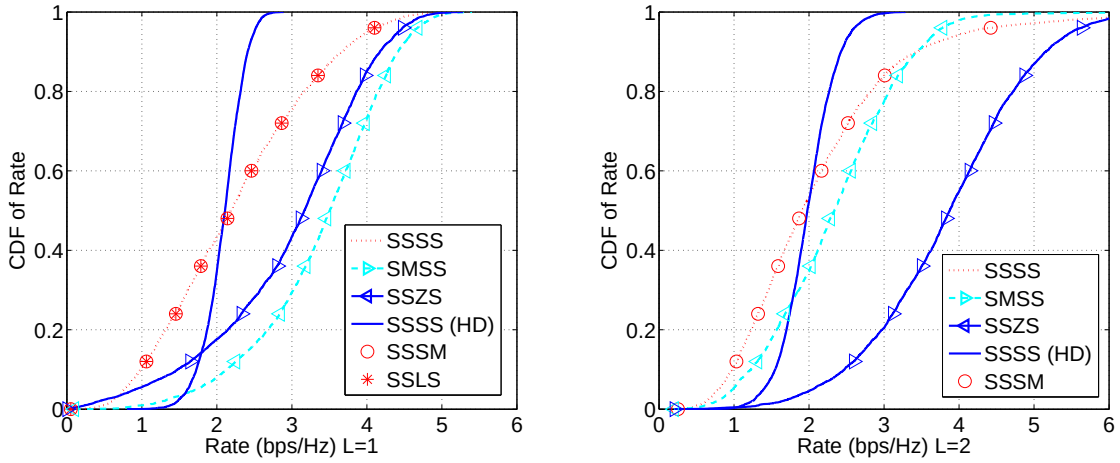

Figure 4.11 High SI. Rate CDFs for SSSS, SZSS, SSSM, SMSS, SSLS and SSSS (HD) designs ($\mathrm{SNR}_{\mathrm{H_{SR}}} = 10$ dB, $\mathrm{INR}_{\mathrm{H_{RR}}} = 10$ dB, $\mathrm{SNR}_{\mathrm{H_{RD}}} = 10$ dB, $K_{\mathrm{SR}} = 1e^{-8}$ dB, $K_{\mathrm{RR}} = 1e^{-8}$ dB, $K_{\mathrm{RD}} = 1e^{-8}$ dB)($N_S = 2$, $N_{RR} = 2$, $N_{RT} = 3$, $N_D = 2$ for L=1), ($N_S = 2$, $N_{RR} = 2$, $N_{RT} = 4$, $N_D = 2$ for L=2) .

in a Rayleigh fading channel. The rate of all of the designs are higher in the Rayleigh fading channel compared with Rician fading channel. This is expected as the Rayleigh fading channel has rich scattering that increases the rank of the channel and improves the diversity of the MIMO system.

The different designs, such as SSSS, SLSS, SMSS, SSZS and SSSM, all have the same performance in the Rician and Rayleigh channel in the one stream case. In Ł = 2 case, the SSZS design has the best performance when compared with all the other designs in the Rayleigh fading channel. It even outperforms SSZS for the Ł = 1 case and its rate is better than SMSS. For the Ł = 2 case, SSZS has a higher rate than the Ł = 1 case and its rate is better than SMSS. The reason is that when there are four antennas at the transmitter and only two antennas at the receiver, the SMSS design lacks enough degrees of freedom to cancel out the interference and noise. In the Rician channel with Ł = 2 scenario, since the channel is a rank deficient, it has a similar performance when Ł = 1.

4.5.1.4 Comparison Between SMSS and SSSS with Various System Sizes

In this section, the e2e SINR is compared by changing the antenna numbers at the source, at the relay and at the destination. We implement SMSS, which is the best overall design and

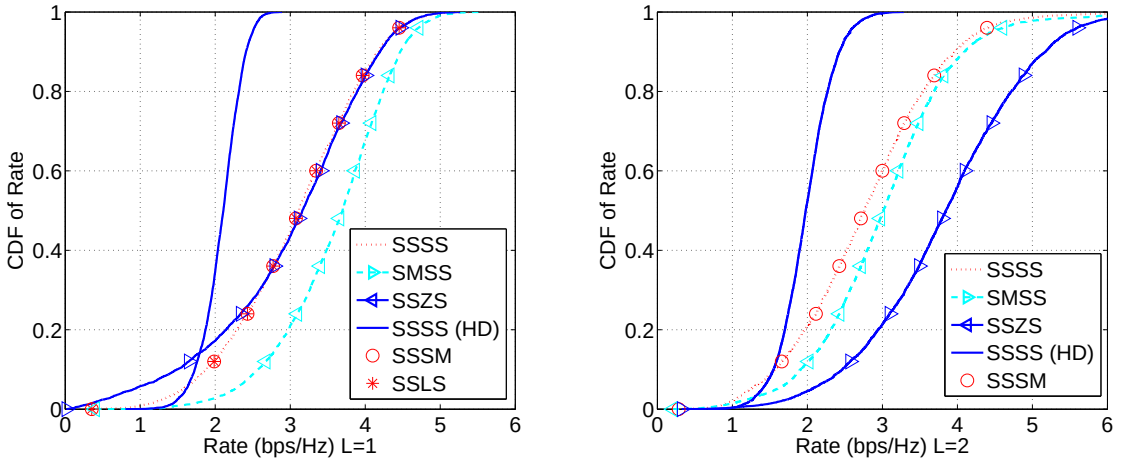

Figure 4.12 Medium SI. Rate CDFs for SSSS, SZSS, SSSM, SMSS, SSLS and SSSS (HD) designs ($\text{SNR}_{\text{H}_{\text{SR}}} = 10$ dB, $\text{INR}_{\text{H}_{\text{RR}}} = 5$ dB, $\text{SNR}_{\text{H}_{\text{RD}}} = 10$ dB, $K_{\text{SR}} = 1e^{-8}$ dB, $K_{\text{RR}} = 1e^{-8}$ dB, $K_{\text{RD}} = 1e^{-8}$ dB)($N_S = 2$, $N_{RR} = 2$, $N_{RT} = 3$, $N_D = 2$ for L=1), ($N_S = 2$, $N_{RR} = 2$, $N_{RT} = 4$, $N_D = 2$ for L=2) .

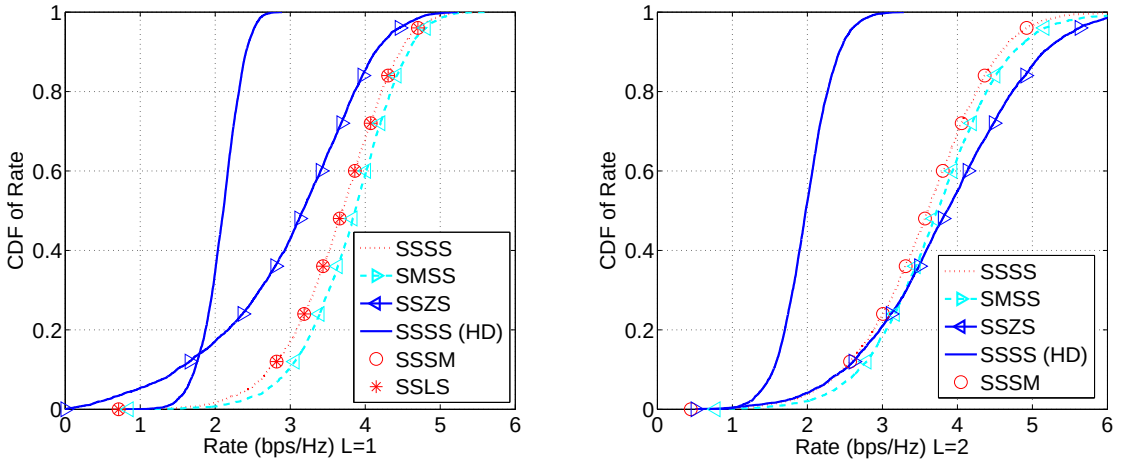

Figure 4.13 Low SI. Rate CDFs for SSSS, SZSS, SSSM, SMSS, SSLS and SSSS (HD) designs ($\text{SNR}_{\text{H}_{\text{SR}}} = 10$ dB, $\text{INR}_{\text{H}_{\text{RR}}} = 0$ dB, $\text{SNR}_{\text{H}_{\text{RD}}} = 10$ dB, $K_{\text{SR}} = 1e^{-8}$ dB, $K_{\text{RR}} = 1e^{-8}$ dB, $K_{\text{RD}} = 1e^{-8}$ dB),($N_S = 2$, $N_{RR} = 2$, $N_{RT} = 3$, $N_D = 2$ for L=1), ($N_S = 2$, $N_{RR} = 2$, $N_{RT} = 4$, $N_D = 2$ for L=2) .

compare it with the SSSS design.

Figure 4.15 shows the comparison between the rate of SMSS and SSSS with various antenna combinations. The configuration, $N_S = 2, N_{RR} = 4, N_{RT} = 4, N_D = 2$ (circle) gives the best performance followed by $N_S = 4, N_{RR} = 2, N_{RT} = 2, N_D = 4$ (line) and then $N_S = 2, N_{RR} = 2, N_{RT} = 2, N_D = 2$ (triangle). The triangle configuration has the least number of antennas so will be used as a benchmark to compare the other configurations. This configuration also has

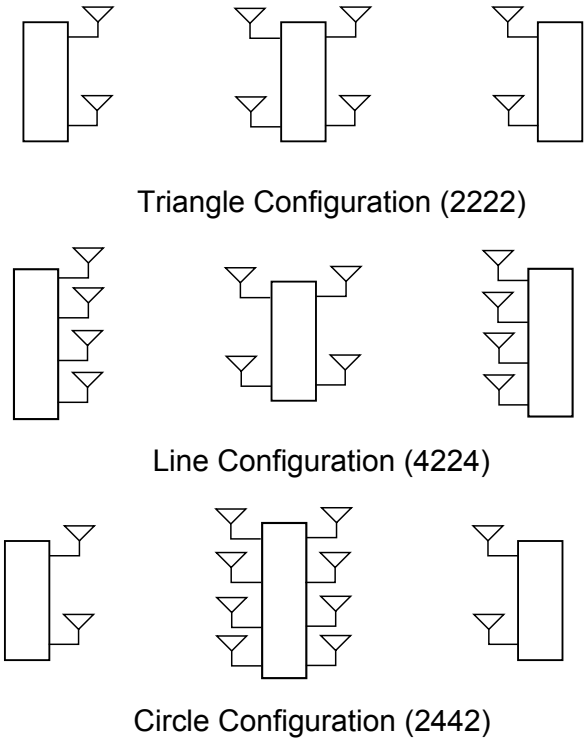

Figure 4.14 Antenna configurations for the compared designs.

the lowest e2e performance when compared to the other designs.

In Figure 4.15, the circle configuration has extra antennas at the relay. This allows more freedom to transmit and receive on the highest SNR channel which will reduce the SI. The line configuration has extra antennas at the source and destination which can only be used to boost the desired signal component. Therefore the performance is reduced when compared with the circle configuration.

From Figure 4.15, the best design is SMSS for the Ł = 1 case. For Ł = 2 case, SSSS has a higher rate at the 90^{th} percentile. The reason is in a Ł = 2 case, SVD is useful as it can diagonalise and avoid interference between streams in the channel by creating parallel channel decomposition.

4.5.2 Near-optimal Solution

In addition to ad-hoc methods, a near-optimal design is used to improve the MIMO system. This design is constructed using optimal RR techniques for the source precoder and destination

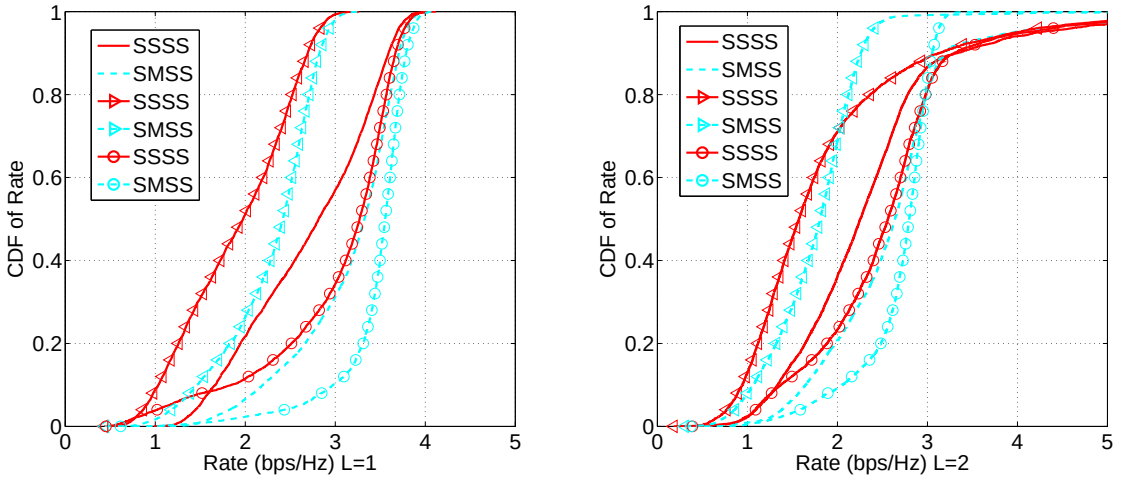

Figure 4.15 Rate CDFs for SSSS and SMSS designs. ($\text{SNR}_{\text{H}_{\text{SR}}} = 5$ dB, $\text{INR}_{\text{H}_{\text{RR}}} = 5$ dB, $\text{SNR}_{\text{H}_{\text{RD}}} = 5$ dB. Line: $N_S = 4, N_{RR} = 2, N_{RT} = 2, N_D = 4$, Triangle: $N_S = 2, N_{RR} = 2, N_{RT} = 2, N_D = 2$, Circle: $N_S = 2, N_{RR} = 4, N_{RT} = 4, N_D = 2$, $K_{\text{SR}} = 10$ dB, $K_{\text{RR}} = 10$ dB, $K_{\text{RD}} = 10$ dB) .

Table 4.9 Precoder and weight vector specifications

Design	$\boldsymbol{M}_S$	$\boldsymbol{W}_R$	$\boldsymbol{M}_R$	$\boldsymbol{W}_D$
ITE	RR	MMSE	SVD	RR

weight vector that are based on (4.69). The relay precoder and weight vector are implemented using SVD and MMSE, respectively, shown in Table 4.9. The number of antennas at each node are $N_S = 2$, $N_{RR} = 2$, $N_{RT} = 3$, $N_D = 2$ for Ł $= 1$ and $N_S = 2$, $N_{RR} = 2$, $N_{RT} = 4$, $N_D = 2$ for Ł $= 2$.

From Figure 4.16 and Figure 4.17, the performance of near-optimal design is similar to the performance of SMSS for both of the scenarios ($\text{INR}_{\text{H}_{\text{RR}}} = 0$ dB and $\text{INR}_{\text{H}_{\text{RR}}} = 10$ dB). This is due to the source node having no interference and the optimal method is transmitting signals on the strongest link that is similar to the SVD method. At the destination receiver, the relay to destination channel, $\boldsymbol{H}_{RD}$ carries both the signal and SI. This is shown in (4.5), where the destination receive weight vector is given by

$$\begin{aligned}\boldsymbol{y}_D = \boldsymbol{W}_D^{\dagger}\boldsymbol{H}_{RD}\boldsymbol{F}_R\boldsymbol{H}_{SR}\boldsymbol{M}_S\boldsymbol{d}_S + \boldsymbol{W}_D^{\dagger}\boldsymbol{H}_{RD}\boldsymbol{F}_R\boldsymbol{H}_{RR}\boldsymbol{x}_R^d \\ + \boldsymbol{W}_D^{\dagger}\boldsymbol{H}_{RD}\boldsymbol{F}_R\boldsymbol{n}_R + \boldsymbol{W}_D^{\dagger}\boldsymbol{n}_D,\end{aligned} \tag{4.77}$$

Therefore, increasing the signal component will also increase the SI component. Hence, the best

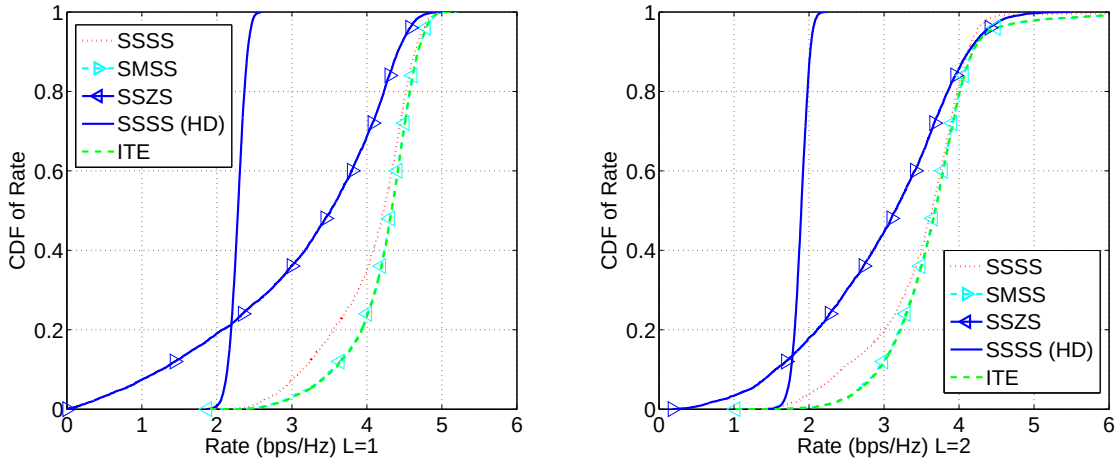

Figure 4.16 Rate CDFs for SSSS and SMSS designs. (Rate CDFs for SSSS, SMSS, SSZS, SSSM, SSSS (HD) and ITE designs. (($\mathrm{SNR}_{\mathrm{H_{SR}}} = 10$ dB, $\mathrm{INR}_{\mathrm{H_{RR}}} = 0$ dB, $\mathrm{SNR}_{\mathrm{H_{RD}}} = 10$ dB, $K_{\mathrm{SR}} = 10$ dB, $K_{\mathrm{RR}} = 10$ dB, $K_{\mathrm{RD}} = 10$ dB)($N_S = 2$, $N_{RR} = 2$, $N_{RT} = 3$, $N_D = 2$ for L=1)($N_S = 2$, $N_{RR} = 2$, $N_{RT} = 4$, $N_D = 2$ for L=2) .

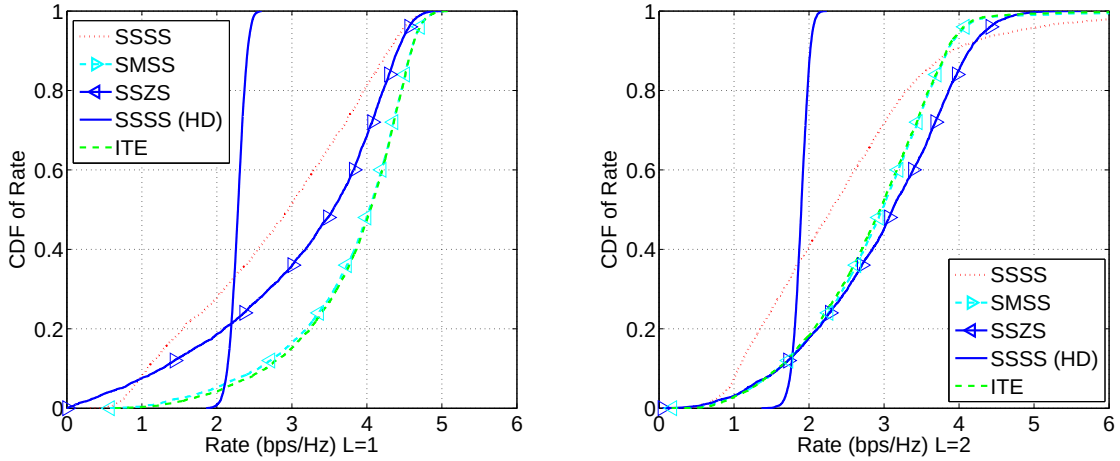

Figure 4.17 Rate CDFs for SSSS and SMSS designs. (Rate CDFs for SSSS, SMSS, SSZS, SSSM, SSSS (HD) and ITE designs. (($\mathrm{SNR}_{\mathrm{H_{SR}}} = 10$ dB, $\mathrm{INR}_{\mathrm{H_{RR}}} = 10$ dB, $\mathrm{SNR}_{\mathrm{H_{RD}}} = 10$ dB, $K_{\mathrm{SR}} = 10$ dB, $K_{\mathrm{RR}} = 10$ dB, $K_{\mathrm{RD}} = 10$ dB)($N_S = 2$, $N_{RR} = 2$, $N_{RT} = 3$, $N_D = 2$ for L=1)($N_S = 2$, $N_{RR} = 2$, $N_{RT} = 4$, $N_D = 2$ for L=2) .

approach is to increase the desired channel component which is similar to SVD.

4.5.3 Precoder and Weight Vector Design Complexity

These ad-hoc designs can increase the performance of the FD MIMO relay system. To compute these designs, such as the channel information, other precoder and/or weight vector values are required. Hence, it useful to know the channel information in calculating these precoder and

weight vector solutions. If these designs require a large amount of information transmitted between each link, such as channel state information, precoder and weight vector matrices, then the rate of the system may decrease. We will compare the information exchange required by SMSS with SSSS, as the SMSS solution gives the overall highest e2e SINR. The SSSS solution will be used as a benchmark.

For SMSS the:

Source TX requires

- $\boldsymbol{H}_{SR}$ (This is transmitted back from the relay to the source.)

Relay RX & TX require

- $\boldsymbol{H}_{RR}$ (This is obtained from channel estimation.)
- $\boldsymbol{H}_{RD}$ (This is transmitted back from the destination to the relay.)
- $\boldsymbol{H}_{SR}\boldsymbol{M}_{S}$ (This is the equivalent channel and is obtained from channel estimation.)

Destination RX requires

- $\boldsymbol{H}_{RD}$ (This is obtained from channel estimation.)

To compute the precoder and weight vectors of the SMSS design, the only information required to be transmitted between each of the nodes is $\boldsymbol{H}_{SR}$ and $\boldsymbol{H}_{RD}$. Therefore, the SMSS design is as efficient as SSSS.

For the SSSS approach at each node, the processing for computing the precoder or weight vector only uses eigenvalue decomposition. The SMSS design requires the processing of the eigenvalue decomposition, matrix multiplication and inverse operation. In general, the computational complexity of eigenvalue decomposition, matrix multiplication and matrix inversion all have $O(n^3)$ complexity [113]. Hence, the overall complexity of SSSS and SMSS are the same, but SMSS

gives a better performance than SSSS. This is because SMSS considers the noise and interference at the relay receiver.

4.6 SUMMARY

In this chapter, we used different precoder and weight vector designs (SSSS, SMSS, SSLS, SSSM, SSZS and SZSS) to increase the SINR of the one path MIMO relay system. We also constrain the average signal power transmitted from the relay by scaling the power of the relay precoder.

The results show that SMSS has the overall best performance. SSZS or SSSS was next depending on the level of SI. When SI is large (INR=10dB), then SSZS has a higher SINR and when SI is low (INR=0dB) then SSSS has a higher SINR. The SSLS and SSSM both have similar performance to SSSS as the signal and SI are both carried in the same relay to destination channel, $\boldsymbol{H}_{RD}$. But has higher complexity in the design.

The one stream case, Ł = 1, has a higher SINR than the two stream case, Ł = 2. The reason is that in the two stream case, the signal power of the two streams is shared where one stream has a higher SNR than the other. This results in a lower overall SNR, whereas for the one stream case the channel with the highest SNR is selected.

The near-optimal method has a similar performance to the SMSS design. This is due to the source having no interference and the optimal method will be similar to the SVD method. At the destination, the channel carries both the signal and SI. Therefore the best approach is to increase the signal component which is similar to the SVD method.

From the different precoder and weight vector designs, the key finding is that the SMSS is the best design as it gives the highest overall e2e SINR. This is because for AF relays, the signals and interference will be combined then amplified at transmitter side, therefore it is more effective to do processing at the receiver side.

Chapter 5

MIMO RELAY MODEL USING INSTANTANEOUS POWER NORMALISATION

In Chapter 4, the relay signal was constrained so that the average power of the signal transmitted from the relay is constant. Using this average power normalisation, there are some difficulties in setting up the system analysis. Firstly, the calculation of the covariance matrix needs to be derived as shown in Section 4.3. Secondly, a numerical method is required to find a scaling factor for the relay precoder, which constrains the relay signal to the correct size.

In this chapter, we consider a different relay power constraint where the relay transmit power is held constant and the relay signal is normalised by its instantaneous power as shown in Section 5.1. In Section 5.2, we derive the estimated SI signal that the relay receives under this scenario. In contrast to Chapter 4, we evaluate performance via the symbol error rate (SER) and the AF FD MIMO relay system is simulated using QPSK transmission. The SER is calculated and the results are shown in Section 5.3. Afterwards, in Section 5.4, we present an initial derivation for the rate of the instantaneous power normalisation approach and discuss the difficulties that arise. This analysis shows why the SER is a more straight forward metric method than calculating the rate for the instantaneous power normalisation approach.

5.1 SYSTEM MODEL

Consider an AF FD MIMO relay system as shown in Figure 4.1, where the signal is transmitted from the source to the relay and the relay amplifies the received desired signal plus SI and noise which then retransmits it to the destination. The power normalisation at the relay for the

transmitted signal is computed using the instantaneous signal power so that the relay transmits with constant power. We simulate this FD MIMO relay system as shown in Figure 4.1 by transmitting QPSK signals and using hard decoding at the destination. We consider the error performance of this AF FD MIMO relay system with different precoder and weight vector designs.

At the source, the complex QPSK signal is multiplied by a precoder before transmission. Using one stream transmission ($Ł = 1$), the transmitted signal is given by

$$\boldsymbol{x}_S = \boldsymbol{M}_S d_S, \tag{5.1}$$

where $\boldsymbol{M}_S$ is the source precoder and d_S is the desired source QPSK signal.

The received signal at the relay, after being multiplied by the relay weight vector, is given by

$$\boldsymbol{y}_R = \boldsymbol{W}_R^{\dagger}(\boldsymbol{H}_{SR}\boldsymbol{x}_S + \boldsymbol{H}_{RR}\boldsymbol{x}_R^D + \boldsymbol{n}_R), \tag{5.2}$$

where $\boldsymbol{H}_{SR}$ and $\boldsymbol{H}_{RR}$ are the source to relay and relay to relay channels, respectively. $\boldsymbol{W}_R$ is the relay weight vector and $\boldsymbol{n}_R$ is the receive noise vector. $\boldsymbol{x}_R^D$ is the delayed relay signal that the relay receives, which is transmitted from the relay transmitter through $\boldsymbol{H}_{RR}$ and this signal is considered as SI.

At the relay transmitter, the relay received signal is multiplied by a relay precoder, which gives the output

$$\boldsymbol{x}_R = \boldsymbol{M}_R \boldsymbol{y}_R, \tag{5.3}$$

where $\boldsymbol{M}_R$ is the relay precoder.

At the destination, the received signal, $\boldsymbol{x}_D$, is multipled by the destination weight vector, $\boldsymbol{W}_D$, which is given by

$$\boldsymbol{x}_D = \boldsymbol{W}_D^{\dagger}(\boldsymbol{H}_{RD}\boldsymbol{x}_R + \boldsymbol{n}_D). \tag{5.4}$$

Here, $\boldsymbol{H}_{RD}$ and $\boldsymbol{n}_D$ are the relay to destination channel and destination noise, respectively.

The SER is calculated by averaging the number of errors that are received at the destination.

The error is calculated by comparing the decoded signal at the destination, a quantised version of $\boldsymbol{x}_D$, with the desired signal at the source, d_S. This process is also known as hard decision decoding.

5.2 RELAY DELAYED SIGNAL CALCULATION

The signal, channel and noise can be randomly generated at any instant of time using Monte Carlo simulation. However, the SI signal is more difficult to generate, as it depends on the previous transmitted signals and also dependent on the relay precoder and weight vector. Hence, below we develop a method to generate the SI term required in the simulations.

Consider the relay signal as a function of time is given by

$$\begin{aligned}\boldsymbol{x}_R(t) &= \boldsymbol{M}_R\boldsymbol{W}_R^{\dagger}(\boldsymbol{H}_{SR}\boldsymbol{M}_S\boldsymbol{x}_S(t) + \boldsymbol{H}_{RR}\boldsymbol{x}_R(t-\tau) + \boldsymbol{n}_R(t)) \\ &= \boldsymbol{M}_R\boldsymbol{W}_R^{\dagger}\boldsymbol{H}_{SR}\boldsymbol{M}_S\boldsymbol{x}_S(t) + \boldsymbol{M}_R\boldsymbol{W}_R^{\dagger}\boldsymbol{H}_{RR}\boldsymbol{x}_R(t-\tau) + \boldsymbol{M}_R\boldsymbol{W}_R^{\dagger}\boldsymbol{n}_R(t). \end{aligned} \tag{5.5}$$

Using (5.5) at times $t-\tau$ and $t-2\tau$ gives

$$\begin{aligned}\boldsymbol{x}_R(t-\tau) &= \boldsymbol{A}\boldsymbol{x}_S(t-\tau) + \boldsymbol{B}\boldsymbol{x}_R(t-2\tau) + \boldsymbol{F}\boldsymbol{n}_R(t-\tau) \\ \boldsymbol{x}_R(t-2\tau) &= \boldsymbol{A}\boldsymbol{x}_S(t-2\tau) + \boldsymbol{B}\boldsymbol{x}_R(t-3\tau) + \boldsymbol{F}\boldsymbol{n}_R(t-2\tau), \end{aligned} \tag{5.6}$$

where

$$\begin{aligned}\boldsymbol{A} &= \boldsymbol{M}_R\boldsymbol{W}_R^{\dagger}\boldsymbol{H}_{SR}\boldsymbol{M}_S \\ \boldsymbol{B} &= \boldsymbol{M}_R\boldsymbol{W}_R^{\dagger}\boldsymbol{H}_{RR} \\ \boldsymbol{F} &= \boldsymbol{M}_R\boldsymbol{W}_R^{\dagger}, \end{aligned} \tag{5.7}$$

and we assume that $\boldsymbol{A}$, $\boldsymbol{B}$ and $\boldsymbol{F}$ are constant over the time period of interest. Substituting

$\boldsymbol{x}_R(t-\tau)$ from (5.6) in (5.5) gives

$$\begin{aligned}\boldsymbol{x}_R(t) &= \boldsymbol{A}\boldsymbol{x}_S(t) + \boldsymbol{B}[\boldsymbol{A}\boldsymbol{x}_S(t-\tau) + \boldsymbol{B}\boldsymbol{x}_R(t-2\tau) + \boldsymbol{F}\boldsymbol{n}_R(t-\tau)] + \boldsymbol{F}\boldsymbol{n}_R(t) \\ &= \boldsymbol{A}\boldsymbol{x}_S(t) + \boldsymbol{B}\boldsymbol{A}\boldsymbol{x}_S(t-\tau) + \boldsymbol{B}\boldsymbol{F}\boldsymbol{n}_R(t-\tau) + \boldsymbol{F}\boldsymbol{n}_R(t) + \boldsymbol{B}^2\boldsymbol{x}_R(t-2\tau). \end{aligned} \tag{5.8}$$

Substituting $\boldsymbol{x}_R(t-2\tau)$ from (5.6) in (5.8) gives

$$\begin{aligned}\boldsymbol{x}_R(t) &= \boldsymbol{A}\boldsymbol{x}_S(t) + \boldsymbol{B}\boldsymbol{A}\boldsymbol{x}_S(t-\tau) + \boldsymbol{B}\boldsymbol{F}\boldsymbol{n}_R(t-\tau) + \boldsymbol{F}\boldsymbol{n}_R(t) \\ &\quad + \boldsymbol{B}^2[\boldsymbol{A}\boldsymbol{x}_S(t-2\tau) + \boldsymbol{B}\boldsymbol{x}_R(t-3\tau) + \boldsymbol{F}\boldsymbol{n}_R(t-2\tau)] \\ &= \boldsymbol{A}\boldsymbol{x}_S + \boldsymbol{B}\boldsymbol{A}\boldsymbol{x}_S(t-\tau) + \boldsymbol{B}^2\boldsymbol{A}\boldsymbol{x}_S(t-2\tau) + \boldsymbol{F}\boldsymbol{n}_R(t) \\ &\quad + \boldsymbol{B}\boldsymbol{F}\boldsymbol{n}_R(t-\tau) + \boldsymbol{B}^2\boldsymbol{F}\boldsymbol{n}_R(t-2\tau) + \boldsymbol{B}^3\boldsymbol{x}_R(t-\tau). \end{aligned} \tag{5.9}$$

Assuming $\boldsymbol{B}^n \to 0$ as $n \to \infty$, (5.9) can be extended to the general form

$$\boldsymbol{x}_R(t) = \sum_{j=0}^{\infty} \boldsymbol{B}^j\boldsymbol{A}\boldsymbol{x}_S(t-j) + \sum_{k=0}^{\infty} \boldsymbol{B}^k\boldsymbol{F}\boldsymbol{n}_R(t-k\tau). \tag{5.10}$$

When the SI is computed, $\boldsymbol{y}_R$ can be calculated and this enables us to find the scaling factor, α, to normalise $\boldsymbol{M}_R^U$. This is given by

$$\alpha = \frac{1}{||\boldsymbol{M}_R^U\boldsymbol{y}_R||^2}, \tag{5.11}$$

and then $\boldsymbol{M}_R$ is normalised by

$$\boldsymbol{M}_R = \alpha\boldsymbol{M}_R^U. \tag{5.12}$$

When the normalised $\boldsymbol{M}_R$ has been calculated using (5.12), the $\boldsymbol{x}_R(t)$ term in (5.10) requires to be recalculated with the new normalised $\boldsymbol{M}_R$, as the initial $\boldsymbol{M}_R$ that is used to calculate for $\boldsymbol{x}_R(t)$ has not been normalised. Thus, we iterate this process until $\boldsymbol{M}_R$ converges to have the correct normalised power.

5.3 SIMULATION RESULTS

The precoder and weight vectors are designed using the SSSS and SMSS designs from Table 4.8. These approaches are considered using the same methods from Chapter 4, SMSS has the best performance and SSSS is used as a benchmark for the FD designs. This is due to the fact that SSSS is optimal when there is no SI. Hence, in the presence of SI, the SSSS design can provide a lower bound for the SMSS design.

The system is simulated by transmitting QPSK symbols from the source to the relay and the relay retransmits the received signal with SI to the destination. At the destination, the error rate is calculated using hard decision decoding.

Figure 5.1 to Figure 5.3, show the performance of the three different system antenna combinations (as shown in Figure 4.14): 2222, 2442 and 4224, respectively. The SNR is set to 5dB and we alter the signal to interference ratio (SIR) at the relay receiver. The figures show the SER performance of the two proposed schemes (SMSS and SSSS) using Monte Carlo simulations (number of trials is 100,000). The results show that the SER decreases as the SIR increases and reaches an error floor when the SIR is high (approximately 25dB). Thus, when the SI is reduced, the system improves its performance. As the SI reduces to a low threshold, the system is noise limited and the SER remains constant.

Figure 5.1 to Figure 5.3 show that the SMSS design has a lower SER than the SSSS design. This is expected from the average relay normalisation results in Chapter 4. However, Figure 5.3 shows that after SIR=10dB, the SMSS and the SSSS design have similar performance. The reason is with only two antennas at the receiver there are limited degrees of freedom for the MMSE design to reduce the interference and noise.

For the different system sizes, the best performance for the SMSS design is 2442 followed by 4224 and then 2222. For the SSSS design, it is 4224 followed by 2442 and then 2222. The reason that the SMSS design obtained a better result in the 2442 system is due to the fact that there are more degrees of freedom to reduce SI and noise. The increase in degrees of freedom is due to increasing the number of antennas at the relay which was also observed in Chapter 4. By having more antennas at the relay, the SMSS design has a higher rate when compared to extra

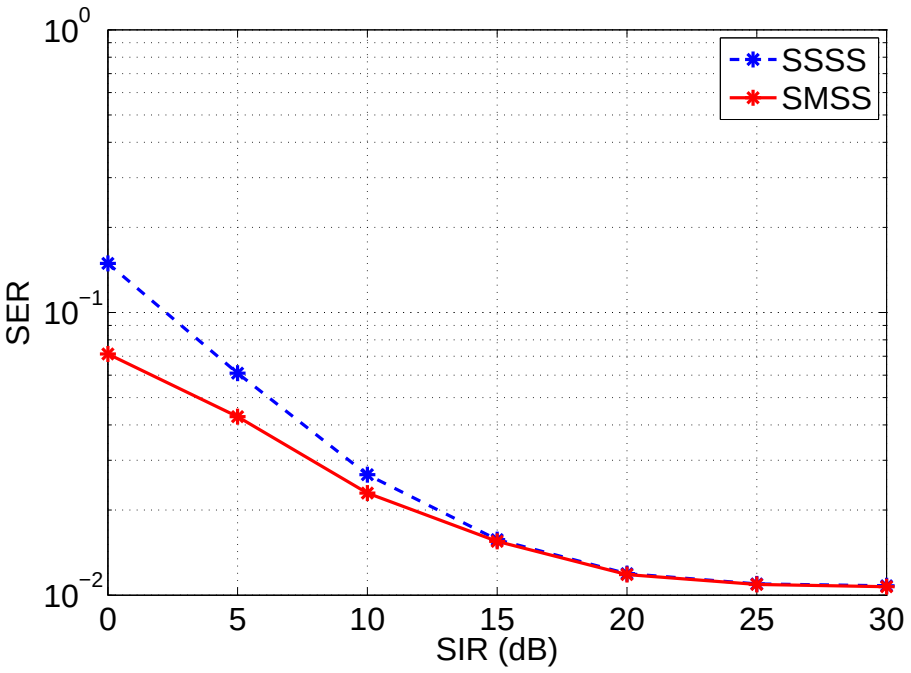

Figure 5.1 The SER of the relay with instantaneous power normalisation for the $N_S = 2$, $N_{RR} = 2$, $N_{RT} = 2$, $N_D = 2$ system with a SNR of 5dB.

antennas at the source and destination.

The results show the SER performance of the FD MIMO relay under an instantaneous power constraint. Hence, the performance cannot be directly compared to the average power normalisation approach since these systems were evaluated via the rate.

5.4 RATE CALCULATION FOR INSTANTANEOUS POWER NORMALISATION

In Chapter 4, most of the simulations consider the e2e rate, which is a useful method for comparing FD and HD relays. Hence, it is also useful method to compute the rate for the instantaneous power normalisation. In this way, the e2e rate results from average power normalisation method and instantaneous power normalisation method can be compared.

To obtain the rate of the MIMO relay system, the e2e SINR needs to be calculated. The SINR is given by

$$\text{SINR} = \frac{\text{E}\{|\text{signal}|^2\}}{\text{E}\{|\text{interference}|^2\} + \text{E}\{|\text{noise}|^2\}}. \tag{5.13}$$

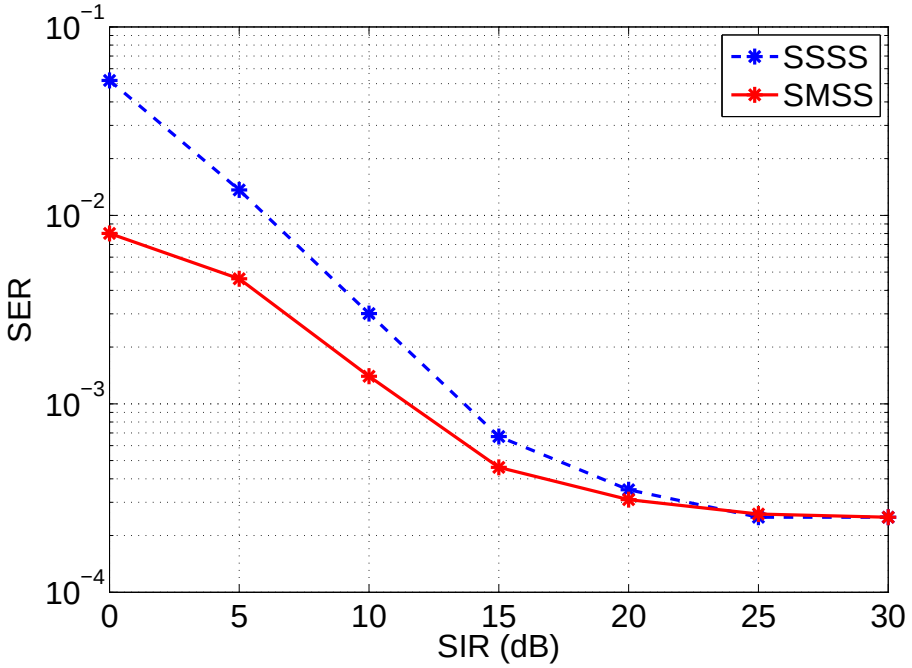

Figure 5.2 The SER of the relay with instantaneous power normalisation for the $N_S = 2$, $N_{RR} = 4$, $N_{RT} = 4$, $N_D = 2$ system with a SNR of 5dB.

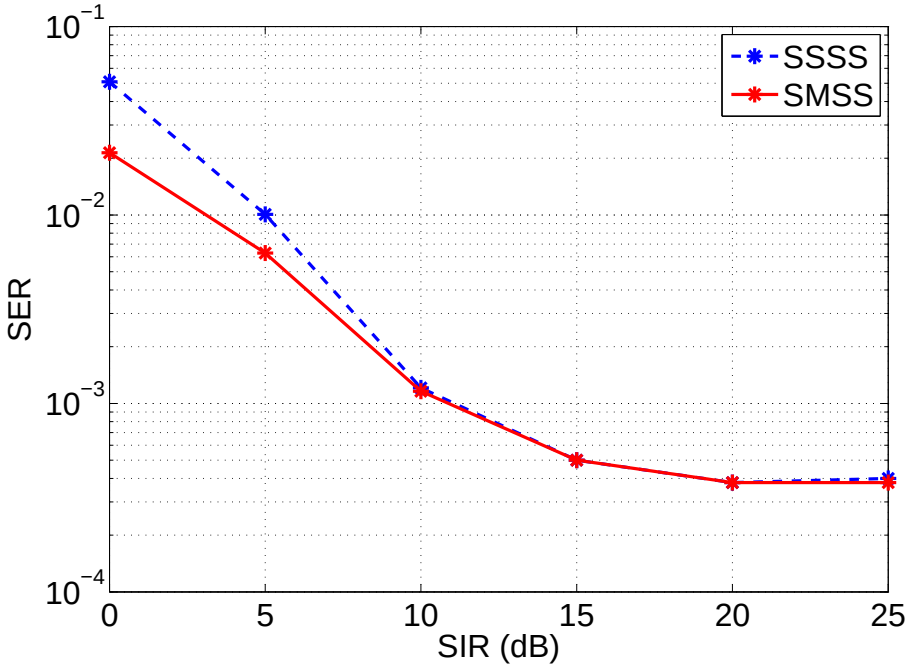

Figure 5.3 The SER of the relay with instantaneous power normalisation for the $N_S = 4$, $N_{RR} = 2$, $N_{RT} = 2$, $N_D = 4$ system with a SNR of 5dB.

In order to compute (5.13), the received signal at the destination is expanded into terms consisting of signal, interference and noise. From (5.4), the destination received signal is given by

$$\begin{aligned}\boldsymbol{y}_D =& \boldsymbol{W}_D^{\dagger}\boldsymbol{H}_{RD}\boldsymbol{M}_R\boldsymbol{W}_R^{\dagger}\boldsymbol{H}_{SR}\boldsymbol{M}_S\boldsymbol{d}_S + \boldsymbol{W}_D^{\dagger}\boldsymbol{H}_{RD}\boldsymbol{M}_R\boldsymbol{W}_R^{\dagger}\boldsymbol{H}_{RR}\boldsymbol{x}_R^D \\ &+ \boldsymbol{W}_D^{\dagger}\boldsymbol{H}_{RD}\boldsymbol{M}_R\boldsymbol{W}_R^{\dagger}\boldsymbol{n}_R + \boldsymbol{W}_D^{\dagger}\boldsymbol{n}_D,\end{aligned} \tag{5.14}$$

which can be decomposed to give

$$\begin{aligned}\text{signal} &= \boldsymbol{W}_D^{\dagger}\boldsymbol{H}_{RD}\boldsymbol{M}_R\boldsymbol{W}_R^{\dagger}\boldsymbol{H}_{SR}\boldsymbol{M}_S\boldsymbol{d}_S, \\ \text{interference} &= \boldsymbol{W}_D^{\dagger}\boldsymbol{H}_{RD}\boldsymbol{M}_R\boldsymbol{W}_R^{\dagger}\boldsymbol{H}_{RR}\boldsymbol{x}_R^D, \\ \text{noise1} &= \boldsymbol{W}_D^{\dagger}\boldsymbol{H}_{RD}\boldsymbol{M}_R\boldsymbol{W}_R^{\dagger}\boldsymbol{n}_R, \\ \text{noise2} &= \boldsymbol{W}_D^{\dagger}\boldsymbol{n}_D.\end{aligned} \tag{5.15}$$

The signal term is given by

$$\begin{aligned}\text{signal} &= \boldsymbol{W}_D^{\dagger}\boldsymbol{H}_{RD}\boldsymbol{M}_R\boldsymbol{W}_R^{\dagger}\boldsymbol{H}_{SR}\boldsymbol{M}_S\boldsymbol{d}_S, \\ \mathrm{E}\{|\text{signal}|^2\} &= \mathrm{E}\{\boldsymbol{W}_D^{\dagger}\boldsymbol{H}_{RD}\boldsymbol{M}_R\boldsymbol{W}_R^{\dagger}\boldsymbol{H}_{SR}\boldsymbol{x}_S\boldsymbol{x}_S^{\dagger}\boldsymbol{H}_{SR}^{\dagger}\boldsymbol{W}_R\boldsymbol{M}_R^{\dagger}\boldsymbol{H}_{RD}^{\dagger}\boldsymbol{W}_D\}, \\ &= \frac{1}{\text{Ł}}\mathrm{E}\{\boldsymbol{W}_D^{\dagger}\boldsymbol{H}_{RD}\boldsymbol{M}_R\boldsymbol{W}_R^{\dagger}\boldsymbol{H}_{SR}\boldsymbol{H}_{SR}^{\dagger}\boldsymbol{W}_R\boldsymbol{M}_R^{\dagger}\boldsymbol{H}_{RD}^{\dagger}\boldsymbol{W}_D\}, \\ &= \frac{1}{\text{Ł}}\mathrm{E}\{\boldsymbol{v}^{\dagger}\boldsymbol{M}_R\boldsymbol{A}\boldsymbol{M}_R^{\dagger}\boldsymbol{v}\}, \\ &= \frac{1}{\text{Ł}}\mathrm{E}\{\alpha^2\boldsymbol{v}^{\dagger}\boldsymbol{M}_R^U\boldsymbol{A}\boldsymbol{M}_R^{U\dagger}\boldsymbol{v}\}, \\ &= \frac{1}{\text{Ł}}\mathrm{E}\left\{\frac{\boldsymbol{v}^{\dagger}\boldsymbol{M}_R^U\boldsymbol{A}\boldsymbol{M}_R^{U\dagger}\boldsymbol{v}}{\boldsymbol{y}_R^{\dagger}\boldsymbol{M}_R^{U\dagger}\boldsymbol{M}_R^U\boldsymbol{y}_R}\right\}.\end{aligned} \tag{5.16}$$

where

$$\begin{aligned} \mathrm{E}\{|\boldsymbol{x}_S|^2\} &= \frac{1}{\mathrm{L}}, \\ \boldsymbol{v} &= \boldsymbol{H}_{RD}^{\dagger}\boldsymbol{W}_D, \\ \boldsymbol{A} &= \boldsymbol{W}_R^{\dagger}\boldsymbol{H}_{SR}\boldsymbol{H}_{SR}^{\dagger}\boldsymbol{W}_R, \\ \boldsymbol{M}_R &= \alpha \boldsymbol{M}_R^U, \\ \boldsymbol{y}_R &= \boldsymbol{W}_R^{\dagger}(\boldsymbol{H}_{SR}\boldsymbol{x}_S + \boldsymbol{H}_{RR}\boldsymbol{x}_R^D + \boldsymbol{n}_R). \end{aligned} \tag{5.17}$$

The interference term is given by

$$\begin{aligned} \text{interference} &= \boldsymbol{W}_D^{\dagger}\boldsymbol{H}_{RD}\boldsymbol{M}_R\boldsymbol{W}_R^{\dagger}\boldsymbol{H}_{RR}\boldsymbol{x}_R^D, \\ \mathrm{E}\{|\text{interference}|^2\} &= \mathrm{E}\{\boldsymbol{W}_D^{\dagger}\boldsymbol{H}_{RD}\boldsymbol{M}_R\boldsymbol{W}_R^{\dagger}\boldsymbol{H}_{RR}\boldsymbol{C}\boldsymbol{H}_{RR}^{\dagger}\boldsymbol{W}_R\boldsymbol{M}_R^{\dagger}\boldsymbol{H}_{RD}^{\dagger}\boldsymbol{W}_D\}, \\ &= \mathrm{E}\{\boldsymbol{v}^{\dagger}\boldsymbol{M}_R\boldsymbol{B}\boldsymbol{M}_R^{\dagger}\boldsymbol{v}\}, \\ &= \mathrm{E}\{\alpha^2\boldsymbol{v}^{\dagger}\boldsymbol{M}_R^U\boldsymbol{B}\boldsymbol{M}_R^{U\dagger}\boldsymbol{v}\} \\ &= \mathrm{E}\left\{\frac{\boldsymbol{v}^{\dagger}\boldsymbol{M}_R^U\boldsymbol{A}\boldsymbol{M}_R^{U\dagger}\boldsymbol{v}}{\boldsymbol{y}_R^{\dagger}\boldsymbol{M}_R^{U\dagger}\boldsymbol{M}_R^U\boldsymbol{y}_R}\right\}, \end{aligned} \tag{5.18}$$

where $\boldsymbol{B} = \boldsymbol{W}_R^{\dagger}\boldsymbol{H}_{RR}\boldsymbol{C}\boldsymbol{H}_{RR}^{\dagger}\boldsymbol{W}_R$ and $\boldsymbol{C} = \mathrm{E}\{\boldsymbol{x}_R\boldsymbol{x}_R^{\dagger}\}$ is the relay covariance matrix. The noise1 term is given by

$$\begin{aligned} \text{noise1} &= \boldsymbol{W}_D^{\dagger}\boldsymbol{H}_{RD}\boldsymbol{M}_R\boldsymbol{W}_R^{\dagger}\boldsymbol{n}_R, \\ \mathrm{E}\{|\text{noise1}|^2\} &= \mathrm{E}\left\{\frac{|\boldsymbol{W}_D^{\dagger}\boldsymbol{H}_{RD}\boldsymbol{M}_R^U\boldsymbol{W}_R^{\dagger}\boldsymbol{n}_R|^2}{|\boldsymbol{M}_R^U\boldsymbol{W}_R^{\dagger}(\boldsymbol{H}_{SR}\boldsymbol{x}_S + \boldsymbol{H}_{RR}\boldsymbol{x}_R^D + \boldsymbol{n}_R)|^2}\right\} \\ &= \mathrm{E}\left\{\frac{|\boldsymbol{A}_n\boldsymbol{n}_R|^2}{|\boldsymbol{B}_n\boldsymbol{x}_S + \boldsymbol{C}_n\boldsymbol{x}_R^D + \boldsymbol{D}_n\boldsymbol{n}_R|^2}\right\}, \end{aligned} \tag{5.19}$$

where

$$\begin{aligned}\boldsymbol{A}_n &= \boldsymbol{W}_D^{\dagger}\boldsymbol{H}_{RD}\boldsymbol{M}_R^U\boldsymbol{W}_R^{\dagger},\\ \boldsymbol{B}_n &= \boldsymbol{M}_R^U\boldsymbol{W}_R^{\dagger}\boldsymbol{H}_{SR},\\ \boldsymbol{C}_n &= \boldsymbol{M}_R^U\boldsymbol{W}_R^{\dagger}\boldsymbol{H}_{RR},\\ \boldsymbol{D}_n &= \boldsymbol{M}_R^U\boldsymbol{W}_R^{\dagger}.\end{aligned} \tag{5.20}$$

The second noise term, noise2, is given by

$$\text{noise2} = \boldsymbol{W}_D^{\dagger}\boldsymbol{n}_D \tag{5.21}$$

so that

$$\mathrm{E}\{|\text{noise2}|^2\} = \mathrm{E}\{\boldsymbol{W}_D^{\dagger}\boldsymbol{W}_D\}, \tag{5.22}$$

where $\mathrm{E}\{\boldsymbol{n}_D\boldsymbol{n}_D^{\dagger}\} = \boldsymbol{I}_{N_D}$.

This makes (5.19) a ratio of quadratic forms with the same Gaussian variables. Furthermore, the quadratic form in the denominator is non-central. Hence, the exact mean of (5.19) as a function of $\boldsymbol{n}_R$ is unknown. In addition, $\boldsymbol{x}_R^D$ that is in the denominator of (5.19) has a complex unknown distribution and is also affected by the power normalisation. As a result of this, the exact distribution of $\boldsymbol{x}_R^D$ is a very challenging problem. Regrettably, taking the expectation of (5.19) is an extremely complex problem and is beyond the scope of this thesis.

5.5 SUMMARY

In this chapter, we used an instantaneous power normalisation approach to constrain the signal and SI that are transmitted from the relay transmitter. In this model, we derived an equation to model the SI that is received by the relay receiver. We simulated the system using an QPSK transmission as the SER result is a more straight forward method than the rate for the instantaneous normalisation approach.

The results from the SMSS and SSSS designs agree with the results in Chapter 4 in the sense

that SMSS has a higher performance. The relative performance for the different system sizes also agrees with the results in Chapter 4, where 2442 has the lowest SER plot followed by 4224 and lastly 2222.

Calculation of the rate using instantaneous power normalisation is extremely difficult and this is a topic for future work.

Chapter 6

CONCLUSIONS AND FUTURE WORK

In this chapter, we conclude our work based on the FD relay designs that are presented in this thesis and summarise our main contributions. Potential future work is also discussed at the end of this chapter.

6.1 CONCLUSION

FD relays can have a higher rate compared to HD relays, but FD relays suffers from SI, where the transmitted signals from the relay are received by the relay receiver which reduce the performance of the relay system.

In this thesis, we derived an e2e SINR equation in a FD MIMO relay which contains the relay SI component. With the use of different precoder and weight vector designs, our goal is to increase the e2e SINR of the MIMO relay system. The precoder designs are SVD, SLNR and ZF. The SVD design transmits signals using the strongest eigenchannel and it is the optimal approach when there is no interference. Maximising the SLNR increases the ratio between the signal over the leakage and noise. ZF completely removes the interference signal, but does not have any control on the desired signal. The weight vector designs are SVD, ZF and MMSE. Both SVD and ZF weight vectors have the same design method as their precoders. For the MMSE weight vector, it increases the signal term while decreasing the interference and noise terms.

In Chapter 3, we construct a two path FD MIMO relay model. This model assumes that the relay transmits and receives instantaneously. By using this approach, the SI term and the source signal term, which are received by the relay receiver, contain the same underlying signal from

the source. This implies that doing processing to remove SI is unlikely to increase the e2e SINR. Hence, in order to model the SI effect, we include a processing delay into the relay system. In this way, the underlying signal in the SI term will be delayed as compared to the underlying signal from the source and is considered as an interference signal.

In Chapter 4, we use a one path FD MIMO relay system with a processing delay at the relay. In this model, we use an average power normalisation to constrain the precoder and weight vector for each of the nodes. Here, constraining the relay precoder has evolved into a very complicated arithmetic problem: Firstly, the relay covariance matrix needs to be solved using a novel mathematical derivation which involves matrix vectorization techniques. Secondly, a numerical approach is required to find the correct scaling factor to scale the relay precoder to have the correct size. Finally, some of the relay precoder and weight vector designs, such as SSLS and SMSS, require the SI value. However, to compute the SI, it requires the values of the relay precoder and weight vector. Thus, an iteration between the precoder/weight vector calculation and the SI calculation is required and this is used in the SSLS design. For the SMSS design, we use an approximation of SI to compute the weight vector which avoids the iterative calculation.

The results indicate that the best scheme is SMSS followed by SSSS or SSZS. The SSZS has a better performance than SSSS when the INR is large (10dB), but not when INR is low (0dB). This suggests that when SI is large, the system can have a higher SINR by nulling SI. However, when SI is low, transmitting signals on the strongest eigenchannel is likely to increase the e2e SINR. Here, the best approach is to decrease SI and increase the desired signal which is given by the SMSS method. It was found that the SSLS and SSSM designs both have similar performance compared to the SSSS design. This suggests that it is ineffective to perform processing to reduce SI at the destination as this channel carries both the SI and the desired signal. The best approach in relation to the SSLS and SSSM techniques is to transmit through the largest eigenchannel which is given by the SSSS design.

For the different system sizes, the highest performing system is 2442 compared with 4224 and 2222. This suggests that having more antennas at the relay provides more degrees of freedom for the relay precoder and weight vector which increases the SINR.

The one stream system has a higher performance of rate than the two stream system. The two stream system has the signal power is shared between the streams. In the one stream system, it uses the highest channel power for transmission. This suggests that for a two stream system, a power allocation scheme is required in order to achieve higher performance when compared to the one stream system.

The near-optimal method proposed in Section 4.4.2 has a similar performance to the SMSS design. This suggests that by using the SVD method to compute the source precoder, with no interference, the result is close to the near-optimal method of precoding. At the destination, the results from the near-optimal method suggest that it is very difficult to increase the signal and decrease SI when they are both carried in the relay to destination channel.

In Chapter 5, we use a one path FD MIMO relay system, which is similar to the model in Chapter 4. However, in this model we use an instantaneous power normalisation instead of an average power normalisation at the relay. The SER plots show the results from the different designs are similar with the results in Chapter 4. In the sense that SMSS has a lower SER than the SSSS design and the best system size performance is 2442. It would be useful to compare the rate between the instantaneous power normalisation and the average power normalisation. Hence, we begin an initial derivation of the rate for the instantaneous power normalisation model but showed that it is extremely difficult. Thus, this is considered beyond the scope of this project and left for future work.

From the different precoder and weight vector designs, the results show that doing processing to reduce SI at the relay receiver (i.e. SMSS) has a better performance than doing processing at the relay transmitter (i.e. SSZS and SSLS). The SMSS design has the best overall performance for the ad-hoc scheme and its performance is similar to the near-optimal scheme. This suggests that ad-hoc methods can produce a high e2e rate with a lower complexity requirement for the precoder and weight vector. In addition, the result from the SMSS design shows that having more antennas at the relay can further increase the performance of the FD MIMO relay system.

This research is successful at showing the performance difference between each of the precoder and weight vector designs. Designs like SSLS and SSSM have similar complexity as the SMSS design, however their performance is less. The SSSS and SSZS designs are less complex, but

SSZS performance increases only in the presence of a high SI.

6.2 FUTURE WORK

This thesis has provided some insights to the precoder and weight vector designs that can reduce the SI and/or increase SNR of the MIMO relay. However, there are some aspects to this work that can be investigated further.

- Derive the SINR for the instantaneous power normalisation model. Therefore, we can compare the results between the instantaneous power normalisation model with the average power normalisation model.
- Analyze the effects of different precoder and weight vector designs on the e2e SINR, in particular, their effectiveness in increasing the signal component and/or decreasing the interference and noise component.
- Compare the precoding and weight vector techniques with other techniques like antenna selection.

REFERENCES

[1] T. Rappaport, *Wireless Communications : Principles and Practice.* Prentice Hall, 2002.

[2] H. Choi, C. Song, H. Park, A. M, and I. Lee, "Pairwise MSE Balancing Transceiver Designs for Multipoint-to-multipoint MIMO AF Relay Systems," in *Proc. VTC*, 2013.

[3] E. Dahlman, S. Parkvall, and J. Skold, *4G LTE/LTE-Advanced for Mobile Broadband.* Academic Press, 2011.

[4] H. Yang and M. Alouini, *Order Statistics in Wireless Communications - Diversity, Adaptation, and Scheduling in MIMO and OFDM Systems.* Cambridge University Press, 2011.

[5] A. Molisch, *Wireless Communications.* John Wiley and Sons, 2011.

[6] M. Simon and M. Alouini, *Digital Communication Over Fading Channels: A Unified Approach to Performance Analysis.* John Wiley and Sons, 2000.

[7] T. Brown, P. Kyritsi, and E. De Carvalho, *Practical Guide to MIMO Radio Channel.* John Wiley and Sons, 2012.

[8] G. Byers and F. Takawira, "Spatially and Temporally Correlated MIMO Channels: Modeling and Capacity Analysis," *IEEE Veh. Technol. Mag.*, vol. 53, no. 3, pp. 634–643, 2004.

[9] E. Larsson and P. Stoica, *Space Time Block Coding for Wireless Commuications.* Cambridge University Press, 2003.

[10] C. Kundu and R. Bose, "Joint Optimal Power Allocation and Relay Location for Amplify-and-Forward Multihop Relaying over Lognormal Channel," in *Proc. VTC*, 2013.

[11] O. Waqar, M. Imran, and M. Dianati, "On the Error Analysis of Fixed-gain Relay Networks over Composite Multipath/Shadowing Channels," in *Proc. VTC*, 2013.

[12] H. Choi, K. Lee, C. Song, H. Kim, and I. Lee, "Weighted Sum Rate Maximization for Multi-User Multi-Relay MIMO Systems with Direct Links," in *Proc. VTC*, 2013.

[13] B. Rankov and A. Wittneben, "On the Capacity of Relay-Assisted Wireless MIMO Channels," in *Proc. SPAWC*, 2004, pp. 323–327.

[14] J. Laneman, G. Wornell, and D. Tse, "An Efficient Protocol for Realizing Cooperative Diversity in Wireless Networks," in *Proc. ISIT*, 2001, p. 294.

[15] H. Fukuzono, Y. Asai, R. Kudo, and M. Mizoguchi, "A Novel Channel Estimation Scheme on Amplify-and-Forward Cooperative OFDM-Based Wireless LAN Systems," in *Proc. VTC*, 2013.

[16] N. Kikuchi, M. Inamori, and Y. Sanada, "Combining of Loop Signals in Frequency Offset Amplify-and-Forward Relay," in *Proc. VTC*, 2013.

[17] G. Zheng, E. Jorswieck, and B. Ottersten, "Cooperative Communications Against Jamming with Half-Duplex and Full-Duplex Relaying," in *Proc. VTC*, 2013.

[18] D. Gesbert, H. Bolcskei, D. Gore, and A. Paulraj, "Outdoor MIMO Wireless Channels: Models and Performance Prediction," *IEEE Trans. Commun.*, vol. 50, no. 12, pp. 1926–1934, 2002.

[19] A. Forouzan and P. Smith, "Background Research into Increasing the Spectral Efficiency of Long-Range Outdoor MIMO Communication Systems," *NZi3, Wireless Research Centre, University of Canterbury, New Zealand*, 2008.

[20] F. Tseng, W. Wu, and J. Wu, "Joint Source/Relay Precoder Design in Amplify-and-Forward Relay Systems Using an MMSE Criterion," in *Proc. WCNC*, 2009, pp. 1–5.

[21] F. Tseng, M. Chang, and W. Wu, "Joint Tomlinson Harashima Source and Linear Relay Precoder Design in Amplify and Forward MIMO Relay Systems via MMSE Criterion," *IEEE Trans. Veh. Technol.*, vol. 60, no. 4, pp. 1687–1698, 2011.

[22] F. Tseng, G. Ke, and W. Wu, "Linear MMSE Transceiver Design with Quality-of-Service Constraints in Amplify-and-Forward MIMO Relay Systems," in *Proc. VTC*, 2010, pp. 1–5.

[23] C. Xing, S. Ma, and Y. Wu, "Robust Joint Design of Linear Relay Precoder and Destination Equalizer for Dual-Hop Amplify-and-Forward MIMO Relay Systems," *IEEE Trans. Signal Process.*, vol. 58, no. 4, pp. 2273–2283, 2010.

[24] F. Rong, "Two-Way Amplify-and-Forward MIMO Relay Communications using Linear MMSE Receiver," in *Proc. AusCTW*, 2011, pp. 55–59.

[25] H. Chun and Y. Lee, "A Spatial Self-Interference Nullification Method for Full Duplex Amplify-And-Forward MIMO Relays," in *Proc. WCNC*, 2010, pp. 1–6.

[26] R. Zhao, L. Yang, W. Zhu, and Z. He, "OFDM Amplify-and-Forward Two-Way Relaying for MIMO Multiuser Networks," in *Proc. ICASSP*, 2010, pp. 3238–3241.

[27] A. Steiner and S. Shamai, "Broadcasting over Two-Hop Relay Fading Channels," in *Proc. IZS*, 2006, pp. 26–29.

[28] K. Lee, H. Kwon, H. Kim, S. Lee, Y. Shim, and L. Park, H. Yong, "AF Wireless Relay Network Analysis under Receiver Power Constraints," in *Proc. VTC*, 2013.

[29] T. Tao and A. Czylwik, "Beamforming Design and Relay Selection for Multiple MIMO AF Relay Systems with Limited Feedback," in *Proc. VTC*, 2013.

[30] Y. Kang and J. Cho, "Capacity of MIMO Wireless Channel with Full-Duplex Amplify-and-Forward Relay," in *Proc. PIMRC*, 2009, pp. 117–121.

[31] T. Riihonen, K. Haneda, S. Werner, and R. Wichman, "SINR Analysis of Full-Duplex OFDM Repeaters," in *Proc. PIMRC*, 2009, pp. 3169–3173.

[32] B. Day, A. Margetts, D. Bliss, and P. Schniter, "Full-Duplex MIMO Relaying: Achievable Rates Under Limited Dynamic Range," *IEEE J. Sel. Areas Commun.*, vol. 30, no. 8, pp. 1541–1553, 2012.

[33] K. Tamaki, A. Raptino, Y. Sugiyama, M. Bandai, S. Saruwatari, and T. Watanabe, "Full Duplex Media Access Control for Wireless Multi-hop Networks," in *Proc. VTC*, 2013.

[34] S. Hong, J. Brand, J. Choi, M. Jain, J. Mehlman, S. Katti, and P. Levis, "Applications of Self-Interference Cancellation in 5G and Beyond," *IEEE Commun. Mag.*, vol. 52, no. 2, pp. 114–121, February 2014.

[35] M. Duarte, "Full Duplex Wireless: Design, Implementation and Characterization," Ph.D. dissertation, Rice University, 2012.

[36] A. Sabharwal, P. Schniter, D. Guo, D. Bliss, S. Rangarajan, and R. Wichman, "In band Full Duplex Wireless: Challenges and Opportunities," *ArXiv e-prints*, Nov. 2013.

[37] J. Vella and S. Zammit, "Performance Improvement of Long Distance MIMO Links Using Cross Polarized Antennas," in *Proc. MELECON*, 2010, pp. 1287–1292.

[38] B. Chalise and L. Vandendorpe, "MIMO Relay Design for Multipoint-to-Multipoint Communications with Imperfect Channel State Information," *IEEE Trans. Signal Process.*, vol. 57, no. 7, pp. 2785–2796, 2009.

[39] C. Chae, T. Tang, R. Heath, and S. Cho, "MIMO Relaying With Linear Processing for Multiuser Transmission in Fixed Relay Networks," *IEEE Trans. Signal Process.*, vol. 56, no. 2, pp. 727–738, 2008.

[40] R. Zhang, C. Chai, and Y. Liang, "Joint Beamforming and Power Control for MIMO Relay Broadcast Channel with QoS Constraints," in *Proc. ACSSC*, 2007, pp. 453–457.

[41] S. Peters and R. Heath, "Nonregenerative MIMO Relaying With Optimal Transmit Antenna Selection," *IEEE Signal Process. Lett.*, vol. 15, pp. 421–424, 2008.

[42] J. Joung and A. Sayed, "Design of Half- and Full-Duplex Relay Systems Based on the MMSE Formulation," in *Proc. SSP*, 2009, pp. 281–284.

[43] T. Riihonen, S. Werner, and R. Wichman, "Mitigation of Loopback Self-Interference in Full-Duplex MIMO Relays," *IEEE Trans. Signal Process.*, vol. 59, no. 12, pp. 5983–5993, 2011.

[44] W. Slingsby and J. McGeehan, "Antenna Isolation Measurements for On-Frequency Radio Repeaters," in *Proc. AP-S*, 1995, pp. 239–243.

[45] E. Aryafar, M. Khojastepour, K. Sundaresan, S. Rangarajan, and M. Chiang, "MIDU: Enabling MIMO Full Duplex," in *Proc. ACM MobiCom*, 2012, pp. 1–12.

[46] H. Suraweera, I. Krikidis, G. Zheng, C. Yuen, and P. Smith, "Low complexity end to end performance optimization in MIMO full duplex relay systems," *IEEE Trans. Wireless Commun.*, 2013.

[47] I. Krikidis, H. Suraweera, S. Yang, and K. Berberidis, "Full Duplex Relaying Over Block Fading Channel: A Diversity Perspective," *IEEE Trans. Wireless Commun.*, vol. 11, no. 12, pp. 4524–4535, 2012.

[48] M. Duarte, C. Dick, and A. Sabharwal, "Experiment-Driven Characterization of Full-Duplex Wireless Systems," *IEEE Trans. Wireless Commun.*, vol. 11, no. 12, pp. 4296–4307, 2012.

[49] C. Anderson, S. Krishnamoorthy, C. Ranson, T. Lemon, W. Newhall, T. Kummetz, and J. Reed, "Antenna Isolation, Wideband Multipath Propagation Measurements, and Interference Mitigation for On-frequency Repeaters," in *Proc. SoutheastCon*, 2004, pp. 110–114.

[50] J. Choi, M. Jain, K. Srinivasan, P. Levis, and S. Katti, "Achieving Single Channel, Full Duplex Wireless Communication," in *Proc. ACM MobiCom*, 2010.

[51] M. Duarte and A. Sabharwal, "Full-Duplex Wireless Communications using Off-the-Shelf Radios: Feasibility and First Results," in *Proc. ASILOMAR*, 2010, pp. 1558–1562.

[52] T. Riihonen, S. Werner, and R. Wichman, "Residual Self-Interference in Full-Duplex MIMO Relays After Null-Space Projection and Cancellation," in *Proc. ASILOMAR*, 2010, pp. 653–657.

[53] Y. Sung, Y. Ahn, B. Nguyen, and K. Kim, "Loop Interference Suppression Strategies Using Antenna Selection in Full Duplex MIMO Relays," in *Proc. ISPACS*, 2011, pp. 1–4.

[54] B. Chun and H. Park, "A Spatial-Domain Joint-Nulling Method of Self-Interference in Full-Duplex Relays," *IEEE Commun. Lett.*, vol. 16, no. 4, pp. 436–438, 2012.

[55] E. Everett, D. Dash, C. Dick, and A. Sabharwal, "Self-Interference Cancellation in Multi-Hop Full-Duplex Networks Via Structured Signaling," in *Proc. Allerton*, 2011, pp. 1619–1626.

[56] P. Larsson and M. Prytz, "MIMO On-Frequency Repeater with Self-Interference Cancellation and Mitigation," in *Proc. VTC*, 2009, pp. 1–5.

[57] A. Scaglione, P. Stoica, S. Barbarossa, G. Giannakis, and H. Sampath, "Optimal Designs for Space-Time Linear Precoders and Decoders," *IEEE Trans. Signal Process.*, vol. 50, no. 5, pp. 1051–1064, 2002.

[58] M. Vu and A. Paulraj, "MIMO Wireless Linear Precoding," *IEEE Signal Process. Mag.*, vol. 24, no. 5, pp. 86–105, 2007.

[59] H. Bahrami and T. Le-Ngoc, "MIMO Precoding Structures for Frequency-Flat and Frequency-Selective Fading Channels," in *Proc. ICCE*, 2006, pp. 193–197.

[60] H. Sampath, P. Stoica, and A. Paulraj, "Generalized Linear Precoder and Decoder Design for MIMO Channels Using the Weighted MMSE Criterion," *IEEE Trans. Commun.*, vol. 49, no. 12, pp. 2198–2206, 2001.

[61] E. Biglieri, R. Calderbank, A. Constantinides, A. Goldsmith, A. Paulraj, and H. Poor, *MIMO Wireless Communications*. Cambridge University Press, 2007.

[62] Q. Spencer, A. Swindlehurst, and M. Haardt, "Zero-Forcing Methods for Downlink Spatial Multiplexing in Multiuser MIMO Channels," *IEEE Trans. Signal Process.*, vol. 52, no. 2, pp. 461–471, 2004.

[63] A. Wiesel, Y. Eldar, and S. Shamai, "Zero-Forcing Precoding and Generalized Inverses," *IEEE Trans. Signal Process.*, vol. 56, no. 9, pp. 4409–4418, 2008.

[64] B. Bandemer, M. Haardt, and S. Visuri, "Linear MMSE Multi-User MIMO Downlink Precoding for Users with Multiple Antennas," in *Proc. PIMRC*, 2006, pp. 1–5.

[65] F. Wang, S. Liew, and D. Guo, "Wireless MIMO Switching with MMSE Relaying," in *Proc. ISIT*, 2012, pp. 1127–1131.

[66] M. Sadek, A. Tarighat, and A. Sayed, "A Leakage-Based Precoding Scheme for Downlink Multi-User MIMO Channels," *IEEE Trans. Wireless Commun.*, vol. 6, no. 5, pp. 1711–1721, 2007.

[67] P. Cheng, M. Tao, and W. Zhang, "A New SLNR-Based Linear Precoding for Downlink Multi-User Multi-Stream MIMO Systems," *IEEE Commun. Lett.*, vol. 14, no. 11, pp. 1008–1010, 2010.

[68] Z. Zeng, Z. Chen, and L. Li, "Iterative Joint Source and Relay Optimization for Multiuser MIMO Relay Systems," in *Proc. VTC*, 2012, pp. 1–5.

[69] Y. Sun, M. Wu, and Q. Guo, "New Interference Suppression Precoding Scheme for Downlink Multi-User Multi-Stream MIMO Systems," in *Proc. VTC*, 2012, pp. 1–5.

[70] Y. Zhang, B. Golkar, E. Sousa, and Q. Zhang, "Efficient User Selection for Downlink Zero-Forcing Based Multiuser MIMO Systems," in *Proc. VTC*, 2011, pp. 1–5.

[71] X. Shao, J. Yuan, and Y. Shao, "Error Performance Analysis of Linear Zero Forcing and MMSE Precoders for MIMO Broadcast Channels," *IEEE Trans. Commun. Technol.*, vol. 1, no. 5, pp. 1067–1074, 2007.

[72] A. Mehana and A. Nosratinia, "High-SNR Analysis of MIMO Linear Precoders," in *Proc. ISIT*, 2012, pp. 2296–2300.

[73] J. Lee and O. Shin, "Full-Duplex Relay Based on Block Diagonalisation in Multiple-Input Multiple-Output Relay Systems," *IEEE Trans. Commun. Technol.*, vol. 4, no. 15, pp. 1817–1826, 2010.

[74] W. Zhang, G. Choi, and M. Xiaoli, "Designing Zero-Forcing Based MIMO Relay Networks with Channel-Controlled ARQ to Achieve Full Diversity," in *Proc. MILCOM*, 2010, pp. 363–368.

[75] C. Wang, E. Au, R. Murch, W. Mow, R. Cheng, and V. Lau, "On the Performance of the MIMO Zero-Forcing Receiver in the Presence of Channel Estimation Error," *IEEE Trans. Wireless Commun.*, vol. 6, no. 3, pp. 805–810, 2007.

[76] C. Siriteanu, Y. Miyanaga, S. Blostein, S. Kuriki, and X. Shi, "MIMO Zero-Forcing Detection Analysis for Correlated and Estimated Rician Fading," *IEEE Trans. Veh. Technol.*, vol. 61, no. 7, pp. 3087–3099, 2012.

[77] Y. Cao, Z. Chen, and F. Yin, "A Leakage-based Nonlinear Precoder for the Multi-user Multi-stream MIMO Broadcast Channel," *Information Technology Journal*, vol. 10, pp. 787–797, 2011.

[78] M. McKay, I. Collings, and A. Tulino, "Achievable Sum Rate of MIMO MMSE Receivers: A General Analytic Framework," *IEEE Trans. Inf. Theory*, vol. 56, no. 1, pp. 396–410, 2010.

[79] F. Dupuy and P. Loubaton, "Diversity of the MMSE Receiver in Flat Fading and Frequency Selective MIMO Channels at Fixed Rate," in *Proc. ASILOMAR*, 2011, pp. 932–936.

[80] R. Rao, H. Tarn, R. Mazahreh, and C. Dick, "A Low Complexity Square Root MMSE MIMO Decoder," in *Proc. ASILOMAR*, 2010, pp. 1463–1467.

[81] A. Mehana and A. Nosratinia, "Diversity of MMSE MIMO Receivers," *IEEE Trans. Inf. Theory*, vol. 58, no. 11, pp. 6788–6805, 2012.

[82] J. Lee and O. Shin, "Full-Duplex Relay Based on Distributed Beamforming in Multiuser MIMO Systems," *IEEE Trans. Veh. Technol.*, no. 99, pp. 1–1, 2011.

[83] A. Talebi and W. Krzymien, "Cooperative MIMO Multiple-Relay System with Optimised Beamforming and Power Allocation," *IEEE Trans. Commun. Technol.*, vol. 4, no. 14, pp. 1677–1686, 2010.

[84] D. Bliss, P. Parker, and A. Margetts, "Simultaneous Transmission and Reception for Improved Wireless Network Performance," in *Proc. SSP*, 2007, pp. 478–482.

[85] H. Ju, E. Oh, and D. Hong, "Improving Efficiency of Resource Usage in Two-Hop Full Duplex Relay Systems Based on Resource Sharing and Interference Cancellation," *IEEE Trans. Wireless Commun.*, vol. 8, no. 8, pp. 3933–3938, 2009.

[86] B. Chun, E. Jeong, J. Joung, Y. Oh, and Y. Lee, "Pre-Nulling for Self-Interference Suppression in Full-Duplex Relays," in *Proc. APSIPA ASC*, 2009.

[87] C. Shang, P. Smith, and G. Woodward, "Linear Transceiver for Full Duplex MIMO Relays," in *Proc. AusCTW*, 2014.

[88] S. Primak and V. Kontorovich, *Wireless Multi-Antenna Channels : Modeling and Simulation.* John Wiley and Sons, 2011.

[89] W. Stallings, *Wireless Communication and Networks.* Upper Saddle River, NJ:Pearson Prentice Hall, 2006.

[90] D. Tse and P. Wiswanath, *Fundamentals of Wireless Communication.* Cambridge University Press, 2005.

[91] F. Farrokhi, A. Lozano, G. Foschini, and R. Valenzuela, "Spectral Efficiency of Wireless Systems With Multiple Transmit and Receive Antennas," in *Proc. PIMRC*, vol. 1, pp. 373–377 vol.1.

[92] J. Shen, Y. Oda, T. Furuno, T. Maruyama, and T. Ohya, "A Novel Approach for Capacity Improvement of 2x2 MIMO in LOS Channel Using Reflectarray," in *Proc. VTC*, 2011, pp. 1–5.

[93] F. Farrokhi, G. Foschini, A. Lozano, and R. Valenzuela, "Link-Optimal Space-Time Processing with Multiple Transmit and Receive Antennas," *IEEE Commun. Lett.*, vol. 5, no. 3, pp. 85–87, 2001.

[94] L. Tsai and D. Shiu, "Channel Modeling and Capacity Evaluation for Relay-Aided MIMO Systems in LOS Environments," in *Proc. ISCIT*, 2007, pp. 796–801.

[95] A. Wittneben and R. B., "Impact of Cooperative Relays on the Capacity of Rank-Deficient MIMO Channels," in *Proc. IST Wirless Commun.*, 2003, pp. 421–425.

[96] F. Farrokhi, A. Lozano, G. Foschini, and R. Valenzuela, "Spectral Efficiency of FDMA/TDMA Wireless Systems with Transmit and Receive Antenna Arrays," *IEEE Trans. Commun.*, vol. 1, no. 4, pp. 591–599, 2002.

[97] H. Haykin, *Communication Systems.* Wiley, 2001.

[98] G. Vitetta, G. Taylor, D. Colavolpe, F. Pancaldi, and P. Martin, *Wireless Communications : Algorithmic Techniques.* Wiley, 2013.

[99] D. Browne, M. Browne, and M. Fitz, "CTH07-4: Singular Value Decomposition of Correlated MIMO Channels," in *Proc. GLOBECOM*, 2006, pp. 1–6.

[100] J. Gentle, *Matrix Algebra: Theory, Computation, and Applications in Statistics*. Springer, 2007.

[101] S. Haykin, *Adaptive Filter Theory*. Prentice Hall, 2002.

[102] H. Van Trees, *Optimum Array Processing*. Wiley, 2002.

[103] P. Sripathi and J. Lehnert, "Optimizing ZF Precoders for MIMO Broadcast Systems," in *Proc. WCNC*, vol. 4, 2006, pp. 1874–1880.

[104] M. Sadek, A. Tarighat, and A. Sayed, "Active Antenna Selection in Multiuser MIMO Communications," *IEEE Trans. Signal Process.*, vol. 55, no. 4, pp. 1498–1510, 2007.

[105] U. Madhow, *Fundamentals of Digital Communication*. Cambridge University Press, 2008.

[106] R. Elliott and W. Krzymien, "Improved and weighted sum rate maximization for successive zero forcing in multiuser MIMO systems," *EURASIP J. Wireless Comm. and Networking*, vol. 2011, no. 1, pp. 1–6, 2011. [Online]. Available: http://dx.doi.org/10.1186/1687-1499-2011-133

[107] R. Ganesan, H. Al-Shatri, T. Weber, and A. Klein, "Cooperative Zero Forcing in Multi-Pair Multi-Relay Networks," in *Proc. PIMRC*, 2012, pp. 1740–1745.

[108] Y. Jiang, M. Varanasi, and J. Li, "Performance Analysis of ZF and MMSE Equalizers for MIMO Systems: An In-Depth Study of the High SNR Regime," *IEEE Trans. Inf. Theory*, vol. 57, no. 4, pp. 2008–2026, 2011.

[109] J. Wang, S. Li, and H. Hao, "Soft-Output MMSE MIMO Detector under MMSE Channel Estimation," in *Proc. ICCCAS*, 2008, pp. 233–236.

[110] A. Tarighat, M. Sadek, and A. Sayed, "A Multi User Beamforming Scheme for Downlink MIMO Channels Based on Maximizing Signal-to-Leakage Ratios," in *Proc. ICASSP*, vol. 3, 2005, pp. iii/1129–iii/1132 Vol. 3.

[111] P. Gill, W. Murray, and M. Wright, *Practical Optimization*. Academic Press, 1981.

[112] R. Horn and C. Johnson, *Matrix Analysis*. Cambridge University Press, 1985.

[113] J. Demmel, I. Dumitriu, and O. Holtz, "Fast Linear Algebra is Stable," *ArXiv e-prints*, Dec. 2006.